

**ONE DIMENSIONAL PHOTONIC CRYSTAL
WAVEGUIDE**

Koray SEVİM

October, 2004

ONE DIMENSIONAL PHOTONIC CRYSTAL WAVEGUIDE

By

Koray SEVİM

A Dissertation Submitted to the
Graduate School in Partial Fulfillment of the
Requirements for the Degree of

MASTER OF SCIENCE

Department: Physics
Major : Physics

İzmir Institute of Technology

İzmir, Turkey

October, 2004

We approve the thesis of **Koray SEVİM**

Date of Signature

22.10.2004

Asst. Prof. Dr. H. Sami SÖZÜER

Supervisor

Department of Physics

22.10.2004

Assoc. Prof. Dr. Orhan ÖZTÜRK

Co-Supervisor

Department of Physics

22.10.2004

Prof. Dr. Doğan DEMİRHAN

Department of Physics, Ege University

22.10.2004

Asst. Prof. Dr. Salih DİNLEYİCİ

Department of Electrical and Electronics Engineering

22.10.2004

Asst. Prof. Dr. Thomas BECHTELER

Department of Electrical and Electronics Engineering

22.10.2004

Prof. Dr. Durmuş Ali DEMİR

Head of Department

ACKNOWLEDGMENTS

First of all, I am deeply grateful to my advisors Asst. Prof. Dr. H. Sami SÖZÜER who was so helpful, patient and enthusiastic. His patience, experience and encouragement are the valuable sources that have kept me on the right track. He has not only shown me the way to carry out the development work but more importantly, he also taught me how to work in a demanding job. I am very grateful for the positive and constructive feedback from the review committee: Assoc. Prof. Dr. Orhan ÖZTÜRK, Asst. Prof. Dr. Salih DİNLEYİCİ, Dr. Asst. Prof. Thomas BECHTELER, and Prof. Dr. Doğan DEMİRHAN.

I also would like to thank to research assistants in department of physics and mathematics of our institution for their help and friendship during this thesis.

Finally, I wish to express my gratitude to Tina. Simple words seem inadequate to express my love for you. Without her love and great patience I would never have been able to accomplish this dissertation.

ABSTRACT

This thesis deals with the implementation of a numerical method to describe how electromagnetic waves propagate through a one-dimensional photonic crystal waveguide. The one-dimensional photonic crystal waveguide is a periodic arrangement of dielectric slabs of alternating dielectric constant with an impurity slab introduced as the guiding layer. This impurity guides, and confines light within a given range of frequencies by producing waveguide modes within the photonic band gap. These modes are different from those of conventional waveguides that use total internal reflection as the basic guiding mechanism. Photonic crystal waveguides are expected to lead to compact photonic integrated circuits.

ÖZET

Elektromanyetik dalgaların bir boyutlu fotonik kristal dalga kılavuzu içerisinde nasıl ilerlediği nümerik metotların uygulanmasıyla açıklanmaktadır. Bir boyutlu fotonik kristal dalga kılavuzu, değişen dielektrik sabitine sahip tabakaların periyodik olarak sıralanmasından ve içerisinde kılavuz tabaka olarak bilinen safsızlığa sahip bir tabakadan meydana gelmektedir. Bu safsızlık, fotonik yasaklanmış bant aralığında dalga kılavuzu modları yaratarak, ışığın verilen belirli bir frekans aralığında ilerlemesini ve hapsedilmesini sağlamaktadır. Elde edilen bu modlar, basit kılavuzlama mekanizması olarak iç tam yansımayı kullanan geleneksel dalga kılavuzlarından farklıdır. Fotonik kristal dalga kılavuzlarının bütünleşmiş yoğun fotonik devrelerde yol gösterici olacağı umulmaktadır.

TABLE OF CONTENTS

LIST OF FIGURES	viii
Chapter 1. INTRODUCTION	1
1.1 History of Photonic Crystals	2
1.2 Applications of Photonic Crystals	5
1.3 Overview of the Thesis	6
Chapter 2. The Plane-Wave Method	7
2.1 E Method	7
2.1.1 3-D Wave Equation in G Space	8
2.1.2 1-D Wave Equation in G Space	11
2.2 H Method	14
2.2.1 3-D Wave Equation in G Space	15
2.2.2 1-D Wave Equation in G Space	17
Chapter 3. ONE-DIMENSIONAL PERFECT PHOTONIC CRYSTAL	18
3.1 Plane-wave Method	18
3.2 Supercell Method	19
Chapter 4. ONE-DIMENSIONAL DIELECTRIC LAYER'S REFLECTION AND TRANSMISSION CALCULATION	22
4.1 One-dimensional Dielectric Layer	22
4.2 Calculation of Transmission and Reflection Coefficients	28
Chapter 5. RANDOMNESS IN PERIODIC LAYERED MEDIA AND ONE- DIMENSIONAL PHOTONIC CRYSTAL	30
5.1 Supercell Method	30
5.2 Randomness in 1-D Photonic Crystal	32
5.3 Randomness in Periodic Layered Media	35
Chapter 6. ONE-DIMENSIONAL PHOTONIC CRYSTAL WAVEGUIDE	41
6.1 Supercell Method: Derivation and Illustration	41
6.2 H Method in One-Dimensional Photonic Crystal Waveguide	43
6.3 1-D Photonic Crystal Waveguide	46
6.3.1 Solution of One-dimensional Photonic Crystal Waveguide for E-polarization	50
6.3.2 Solution of One-dimensional Photonic Crystal Waveguide for B-polarization	52
6.4 Results and Discussion on 1-D Photonic Crystal Waveguide	54
6.4.1 Analytical Solution of Single Slab Symmetric Waveguide	54
6.4.2 1-D Photonic Crystal Waveguide	59

Chapter 7. DISCUSSION AND CONCLUSIONS	77
7.1 FUTURE WORKS	78
Appendix A.DERIVATION OF EIGENVALUE EQUATION OF H METHOD	79
REFERENCES	83

LIST OF FIGURES

Figure 1.1	Number of published works per year. Data was obtained by searching for “photonic crystal OR photonic band” at the ISI Web of Science.	3
Figure 1.2	Number of US patents issued per year related to photonic crystals. Data was obtained by searching “photonic crystal OR photonic band” at the US Patent Office website http://www.uspto.gov	4
Figure 2.1	1-D Photonic Crystal Band Diagram for $\epsilon_a = 1$, $\epsilon_b = 13$, filling ratio $\beta = 0.5$, number of plane-waves = 100, where the filling ratio is $\frac{d_a}{d_a+d_b}$. Shaded regions show the photonic band gaps.	14
Figure 3.1	Filling ratio vs k(wave vector) for $\epsilon(a) = 1$, $\epsilon(b) = 13$	18
Figure 3.2	Band Structure of One-Dimensional Photonic Crystal (Supercell Method) for $\epsilon_a = 13$, $\epsilon_b = 1$, $d_a = 1$, $d_b = 3.6055$, increasing number of layer, where white regions are band gaps	20
Figure 3.3	Band structure of 1D photonic crystal with plane-wave method and supercell method, where $\epsilon_a = 13$, $\epsilon_b = 1$, $d_a = 1$, $d_b = 3.6055$, number of plane-waves = 3000 for both method and supercell size = 101 for supercell method.	21
Figure 4.1	Illustration of 1D Dielectric Layer.	22
Figure 4.2	$\ln(\text{Transmission})$ versus frequency for $\epsilon_1 = 1$, $\epsilon_2 = 13$, $d_1 = 3.6055$, $d_2 = 1$	29
Figure 5.1	General Picture of the Supercell Method where ϵ_i is dielectric constant of each medium, d_i is the thickness of each medium, and supercell size is taken 2π	31
Figure 5.2	Density of States graph of periodic structure for $\epsilon_a = 13$, $\epsilon_b = 1$, $d_a = 1$, $d_b = 3.6055$, number of plane-waves = 10000, and number of layers = 500.	32
Figure 5.3	Density of States graph for 1% randomness where $\epsilon_a = 13$, $\epsilon_b = 1$, $d_a = 1$, $d_b = 3.6055$, number of plane-waves = 10000, and number of layers = 500.	33
Figure 5.4	Density of States graph for 10% randomness where $\epsilon_a = 13$, $\epsilon_b = 1$, $d_a = 1$, $d_b = 3.6055$, number of plane-waves = 10000, and number of layers = 500.	33
Figure 5.5	Density of States graph for 50% randomness where $\epsilon_a = 13$, $\epsilon_b = 1$, $d_a = 1$, $d_b = 3.6055$, number of plane-waves = 10000, and number of layers = 500.	34
Figure 5.6	Density of States graph for 100% randomness where $\epsilon_a = 13$, $\epsilon_b = 1$, $d_a = 1$, $d_b = 3.6055$, number of plane-waves = 10000, and number of layers = 500.	34

Figure 5.7	Frequency vs % Randomness where $\epsilon_a = 13$, $\epsilon_b = 1$, $d_a = 1$, $d_b = 3.6055$, number of plane-waves = 10000, and number of layers = 500.	35
Figure 5.8	Band structure of 1D photonic crystal and 1st three band gaps of the same structure with 10% randomness for (1 sample) where $\epsilon_a = 13$, $\epsilon_b = 1$, $d_a = 1$, $d_b = 3.6055$, number of plane-waves = 10000.	35
Figure 5.9	Band structure of 1D photonic crystal and 1st three band gaps of the same structure with 10% randomness (for 50 sample) where $\epsilon_a = 13$, $\epsilon_b = 1$, $d_a = 1$, $d_b = 3.6055$, number of plane-waves = 10000.	36
Figure 5.10	Band structure of 1D photonic crystal and 1st three band gaps of the same structure with 10% randomness (for 100 sample) where $\epsilon_a = 13$, $\epsilon_b = 1$, $d_a = 1$, $d_b = 3.6055$, number of plane-waves = 10000.	36
Figure 5.11	$\ln(\text{Transmission})$ of periodic layered structure where $\epsilon_a = 13$, $\epsilon_b = 1$, $d_a = 1$, $d_b = 3.6055$	37
Figure 5.12	$\ln(\text{Transmission})$ vs Normalized frequency for 10% and 25% randomness where $\epsilon_a = 13$, $\epsilon_b = 1$, $d_a = 1$, $d_b = 3.6055$	38
Figure 5.13	$\ln(\text{Transmission})$ vs Normalized frequency for 50% and 100% randomness where $\epsilon_a = 13$, $\epsilon_b = 1$, $d_a = 1$, $d_b = 3.6055$. Making the comparison between graphs for different number of slabs and same percent randomness for instance this figure and previous figure we can easily see that if we increase the number of slabs we can minimize the fluctuations in transmission.	39
Figure 5.14	$\ln(\text{Transmission})$ vs Normalized frequency with different sample size for 40% randomness where $\epsilon_a = 13$, $\epsilon_b = 1$, $d_a = 1$, $d_b = 3.6055$	40
Figure 6.1	Illustration of Supercell, where ϵ_i dielectric constant of impurity layer, d_i thickness of impurity layer, ϵ_b dielectric constant of b type material, d_b thickness of b type material, ϵ_a dielectric constant of a type material, d_a thickness of a type material, n_{ϵ_a} number of epsilon of a type material, $a \equiv d_a + d_b$ lattice constant, A superlattice constant (Taken 2π).	42
Figure 6.2	1D Waveguide, where d_i thickness of impurity layer, $d_a \equiv$ thickness of a type material, $d_b \equiv$ thickness of b type material, $\epsilon_i \equiv$ dielectric constant of impurity layer, $\epsilon_a \equiv$ dielectric constant of a type material, $\epsilon_b \equiv$ dielectric constant of b type material and em waves moving in y direction.	47
Figure 6.3	Figure of Single Slab Symmetric Waveguide, where $\epsilon_1 \equiv$ dielectric constant of guiding layer, $\epsilon_2 \equiv$ dielectric constant of outside.	55
Figure 6.4	Exact and Numerical Solution of Single Slab Symmetric Waveguide for $\epsilon_1 = 13$, $\epsilon_2 = 1$, $d_1 = 0.1$, $d_2 = 0.05$ for E Polarization and B Polarization. Straight and dashed lines denote even and odd modes respectively.	57

Figure 6.5	Exact and Numerical Solution and Band Structure of Single Slab Symmetric Waveguide for $\epsilon_1 = 13$, $\epsilon_2 = 1$, $d_1 = 0.1$, $d_2 = 0.05$ for E Polarization. First even, first odd, and second even modes are given.	58
Figure 6.6	Perfect Periodic Structure for $\epsilon_a = 2.43$, $\epsilon_b = 12.25$, $\epsilon_i = 2.43$, $d_a : d_b = 1 : 2$, $d_i = d_a$, $\beta = 0.32786$ and Structure with defect for $\epsilon_a = 2.43$, $\epsilon_b = 12.25$, $\epsilon_i = 1$, $d_a : d_b = 1 : 2$, $d_i \equiv \frac{2}{3}(d_a + d_b)$, $\beta = 0.32786$ for E-Polarization.	60
Figure 6.7	Comparison of guided modes for $\epsilon_a = 2.43$, $\epsilon_b = 12.25$, $\epsilon_i = 1$, $d_a : d_b = 1 : 2$, $d_i \equiv \frac{2}{3}(d_a + d_b)$, $\beta = 0.32786$	61
Figure 6.8	Comparison of guided modes [25] for $\epsilon_a = 2.43$, $\epsilon_b = 12.25$, $\epsilon_i = 1$, $d_a : d_b = 1 : 2$, $d_i = \frac{2}{3}(d_a + d_b)$	62
Figure 6.9	Dispersion relation and $E(x)$ vs x graph of 1st even mode for $\epsilon_a = 13$, $\epsilon_b = 1$, $\epsilon_i = 13$, $d_a = 0.02$, $d_b = 0.08$, $d_i = 0.1$ (B-polarization).	63
Figure 6.10	Dispersion relation and $E(x)$ vs x graph of 1st odd mode for $\epsilon_a = 13$, $\epsilon_b = 1$, $\epsilon_i = 13$, $d_a = 0.02$, $d_b = 0.08$, $d_i = 0.1$ (B-polarization).	64
Figure 6.11	Dispersion relation and $E(x)$ vs x graph of 2nd even mode for $\epsilon_a = 13$, $\epsilon_b = 1$, $\epsilon_i = 13$, $d_a = 0.02$, $d_b = 0.08$, $d_i = 0.1$ (B-polarization).	65
Figure 6.12	Dispersion relation and $E(x)$ vs x graph of 1st even mode for $\epsilon_a = 13$, $\epsilon_b = 1$, $\epsilon_i = 13$, $d_a = 0.02$, $d_b = 0.08$, $d_i = 0.1$ (E-polarization).	67
Figure 6.13	Dispersion relation and $E(x)$ vs x graph of 1st odd mode for $\epsilon_a = 13$, $\epsilon_b = 1$, $\epsilon_i = 13$, $d_a = 0.02$, $d_b = 0.08$, $d_i = 0.1$ (E-polarization).	68
Figure 6.14	Dispersion relation and $E(x)$ vs x graph of 2nd even mode for $\epsilon_a = 13$, $\epsilon_b = 1$, $\epsilon_i = 13$, $d_a = 0.02$, $d_b = 0.08$, $d_i = 0.1$ (E-polarization).	69
Figure 6.15	Dispersion relation and $E(x)$ vs x graph of 1st even mode for $\epsilon_a = 13$, $\epsilon_b = 1$, $\epsilon_i = 1$, $d_a = 0.02$, $d_b = 0.08$, $d_i = 0.1$ (E-polarization).	70
Figure 6.16	Dispersion relation and $E(x)$ vs x graph of 1st odd mode for $\epsilon_a = 13$, $\epsilon_b = 1$, $\epsilon_i = 1$, $d_a = 0.02$, $d_b = 0.08$, $d_i = 0.1$ (E-polarization).	71
Figure 6.17	Dispersion relation and $E(x)$ vs x graph for $\epsilon_a = 13$, $\epsilon_b = 1$, $\epsilon_i = 13$, $d_a = 0.02$, $d_b = 0.08$, $d_i = 0.1$ and analytical solution of single slab waveguide for $\epsilon_i = 13$, $\epsilon_1 = 0.001$ (E-polarization). In this graph, if we choose the dielectric constant of outside region close to zero we have obtain the same guided modes in the case of one dimensional photonic crystal waveguide. This kind of materials which have zero dielectric constant known as perfect dielectric materials.	72
Figure 6.18	Band diagrams of one-dimensional photonic crystal waveguide for increasing ϵ_i , where $\epsilon_a = 13$, $\epsilon_b = 1$ (E-Polarization).	73

Figure 6.19 Band diagrams of one-dimensional photonic crystal waveguide for increasing ϵ_i , where $\epsilon_a = 13$, $\epsilon_b = 1$ (E-Polarization). . . .	74
Figure 6.20 Band diagrams of one-dimensional photonic crystal waveguide for increasing ϵ_i , where $\epsilon_a = 13$, $\epsilon_b = 1$ (B-Polarization). . . .	75
Figure 6.21 Band diagrams of one-dimensional photonic crystal waveguide for increasing ϵ_i , where $\epsilon_a = 13$, $\epsilon_b = 1$ (B-Polarization). . . .	76

Chapter 1

INTRODUCTION

As the world demands ever more of computers and communications we turn increasingly to optical devices whose bandwidth and speed of execution offer great potential. However materials science has lagged behind in this rush into the optical domain : optical properties of materials are not always well matched to the functions we seek. This is in contrast to the vast range of electronic properties available to us. In the electronic domain one can almost make materials to order. The root cause of this richness in electronic properties is the interaction of electrons with the periodic structure of the materials. It is this interaction that decides whether a material will be a metal, a semiconductor, or an insulator, and can be further exploited to fine tune the detailed electronic properties. Change the structure, change the properties.

It was this concept that led Yablonovitch [1] to propose that we try the same trick with light. He had in mind that just as a semiconductor has a forbidden band of energies within which no electron could enter the crystal, so it should be possible to make a periodic dielectric such that in a forbidden range of frequencies no photon could enter into or propagate within the crystal. This idea created the concept of photonic crystal which has a periodically modulated dielectric constant with a lattice constant that is comparable to desired wavelength. Structure of a photonic crystal consists of periodically arranged blocks and that is why it is a “crystal”. It is said to be “photonic” because these materials affect the propagation properties of photons.

There is a conceptual analogy between the behavior of electromagnetic waves in periodic dielectric structures and electron waves in natural crystals. Photonic crystals are theoretically analyzed by using the solutions of Maxwell’s equations in a periodic medium, while the electronic structure of natural crystals are analyzed by the Schrödinger equation. But this is not a complete analogy. For instance, one important difference between the electronic and photonic band structures is that the electrons are massive whereas photons have no mass. Therefore, the dispersion relation, which is the relationship between the wave-vector

and frequency for electrons in crystals is parabolic while in the photonic case it is linear. There are a few other differences between electronic and photonic band structures. The translation vectors for photonic crystals are much larger than those for the electron systems and the photonic reciprocal space has a Brillouin zone much smaller than that for electrons. Electrons have spin 1/2, but frequently this spin is ignored, and the Schrödinger equation is treated in a scalar wave approximation. In contrast, photons have spin 1, but for 2D and 3D systems it is never a good approximation to neglect polarization in photonic crystal calculations.

In vacuum a well known equation $\omega = ck$ is valid for free photons known as dispersion relation of the radiation field, where c is speed of light in vacuum. If photons are propagating through a homogeneous and isotropic dielectric then $\omega = ck/n$, where n is the refractive index of the dielectric material. As can be seen, the frequency (and therefore photon energy) depends linearly on the ratio of the wave-vector and the material refractive index.

1.1 History of Photonic Crystals

The interest of researchers in the field of photonic crystals has been increasingly growing since they were proposed in 1987. The amount of publications show a spectacular exponential growth. The number of papers published and number of patents issued each year is so high that it is really hard to keep track of even the most significant and valuable papers.

In this section a brief summary of the most important and crucial work related to photonic crystals will be presented.

In 1987, two independent works appeared. The first one was published by Yablonovitch [1] and dealt with the “inhibition of spontaneous emission of electromagnetic radiation using a three dimensionally periodic structure”. The lattice that was proposed should have a photonic band gap and a region of forbidden energy states. The second paper was published by John [4] that was titled “Anderson localization of photons in disordered dielectric superlattices”. These two works are considered as the starting point of the research field.

The spontaneous emission rate of an excited state of a quantum system is given, to first order, by Fermi’s Golden Rule:

$$\Gamma(\omega) = \frac{2\pi}{\hbar^2} \langle |M|^2 \rangle D(\omega), \quad (1.1)$$

where M_{ij} is the matrix element of the interaction Hamiltonian, $H_{\text{int}} : \langle \psi_f | H_{\text{int}} | \psi_i \rangle$.

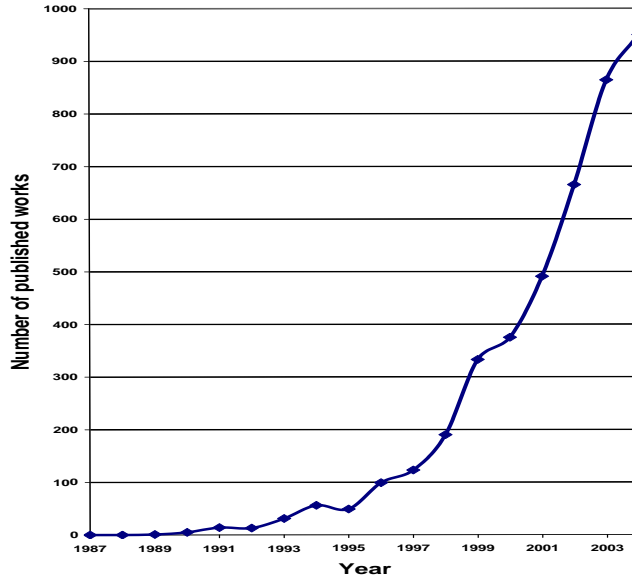


Figure 1.1: Number of published works per year. Data was obtained by searching for “photonic crystal OR photonic band” at the ISI Web of Science.

The density of states of the radiation field in the volume V of vacuum, $D(\omega)$, is proportional to ω^2 :

$$D(\omega) = \frac{\omega^2 V}{\pi^2 c^3} \quad (1.2)$$

By modifying $D(\omega)$, one can change the spontaneous emission rate, and thus the optical properties of materials. For this purpose, photonic crystals can be used as the density of states can be radically altered within a photonic crystal. It was this that motivated Yablonovitch to seek a periodic dielectric structure that possessed a band of “forbidden frequencies.”

In 1990, Satpathy *et al.* [6] and Leung *et al.* [7] independently published a scalar implementation of the plane-wave method to photonic band calculations. Shortly after, both groups improved the plane-wave method. This time theoretical calculations and experimental data showed almost excellent agreement. But whereas Yablonovitch had predicted a photonic bandgap between the 2nd and the 3rd bands for a structure that consisted of slightly overlapping spherical voids arranged in the periodicity of the face-centered cubic (fcc) lattice, the calculations showed that there was no such gap, and that the experimental data was in error.

In 1992, Sözüer *et al* [8] further improved the plane-wave method to show the behavior of higher energy bands. Surprisingly, they showed that between the 8th and the 9th bands of the same structure that Yablonovitch had studied, a complete photonic band gap was formed for a fcc lattice of air holes in a

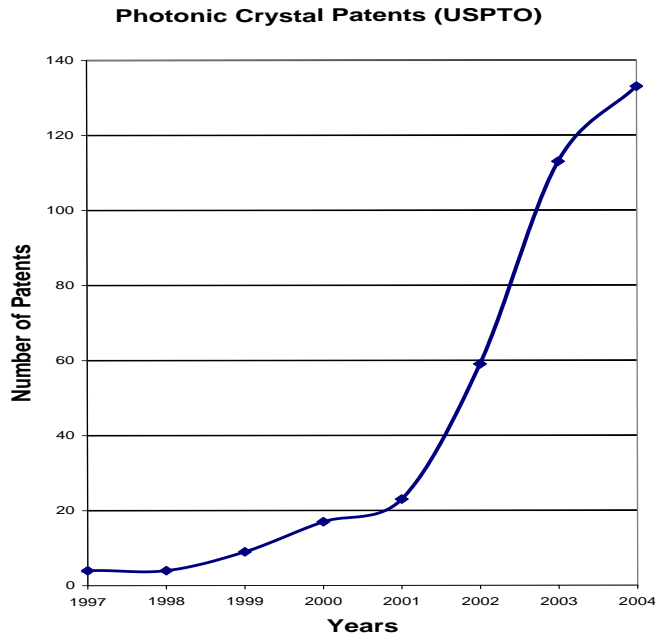


Figure 1.2: Number of US patents issued per year related to photonic crystals. Data was obtained by searching “photonic crystal OR photonic band” at the US Patent Office website <http://www.uspto.gov>.

semiconductor when the refractive index contrast was above 2.8. About one year later Sözüer *et al.* [9] investigated the photonic bands in the simple-cubic lattice (scaffold structure) and calculated the effective long-wavelength dielectric constant.

In the beginning of 1994, a new structure with a complete photonic band gap was proposed by two independent groups [10, 11]. The so-called woodpile structure has a tetragonal symmetry and a complete photonic band gap between the 2nd and 3rd bands.

In 1995, artificial opals [12] were a method that all research laboratories could afford to manufacture and soon many other groups were interested. Furthermore, loading the opal voids with a high refractive index material and then etching away the opal template would result in a structure of air spheres in a dielectric material matrix. Such a structure was precisely the kind of crystal for which Sözüer *et al.* [8] had predicted a complete photonic band gap.

In 1996, Lin *et al.* [13] observed that photons were strongly dispersed in 2D crystals when their frequency was close to the band gap edges. P. St. J. Russell’s group was the first to demonstrate all-silica single-mode optical fiber with photonic crystal cladding [14].

One year later, Birks *et al.* [15] demonstrated early photonic crystal fiber

with some unusual properties. In 1998, Knight *et al.* [16] actually produced the first photonic crystal fiber. The first photonic crystal laser working in the near infrared (NIR) was presented by Fleming *et al.* [17] in 1999. In May of 2000, an inverse opal of silicon was presented by Blanco *et al.* [18].

By 2004, there have been many publications which are mainly related with the different kind of photonic crystal optical fibers and electromagnetic wave guidance.

1.2 Applications of Photonic Crystals

There are many conventional applications of photonic band structures such as perfect dielectric mirrors, resonant cavities, lasers, photonic crystal waveguides, and photonic crystal fibers. Photonic crystals can be used as perfect dielectric mirrors because the reflectivity of photonic crystals derives from their geometry and periodicity, not from a complicated atomic scale property. They should be essentially lossless. Such materials are widely available all the way from the ultraviolet regime to the microwave. Using of the materials with nonlinear properties for construction of photonic crystal lattices open new possibilities for molding the flow of light.

Photonic band gap materials show potential of changing the whole scenario of light guiding in the near future. In traditional waveguides operated at optical range, light is guided by total internal reflection at the boundary of the waveguide. This is quite different from the waveguide operated at microwave range, where the metallic waveguides are used. Though in some sense, the propagation of microwaves in such waveguides can also be regarded as internal reflection, there is no restriction on the reflection angle. For waves at optical frequencies, the metallic waveguides result in great loss, so the dielectric waveguides are the natural choice. But the reflection is restricted to small incidence angles with respect to the waveguide surface. The discovery of photonic crystals put a new alteration on light guiding. When the frequency of the light falls in the gap of the photonic crystal, it is not able to propagate in the crystal. When such light is incident on the surface of the crystal, it will be completely reflected for any incident angle. This provides a great deal of flexibility for the guiding of light. A prominent example is to guide the light through a sharp bend with very high efficiency.[2] For photonic waveguides, extensive numerical calculations and experimental study have been conducted by several groups.[3, 5]

1.3 Overview of the Thesis

In this study we review the optical properties of one-dimensional photonic crystals and one-dimensional photonic crystal waveguides using two different numerical methods. We also investigated transmission spectra of finite periodic dielectric layers. We investigated the effects of random perturbations on the periodic geometry and found that the bandgaps are quite robust to such random variations that could possibly result during an actual manufacturing process.

In chapter 2 we outline the plane-wave method in one and three dimensions. We also show E and H methods and give the derivations and comparison between these two methods.

In chapter 4 the calculation of transmission and reflection coefficients of periodic dielectric media is shown and information about the used method is explained.

In the Randomness in Periodic Layered Media and 1-D Photonic Crystal chapter, effects of random parameters and importance of randomness in dielectric layers and one-dimensional photonic crystals are reviewed and also derivation of the supercell method is given for a disordered one-dimensional photonic crystal.

In the last chapter, derivation of the supercell method is given and properties of one-dimensional photonic crystal waveguides and some guided modes both E-polarization (TE) and B-polarization (TM) are shown. Additionally we have compared analytical and numerical solutions of a single slab symmetric waveguide at both E (TE) and B (TM) polarizations.

Chapter 2

The Plane-Wave Method

The Plane-wave method, is a straightforward way of solving for eigenvalues and eigenfunctions of the equation which is obtained from the Maxwell's equations. The basic idea is to expand the dielectric constant as well as the periodic part of Bloch function in a discrete Fourier series expressed on the plane-wave basis [8],[19], [20], [21]. This method can be very versatile when the medium is periodic.

Unfortunately the plane-wave method does not seem very suitable if the photonic crystals has defects. However, many structures having a point defect have already been studied with this method using a supercell method. In section 6.1, we are going to consider the supercell method for photonic crystals with defects.

2.1 E Method

We start with macroscopic Maxwell's equations in a lossless, charge-free region of space:

$$\nabla \cdot \mathbf{D} = 0 \tag{2.1}$$

$$\nabla \cdot \mathbf{B} = 0 \tag{2.2}$$

$$\nabla \times \mathbf{E} = -\frac{\partial \mathbf{B}}{\partial t} \tag{2.3}$$

$$\nabla \times \mathbf{H} = \frac{\partial \mathbf{D}}{\partial t}. \tag{2.4}$$

where \mathbf{E} and \mathbf{H} are the macroscopic electric and magnetic fields, \mathbf{D} is the displacement field, \mathbf{B} is the magnetic induction field. The displacement field is $\mathbf{D} = \epsilon_0 \epsilon(x) \mathbf{E}$ where $\epsilon(x)$ is relative dielectric permittivity and the magnetic induction field $\mathbf{B} = \mu_0 \mu \mathbf{H}$ where μ is the relative magnetic permeability. For most dielectric materials of interest, the relative magnetic permeability is close to unity

and we may set $\mathbf{B} = \mu_0 \mathbf{H}$ in the Eq. (2.4). Taking the curl of both sides of Eq. (2.3),

$$\nabla \times (\nabla \times \mathbf{E}) = -\nabla \times \frac{\partial \mathbf{B}}{\partial t} = \frac{\partial (\nabla \times \mathbf{B})}{\partial t}, \quad (2.5)$$

where we interchange the order of time and space derivatives. We can substitute Eq. (2.4) in the right hand side of the Eq. (2.5) which yields:

$$\nabla \times (\nabla \times \mathbf{E}) = -\mu_0 \frac{\partial}{\partial t} \left(\frac{\partial \mathbf{D}}{\partial t} \right) = -\frac{1}{c^2} \frac{\partial^2}{\partial t^2} (\epsilon \mathbf{E}) \quad (2.6)$$

where we used $\mathbf{D} = \epsilon_0 \epsilon(x) \mathbf{E}$ and $1/c^2 = \epsilon_0 \mu_0$. or

$$\nabla \times (\nabla \times \mathbf{E}) + \frac{1}{c^2} \frac{\partial^2}{\partial t^2} (\epsilon \mathbf{E}) = 0. \quad (2.7)$$

Eq. (2.7) is the general form of the electromagnetic wave equation in real space.

2.1.1 3-D Wave Equation in G Space

In Eq. (2.7) we can separate out the time dependence using

$$\mathbf{E}(\mathbf{r}, t) = \mathbf{E}(\mathbf{r}) e^{i\omega t}, \quad (2.8)$$

which yields

$$\nabla \times (\nabla \times \mathbf{E}(\mathbf{r})) \frac{\omega^2}{c^2} \epsilon(\mathbf{r}) \mathbf{E}(\mathbf{r}). \quad (2.9)$$

For a dielectric constant that is periodic, $\epsilon(\mathbf{r} + \mathbf{R}) = \epsilon(\mathbf{r})$, where \mathbf{R} is a lattice vector, one can expand $\epsilon(\mathbf{r})$ in terms of the reciprocal lattice vectors \mathbf{G} . Thus $\epsilon(\mathbf{r})$ can be written as:

$$\epsilon(\mathbf{r}) = \sum_{\mathbf{G}} \epsilon(\mathbf{G}) e^{i\mathbf{G} \cdot \mathbf{r}}. \quad (2.10)$$

In general the Fourier transform of the dielectric lattice constant $\epsilon(\mathbf{r})$ can be written as

$$\epsilon(\mathbf{q}) = \frac{1}{(2\pi)^3} \int d\mathbf{r} e^{-i\mathbf{q} \cdot \mathbf{r}} \epsilon(\mathbf{r}) = \sum_{\mathbf{G}} \delta(\mathbf{q} - \mathbf{G}) \epsilon(\mathbf{G}) \quad (2.11)$$

$$\begin{aligned} \epsilon(\mathbf{G}) &= \frac{1}{V_{\text{cell}}} \int_{\text{WS cell}} d\mathbf{r} e^{-i\mathbf{G} \cdot \mathbf{r}} \epsilon(\mathbf{r}) \\ &= \frac{1}{V_{\text{cell}}} \int_{\text{WS cell}} d\mathbf{r} e^{-i\mathbf{G} \cdot \mathbf{r}} \left[\epsilon_b + \sum_{\mathbf{R}} \epsilon_0(\mathbf{r} - \mathbf{R}) \right] \\ &= \epsilon_b \delta_{\mathbf{G}0} + \frac{1}{V_{\text{cell}}} \sum_{\mathbf{R}} \int_{\text{WS cell}} d\mathbf{r} e^{-i\mathbf{G} \cdot (\mathbf{r} - \mathbf{R})} \epsilon_0(\mathbf{r} - \mathbf{R}) \end{aligned} \quad (2.12)$$

$$\begin{aligned}
&= \epsilon_b \delta_{\mathbf{G}0} + \frac{1}{V_{\text{cell}}} \int_{\text{all } \mathbf{r}} d\mathbf{r} e^{-i\mathbf{G}\cdot\mathbf{r}} \epsilon_0(\mathbf{r}) \\
&= \epsilon_b \delta_{\mathbf{G}0} + \epsilon_0(\mathbf{G})
\end{aligned}$$

where

$$\epsilon_0(\mathbf{G}) \equiv \frac{1}{V_{\text{cell}}} \int_{\text{all } \mathbf{r}} d\mathbf{r} e^{-i\mathbf{G}\cdot\mathbf{r}} \epsilon_0(\mathbf{r}) \quad (2.13)$$

Here the volume of the primitive cell of the lattice is taken as Wigner-Seitz (WS) cell, \mathbf{G} is the reciprocal lattice vector, ϵ_b is the dielectric constant of the background, and \mathbf{q} is taken as $(\mathbf{k} + \mathbf{G})$.

And also $\mathbf{E}(\mathbf{r})$ can be written as

$$\mathbf{E}(\mathbf{r}) = \int_{\text{all } \mathbf{q}} d\mathbf{q} e^{i\mathbf{q}\cdot\mathbf{r}} \mathbf{E}(\mathbf{q}). \quad (2.14)$$

If we have an integral which is over all \mathbf{q} , it can be replaced in the calculations as an integral $d\mathbf{k}$ times summation over reciprocal lattice vectors.

$$\int d\mathbf{q} = \int d\mathbf{k} \sum_{\mathbf{G}'} \quad (2.15)$$

Taking the curl of $\mathbf{E}(\mathbf{r})$

$$\nabla \times \mathbf{E}(\mathbf{r}) = \int d\mathbf{q} e^{i\mathbf{q}\cdot\mathbf{r}} i\mathbf{q} \times \mathbf{E}(\mathbf{q}). \quad (2.16)$$

Retaking the curl of Eq. (2.16)

$$\nabla \times \nabla \times \mathbf{E}(\mathbf{r}) = - \int d\mathbf{q} e^{i\mathbf{q}\cdot\mathbf{r}} \mathbf{q} \times \mathbf{q} \times \mathbf{E}(\mathbf{q}). \quad (2.17)$$

On the right hand side of Eq. (2.9)

$$= \frac{\omega^2}{c^2} \sum_{\mathbf{G}} \epsilon(\mathbf{G}) e^{i\mathbf{G}\cdot\mathbf{r}} \int d\mathbf{q} e^{i\mathbf{q}\cdot\mathbf{r}} \mathbf{E}(\mathbf{q}). \quad (2.18)$$

Using the integral property

$$= \frac{\omega^2}{c^2} \sum_{\mathbf{G}} \epsilon(\mathbf{G}) e^{i\mathbf{G}\cdot\mathbf{r}} \int d\mathbf{k} \sum_{\mathbf{G}'} e^{i(\mathbf{k}+\mathbf{G}')\cdot\mathbf{r}} \mathbf{E}(\mathbf{k} + \mathbf{G}') \quad (2.19)$$

where $\mathbf{q} \equiv \mathbf{k} + \mathbf{G}'$.

$$= \frac{\omega^2}{c^2} \int d\mathbf{k} \sum_{\mathbf{G}} \sum_{\mathbf{G}'} \epsilon(\mathbf{G}) e^{i(\mathbf{k}+\mathbf{G}+\mathbf{G}')\cdot\mathbf{r}} \mathbf{E}(\mathbf{k} + \mathbf{G}') \quad (2.20)$$

Using $\mathbf{G} + \mathbf{G}' \equiv \mathbf{G}''$ and $\mathbf{G} \equiv \mathbf{G}'' - \mathbf{G}'$ into Eq. (2.20)

$$= \frac{\omega^2}{c^2} \int d\mathbf{k} \sum_{\mathbf{G}''} \sum_{\mathbf{G}'} \epsilon(\mathbf{G}'' - \mathbf{G}') e^{i(\mathbf{k} + \mathbf{G}'') \cdot \mathbf{r}} \mathbf{E}(\mathbf{k} + \mathbf{G}'). \quad (2.21)$$

Changing summation indices as $\mathbf{G}'' \rightarrow \mathbf{G}'$ and $\mathbf{G}' \rightarrow \mathbf{G}$ then

$$= \frac{\omega^2}{c^2} \int d\mathbf{k} \sum_{\mathbf{G}'} \sum_{\mathbf{G}} \epsilon(\mathbf{G}' - \mathbf{G}) e^{i(\mathbf{k} + \mathbf{G}') \cdot \mathbf{r}} \mathbf{E}(\mathbf{k} + \mathbf{G}). \quad (2.22)$$

Using the integral property again, which yields:

$$= \frac{\omega^2}{c^2} \int d\mathbf{q} e^{i\mathbf{q} \cdot \mathbf{r}} \sum_{\mathbf{G}} \epsilon(\mathbf{G}' - \mathbf{G}) \mathbf{E}(\mathbf{k} + \mathbf{G}). \quad (2.23)$$

Writing Eq. (2.17) and Eq. (2.23) into the Eq. (2.9)

$$- \int d\mathbf{q} e^{i\mathbf{q} \cdot \mathbf{r}} \mathbf{q} \times \mathbf{q} \times \mathbf{E}(\mathbf{q}) = \frac{\omega^2}{c^2} \int d\mathbf{q} e^{i\mathbf{q} \cdot \mathbf{r}} \sum_{\mathbf{G}} \epsilon(\mathbf{G}' - \mathbf{G}) \mathbf{E}(\mathbf{k} + \mathbf{G}). \quad (2.24)$$

We can write

$$- \int d\mathbf{q} e^{i\mathbf{q} \cdot \mathbf{r}} \left\{ \mathbf{q} \times \mathbf{q} \times \mathbf{E}(\mathbf{q}) + \frac{\omega^2}{c^2} \sum_{\mathbf{G}} \epsilon(\mathbf{G}' - \mathbf{G}) \mathbf{E}(\mathbf{k} + \mathbf{G}) \right\} = 0. \quad (2.25)$$

Since $e^{i\mathbf{q} \cdot \mathbf{r}}$ is linearly independent, the expression in the parenthesis must be equal to zero to satisfy this equality. According to this reason, we can write,

$$-\mathbf{q} \times \mathbf{q} \times \mathbf{E}(\mathbf{q}) \frac{\omega^2}{c^2} \sum_{\mathbf{G}} \epsilon(\mathbf{G}' - \mathbf{G}) \mathbf{E}(\mathbf{k} + \mathbf{G}). \quad (2.26)$$

And using $\mathbf{q} \equiv \mathbf{k} + \mathbf{G}'$ into Eq. (2.26)

$$-(\mathbf{k} + \mathbf{G}') \times (\mathbf{k} + \mathbf{G}') \times \mathbf{E}(\mathbf{k} + \mathbf{G}') = \frac{\omega^2}{c^2} \sum_{\mathbf{G}} \epsilon(\mathbf{G}' - \mathbf{G}) \mathbf{E}(\mathbf{k} + \mathbf{G}). \quad (2.27)$$

In more convenient form

$$-(\mathbf{k} + \mathbf{G}') \times (\mathbf{k} + \mathbf{G}') \times \mathbf{E}_k(\mathbf{G}') = \frac{\omega^2}{c^2} \sum_{\mathbf{G}} \epsilon(\mathbf{G}' - \mathbf{G}) \mathbf{E}_k(\mathbf{G}). \quad (2.28)$$

This is the generalized eigenvalue equation and $(\mathbf{k} + \mathbf{G}') \times (\mathbf{k} + \mathbf{G}') \times \mathbf{E}_k(\mathbf{G}')$ and $\epsilon(\mathbf{G}' - \mathbf{G})$ must be hermitian and hermitian, positive definite. If we would like to solve our photonic band gap structure in 3-D using E method we should use Eq. (2.28).

2.1.2 1-D Wave Equation in G Space

From Eq. (2.7), one-dimensional time dependent wave equation in a lossless periodic dielectric structure can be written for $\mu(x) = 1$, $\sigma(x) = 0$ and the dielectric constant is $\epsilon(x, y, z) = \epsilon(x)$ in one-dimension,

$$\frac{\partial^2}{\partial x^2} E(x, t) - \frac{1}{c^2} \frac{\partial^2}{\partial t^2} \epsilon(x) E(x, t) = 0, \quad (2.29)$$

We consider a linear, isotropic and positive definite medium in a lattice with the dielectric lattice constant

$$\epsilon(x) = \epsilon(x + a) > 0,$$

where a is the lattice constant. We can separate out the time dependence by expanding the fields into a set of harmonic modes:

$$E(x, t) = E(x) e^{i\omega t} \quad (2.30)$$

After these assumptions we are going to substitute the electric field into our one-dimensional time dependent wave equation to obtain the wave equation only in spatial domain.

$$\begin{aligned} \frac{\partial^2}{\partial x^2} (E(x) e^{i\omega t}) - \frac{1}{c^2} \frac{\partial^2}{\partial t^2} \epsilon(x) E(x) e^{i\omega t} &= 0, \\ e^{i\omega t} \frac{\partial^2 E(x)}{\partial x^2} + \frac{\omega^2}{c^2} \epsilon(x) E(x) e^{i\omega t} &= 0, \\ \frac{\partial^2 E(x)}{\partial x^2} + \frac{\omega^2}{c^2} \epsilon(x) E(x) &= 0, \end{aligned} \quad (2.31)$$

where $E(x)$ is perpendicular to x coordinate. We expand both $E(x)$ and $\epsilon(x)$ in terms of Bloch plane-waves. We have a periodic dielectric structure, therefore we can write $\epsilon(x)$ as

$$\epsilon(x) = \sum_G \epsilon(G) e^{iGx} \quad (2.32)$$

$$E(x) = \int_{\text{all } q} dq E(q) e^{iqx} \quad (2.33)$$

$$\epsilon(G) = \frac{1}{V_{\text{cell}}} \int \epsilon(x) e^{-iGx} \quad (2.34)$$

$$E(q) = \frac{1}{V_{\text{cell}}} \int dx E(x) e^{-iqx} \quad (2.35)$$

and we rewrite the integral over all q as an integral over Brillouin zone (BZ) and summation over reciprocal lattice vector G .

$$\int_{\text{all } q} = \int_{\text{BZ}} \sum_G \quad (2.36)$$

where $q = k + G$. This integral transformation can be thought as a transformation between real space and reciprocal lattice space. Substituting $\epsilon(x)$ and $E(x)$ into time independent wave Eq. (2.31)

$$\frac{\partial^2}{\partial x^2} \int_{\text{all } q} dq E(q) e^{iqx} + \frac{\omega^2}{c^2} \sum_G \epsilon(G) e^{iGx} \int_{\text{all } q} dq E(q) e^{iqx} = 0 \quad (2.37)$$

$$\int_{\text{all } q} dq (-q^2) E(q) e^{iqx} + \frac{\omega^2}{c^2} \sum_G \epsilon(G) e^{iGx} \int_{\text{all } q} dq E(q) e^{iqx} = 0. \quad (2.38)$$

Using (2.36) and $q = k + G$

$$\begin{aligned} & - \int_{\text{BZ}} dk \sum_{G'} (k + G')^2 E(k + G') e^{i(k+G')x} + \\ & \frac{\omega^2}{c^2} \sum_G \epsilon(G) e^{iGx} \int_{\text{BZ}} dk \sum_{G'} E(k + G') e^{i(k+G')x} = 0. \end{aligned} \quad (2.39)$$

Taking $G'' \equiv G' + G$

$$\begin{aligned} & \int_{\text{BZ}} dk e^{ikx} \left[- \sum_{G'} (k + G')^2 E(k + G') e^{iG'x} + \right. \\ & \left. \frac{\omega^2}{c^2} \sum_{G'} \sum_{G''-G'} \epsilon(G'' - G') E(k + G') e^{iG''x} \right] = 0. \end{aligned} \quad (2.40)$$

We can rewrite this equation as

$$\begin{aligned} & \int_{\text{BZ}} dk e^{ikx} \left[- \sum_{G'} (k + G')^2 E(k + G') e^{iG'x} + \right. \\ & \left. \frac{\omega^2}{c^2} \sum_{G'} \sum_{G''} \epsilon(G'' - G') E(k + G') e^{iG''x} \right] = 0. \end{aligned} \quad (2.41)$$

Now we would like to return first G' and G . Changing our summation indices as $G' \rightarrow G$ and $G'' \rightarrow G'$ in Eq. (2.41)

$$\int_{\text{BZ}} dk e^{ikx} \left[- \sum_{G'} (k + G')^2 E(k + G') e^{iG'x} + \frac{\omega^2}{c^2} \sum_G \sum_{G'} \epsilon(G' - G) E(k + G) e^{iG'x} \right] = 0$$

$$\begin{aligned} & \int_{\text{BZ}} dk e^{ikx} \sum_{G'} e^{iG'x} \left[-(k + G')^2 E(k + G') + \right. \\ & \left. \frac{\omega^2}{c^2} \sum_G \epsilon(G' - G) E(k + G) \right] = 0. \end{aligned} \quad (2.42)$$

Using (2.36) again

$$\int_{\text{all } \mathbf{q}} dq e^{iqx} \left\{ -|k + G'|^2 E(k + G') + \frac{\omega^2}{c^2} \sum_G \epsilon(G' - G) E(k + G) \right\} = 0. \quad (2.43)$$

According to this integral in Eq. (2.43), we can say that the expression in the parenthesis must be equal to zero.

$$-|k + G'|^2 E(k + G') + \frac{\omega^2}{c^2} \sum_G \epsilon(G' - G) E(k + G) = 0 \quad (2.44)$$

For a given k value $E_k(G) \equiv E(k + G)$ Eq. (2.1.2) becomes:

$$|k + G'|^2 E_k(G') = \frac{\omega^2}{c^2} \sum_G \epsilon(G' - G) E_k(G) \quad (2.45)$$

or in an easier more convenient notation

$$|k + G|^2 E_G = \frac{\omega^2}{c^2} \sum_{G'} \epsilon(G - G') E_{G'}. \quad (2.46)$$

For simplicity, we have dropped the script k . These equations define an infinite-dimensional generalized eigenvalue problem of the form

$$Ax = \lambda Bx, \quad (2.47)$$

where $A_{GG'} = |k + G|^2 \delta_{GG'}$, $B_{GG'} = \epsilon(G - G')$, $x_G = E(G)$, and $\lambda = \frac{\omega^2}{c^2}$. We note that A and B are Hermitian matrices, and in addition B is positive definite. Because of real $\epsilon(x)$ and $\epsilon(x) > 0$ respectively, B is a Hermitian and positive definite matrix. Eq. (2.46) can now be solved numerically using standard techniques to give all the allowed frequencies ω for a given wavevector k .

To illustrate the matrices, consider a basis that consists of three reciprocal lattice vectors G_1 , G_2 , and G_3 . One would then obtain, for A , B , and x ,

$$A = \begin{bmatrix} |k + G_1|^2 & 0 & 0 \\ 0 & |k + G_2|^2 & 0 \\ 0 & 0 & |k + G_3|^2 \end{bmatrix}$$

$$B = \begin{bmatrix} \epsilon(G_1 - G_1) & \epsilon(G_1 - G_2) & \epsilon(G_1 - G_3) \\ \epsilon(G_2 - G_1) & \epsilon(G_2 - G_2) & \epsilon(G_2 - G_3) \\ \epsilon(G_3 - G_1) & \epsilon(G_3 - G_2) & \epsilon(G_3 - G_3) \end{bmatrix}$$

and x matrix

$$x = \begin{bmatrix} E(G_1) \\ E(G_2) \\ E(G_3) \end{bmatrix}$$

Of course, a basis of just 3 G points would be inadequate for solving an actual problem. One would typically need ~ 100 plane waves for band structure calculations in 1D to obtain reliable results. The band diagram displayed in Fig. (2.1) was obtained with an expansion using 100 plane waves:

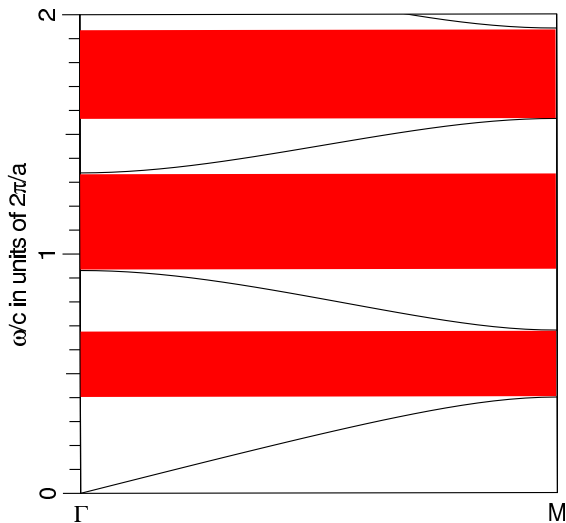


Figure 2.1: 1-D Photonic Crystal Band Diagram for $\epsilon_a = 1$, $\epsilon_b = 13$, filling ratio $\beta = 0.5$, number of plane-waves = 100, where the filling ratio is $\frac{d_a}{d_a+d_b}$. Shaded regions show the photonic band gaps.

2.2 H Method

In the previous section, the \mathbf{B} field was eliminated from Maxwell's equations and a second order equation for \mathbf{E} was obtained. Alternatively, one could eliminate the \mathbf{E} field from the equations and find an equation for \mathbf{B} :

$$\nabla \times \mathbf{E} = -\frac{\partial \mathbf{B}}{\partial t} \quad (2.48)$$

$$\nabla \times \mathbf{H} = \frac{\partial \mathbf{D}}{\partial t}. \quad (2.49)$$

Using two of the Maxwell's equations and taking the curl of Eq. (2.49),

$$\nabla \times \mathbf{H} = \frac{\partial \mathbf{D}}{\partial t} \epsilon_0 \epsilon(\mathbf{r}) \frac{\partial \mathbf{E}}{\partial t} \quad (2.50)$$

Dividing by $\epsilon(\mathbf{r})$ and taking the curl, one obtains

$$\nabla \times \frac{1}{\epsilon(\mathbf{r})} \nabla \times \mathbf{H} = \epsilon_0 \frac{\partial(\nabla \times \mathbf{E})}{\partial t}. \quad (2.51)$$

Using Eq. (2.48), one obtains

$$\nabla \times \frac{1}{\epsilon(\mathbf{r})} \nabla \times \mathbf{H} = -\frac{1}{c^2} \mu \frac{\partial^2 \mathbf{H}}{\partial t^2}. \quad (2.52)$$

For most dielectric materials of interest, the relative magnetic permeability is close to unity and we may set $\mathbf{B} = \mu_0 \mathbf{H}$ in Eq. (2.48). As before, we are looking for harmonic solutions of the form

$$\mathbf{H}(\mathbf{r}, t) = \mathbf{H}(\mathbf{r}) e^{i\omega t}, \quad (2.53)$$

which, upon substitution into Eq.(2.52) yields

$$\nabla \times \left[\frac{1}{\epsilon(\mathbf{r})} \nabla \times \mathbf{H} \right] = \frac{\omega^2}{c^2} \mathbf{H}. \quad (2.54)$$

Eq. (2.54) is the wave equation for \mathbf{H} which can also be written as

$$\nabla \times [\eta(\mathbf{r}) \nabla \times \mathbf{H}] \frac{\omega^2}{c^2} \mathbf{H} \quad (2.55)$$

where $\eta(\mathbf{r}) \equiv \frac{1}{\epsilon(\mathbf{r})}$.

For the H method we have two choices. The first one is choosing $\frac{1}{\epsilon(\mathbf{r})} \equiv \eta(\mathbf{r})$ and the other one is doing our calculation with ϵ^{-1} . In some of the problems second one converges very well. Of course it depends on the structure that you would like to solve.

2.2.1 3-D Wave Equation in \mathbf{G} Space

Since the dielectric constant is periodic, we can expand $\eta(\mathbf{r})$ in terms of reciprocal lattice vector \mathbf{G} . $\eta(\mathbf{r})$ can be written as an summation over all reciprocal lattice vectors

$$\eta(\mathbf{r}) = \sum_{\mathbf{G}} \eta(\mathbf{G}) e^{i\mathbf{G}\cdot\mathbf{r}}. \quad (2.56)$$

And also $\mathbf{H}(\mathbf{r})$ can be written as

$$\mathbf{H}(\mathbf{r}) = \int_{\text{all } \mathbf{q}} d\mathbf{q} e^{i \mathbf{q} \cdot \mathbf{r}} \mathbf{H}(\mathbf{q}). \quad (2.57)$$

If we have an integral which is over all \mathbf{q} , it can be replaced in the calculations as an integral $d\mathbf{k}$ times summation over reciprocal lattice vectors.

$$\int_{\text{all } \mathbf{q}} d\mathbf{q} \int_{BZ} d\mathbf{k} \sum_{\mathbf{G}'} \quad (2.58)$$

Taking the curl of $\mathbf{H}(\mathbf{r})$

$$\nabla \times \mathbf{H}(\mathbf{r}) = \int d\mathbf{q} e^{i \mathbf{q} \cdot \mathbf{r}} i \mathbf{q} \times \mathbf{H}(\mathbf{q}). \quad (2.59)$$

Multiplying Eq. (2.59) with $\eta(\mathbf{r})$ and using the identity $\mathbf{q} \equiv \mathbf{k} + \mathbf{G}$, Eq. (2.59) can be written as:

$$\begin{aligned} \eta(\mathbf{r}) \nabla \times \mathbf{H}(\mathbf{r}) &= \sum_{\mathbf{G}} \eta(\mathbf{G}) e^{i \mathbf{G} \cdot \mathbf{r}} \int d\mathbf{q} e^{i \mathbf{q} \cdot \mathbf{r}} i \mathbf{q} \times \mathbf{H}(\mathbf{q}) \\ &= i \sum_{\mathbf{G}} \eta(\mathbf{G}) e^{i \mathbf{G} \cdot \mathbf{r}} \int d\mathbf{k} \sum_{\mathbf{G}'} e^{i (\mathbf{k} + \mathbf{G}') \cdot \mathbf{r}} (\mathbf{k} + \mathbf{G}') \times \mathbf{H}(\mathbf{k} + \mathbf{G}') \\ &= i \sum_{\mathbf{G}} \sum_{\mathbf{G}'} \eta(\mathbf{G}) \int d\mathbf{k} e^{i (\mathbf{k} + \mathbf{G} + \mathbf{G}') \cdot \mathbf{r}} (\mathbf{k} + \mathbf{G}') \times \mathbf{H}(\mathbf{k} + \mathbf{G}'). \end{aligned}$$

Taking the curl of $\eta(\mathbf{r}) \nabla \times \mathbf{H}(\mathbf{r})$ one more time Eq. (2.59) becomes:

$$\begin{aligned} \nabla \times \eta(\mathbf{r}) \nabla \times \mathbf{H}(\mathbf{r}) &= i \sum_{\mathbf{G}} \sum_{\mathbf{G}'} \eta(\mathbf{G}) \int d\mathbf{k} e^{i (\mathbf{k} + \mathbf{G} + \mathbf{G}') \cdot \mathbf{r}} i (\mathbf{k} + \mathbf{G} + \mathbf{G}') \times (\mathbf{k} + \mathbf{G}') \times \mathbf{H}(\mathbf{k} + \mathbf{G}') \\ &= - \int d\mathbf{k} \left\{ \sum_{\mathbf{G}} \sum_{\mathbf{G}'} (\mathbf{k} + \mathbf{G} + \mathbf{G}') \times \eta(\mathbf{G}) (\mathbf{k} + \mathbf{G}') \times \mathbf{H}(\mathbf{k} + \mathbf{G}') \right\} e^{i (\mathbf{k} + \mathbf{G} + \mathbf{G}') \cdot \mathbf{r}}. \end{aligned}$$

Changing the index of summations as $\mathbf{G}'' \equiv \mathbf{G}' + \mathbf{G}$

$$\begin{aligned} \nabla \times \eta(\mathbf{r}) \nabla \times \mathbf{H}(\mathbf{r}) &= - \int d\mathbf{k} \left\{ \sum_{\mathbf{G}'' = \mathbf{G}} \sum_{\mathbf{G}'} (\mathbf{k} + \mathbf{G}'') \times \eta(\mathbf{G}'' - \mathbf{G}') (\mathbf{k} + \mathbf{G}') \times \mathbf{H}(\mathbf{k} + \mathbf{G}') \right\} e^{i (\mathbf{k} + \mathbf{G}'') \cdot \mathbf{r}} \\ &= - \int d\mathbf{k} \left\{ \sum_{\mathbf{G}'} \sum_{\mathbf{G}} (\mathbf{k} + \mathbf{G}') \times \eta(\mathbf{G}' - \mathbf{G}) (\mathbf{k} + \mathbf{G}) \times \mathbf{H}(\mathbf{k} + \mathbf{G}) \right\} e^{i (\mathbf{k} + \mathbf{G}') \cdot \mathbf{r}} \\ &= - \int d\mathbf{k} \sum_{\mathbf{G}'} e^{i (\mathbf{k} + \mathbf{G}') \cdot \mathbf{r}} \left\{ \sum_{\mathbf{G}} (\mathbf{k} + \mathbf{G}') \times \eta(\mathbf{G}' - \mathbf{G}) (\mathbf{k} + \mathbf{G}) \times \mathbf{H}(\mathbf{k} + \mathbf{G}) \right\} \end{aligned}$$

where the substitution $\mathbf{G}'' \rightarrow \mathbf{G}'$ and $\mathbf{G}' \rightarrow \mathbf{G}$ was used in the second step.

Using the integration property again,

$$\begin{aligned} & \nabla \times (\eta(\mathbf{r})\nabla \times \mathbf{H}(\mathbf{r})) \\ &= -\int d\mathbf{q}e^{i\mathbf{q}\cdot\mathbf{r}} \left\{ \sum_{\mathbf{G}} (\mathbf{k} + \mathbf{G}') \times \eta(\mathbf{G}' - \mathbf{G})(\mathbf{k} + \mathbf{G}) \times \mathbf{H}(\mathbf{k} + \mathbf{G}) \right\}. \end{aligned} \quad (2.60)$$

Substituting Eq. (2.60) into Eq. (2.55) and rearranging

$$\int d\mathbf{q}e^{i\mathbf{q}\cdot\mathbf{r}} \left\{ \sum_{\mathbf{G}} (\mathbf{k} + \mathbf{G}') \times \eta(\mathbf{G}' - \mathbf{G})(\mathbf{k} + \mathbf{G}) \times \mathbf{H}(\mathbf{k} + \mathbf{G}) + \frac{\omega^2}{c^2} \mathbf{H}(\mathbf{k} + \mathbf{G}') \right\} = 0.$$

In order to satisfy this equality, the expression in the curly braces must vanish

$$-\sum_{\mathbf{G}} (\mathbf{k} + \mathbf{G}') \times \eta(\mathbf{G}' - \mathbf{G})(\mathbf{k} + \mathbf{G}) \times \mathbf{H}(\mathbf{k} + \mathbf{G}) = \frac{\omega^2}{c^2} \mathbf{H}(\mathbf{k} + \mathbf{G}'). \quad (2.61)$$

The equation above is an ordinary eigenvalue problem in the form

$$AH = \frac{\omega^2}{c^2} H. \quad (2.62)$$

In Eq. (2.61) we have $3N \times 3N$ matrix equation and we can reduce in $2N \times 2N$ eigenvalue problem (see Appendix A) by similarity transformation choosing appropriate bases vectors as in the form

$$\sum_{\mathbf{G}} |\mathbf{k} + \mathbf{G}'| |\mathbf{k} + \mathbf{G}| \eta(\mathbf{G}' - \mathbf{G}) \begin{bmatrix} \mathbf{e}'_2 \cdot \mathbf{e}_2 & -\mathbf{e}'_1 \cdot \mathbf{e}_2 \\ -\mathbf{e}'_2 \cdot \mathbf{e}_1 & \mathbf{e}'_1 \cdot \mathbf{e}_1 \end{bmatrix} \begin{bmatrix} \mathbf{H}_1(\mathbf{G}) \\ \mathbf{H}_2(\mathbf{G}) \end{bmatrix} = \frac{\omega^2}{c^2} \begin{bmatrix} \mathbf{H}_1(\mathbf{G}') \\ \mathbf{H}_2(\mathbf{G}') \end{bmatrix}.$$

2.2.2 1-D Wave Equation in \mathbf{G} Space

In this section we derive H method in one-dimension. We start with the Eq. (2.61) and writing it in one-dimension by setting $\mathbf{k} \equiv k \mathbf{i}$, $\mathbf{G} \equiv G \mathbf{i}$, $\mathbf{G}' \equiv G' \mathbf{i}$, and $\mathbf{H} \equiv H_z \mathbf{k}$, where \mathbf{H} is perpendicular to x coordinate. For a given G ,

$$(k + G') \mathbf{i} \times \{ \eta(G' - G)(k + G) \mathbf{i} \times H_z \mathbf{k} \} = \frac{\omega^2}{c^2} H_z \mathbf{k}. \quad (2.63)$$

Taking the first curl, we have

$$(k + G') \mathbf{i} \times \eta(G' - G)(k + G) H_z \mathbf{j} = \frac{\omega^2}{c^2} H_z \mathbf{k}. \quad (2.64)$$

Taking the second curl, we have

$$(k + G') \eta(G' - G)(k + G) H_z \mathbf{k} = \frac{\omega^2}{c^2} H_z \mathbf{k}. \quad (2.65)$$

Eq. (2.65) can be written for all G

$$-\sum_G (k + G') \eta(G' - G)(k + G) H_z = \frac{\omega^2}{c^2} H_z. \quad (2.66)$$

This is the ordinary eigenvalue problem in the form

$$AH_z = \lambda H_z \quad (2.67)$$

Chapter 3

ONE-DIMENSIONAL PERFECT PHOTONIC CRYSTAL

One-dimensional photonic crystals are the simplest photonic crystals and serve as a “textbook” case to understand the fundamental properties of the problem. Furthermore the convergence of the plane-wave method is excellent for these structures, making them ideal as a starting point for studying various complications such as randomness, point defects etc. without having to worry about computational resources. In this chapter we are going to show the band structures of one-dimensional perfect photonic crystal calculated with the plane-wave and supercell methods.

3.1 Plane-wave Method

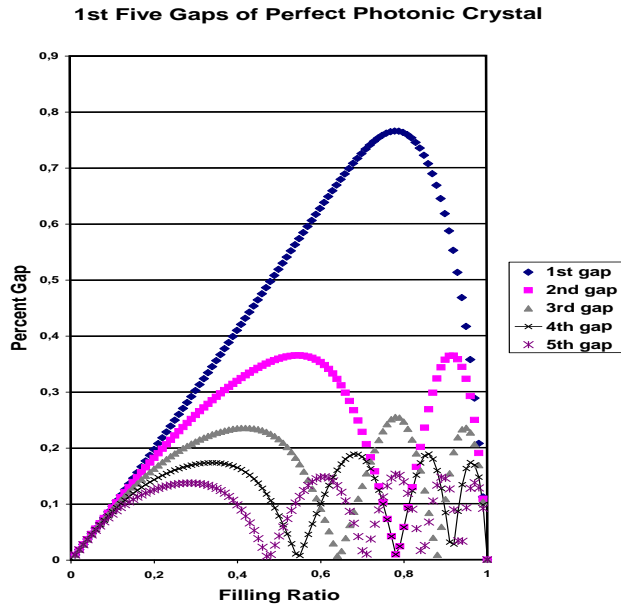


Figure 3.1: Filling ratio vs k (wave vector) for $\epsilon(a) = 1$, $\epsilon(b) = 13$.

In this section we show the band diagrams of one-dimensional photonic crystal calculated by using the plane-wave method. First of all we start with the filling ratio factor which is $\frac{d_a}{d_a + d_b}$.

In our calculations we have used the quarter wave stack which gives the maximum band gap for the lowest gap and higher odd numbered gaps. The even numbered gaps 2, 4, 6, .. are zero for this choices of d_a, d_b . In the Fig. (3.1), the first five band gaps are shown and according to the figure we have chosen the filling ratio as 0.78 that means $d_a\sqrt{\epsilon_a}$ and $d_b = \sqrt{\epsilon_b}$.

3.2 Supercell Method

In this section, we show the band diagrams of a one-dimensional photonic crystal calculated by using the supercell method and compare two band diagrams. In this method, we have chosen the big unit cell (supercell) and calculated photonic band gaps. This method allows the inclusion impurities into the photonic crystal.

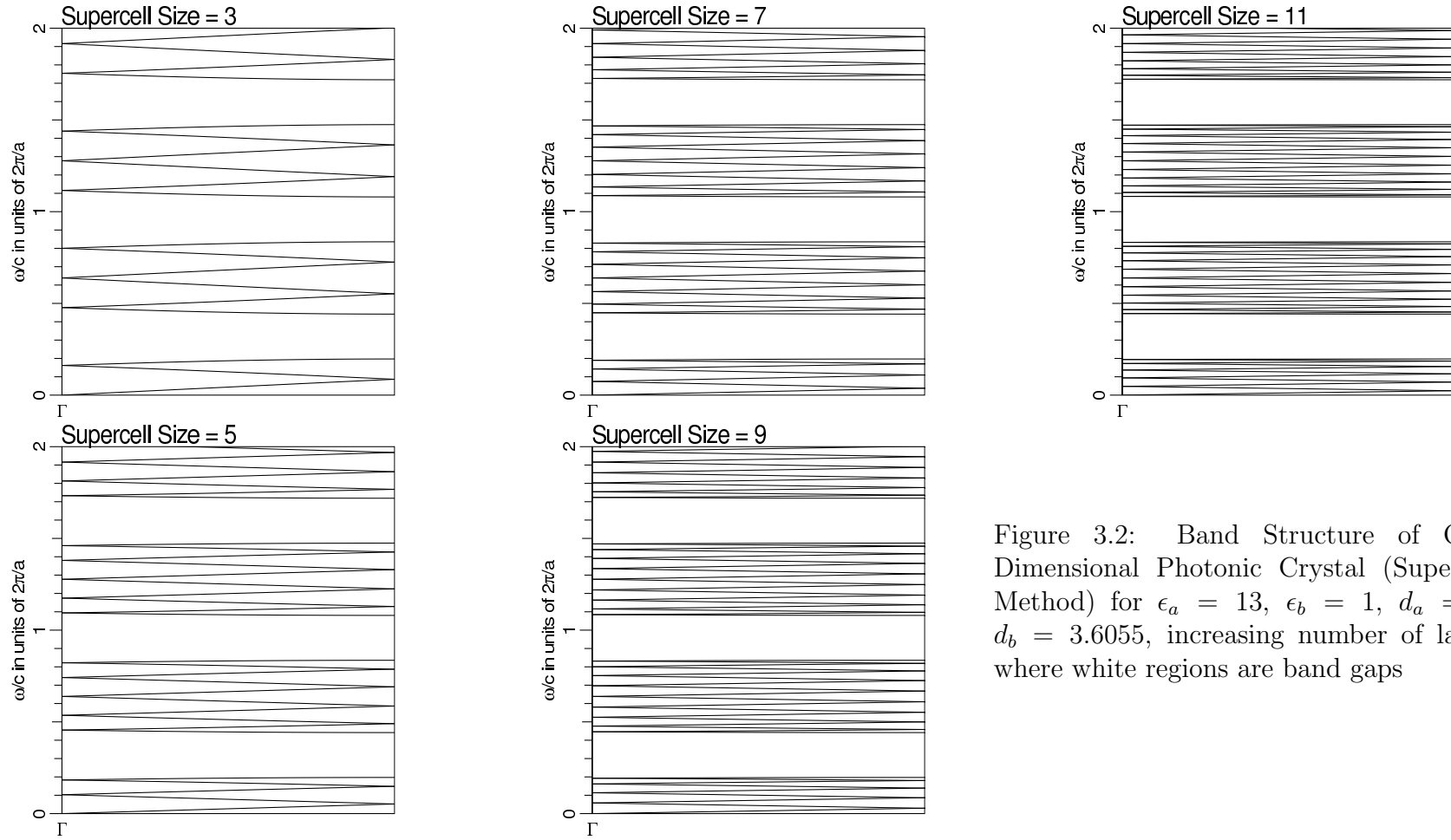


Figure 3.2: Band Structure of One-Dimensional Photonic Crystal (Supercell Method) for $\epsilon_a = 13$, $\epsilon_b = 1$, $d_a = 1$, $d_b = 3.6055$, increasing number of layer, where white regions are band gaps

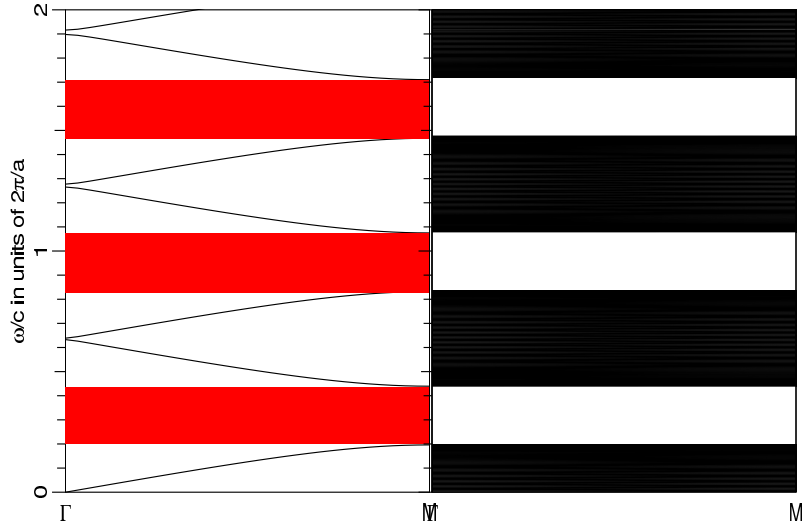


Figure 3.3: Band structure of 1D photonic crystal with plane-wave method and supercell method, where $\epsilon_a = 13$, $\epsilon_b = 1$, $d_a = 1$, $d_b = 3.6055$, number of plane-waves = 3000 for both method and supercell size = 101 for supercell method.

In Fig. (3.3), comparison between plane-wave and supercell methods is given for the same medium parameters. In Fig. (3.2)

Chapter 4

ONE-DIMENSIONAL DIELECTRIC LAYER'S REFLECTION AND TRANSMISSION CALCULATION

In this chapter, we are going to show and derive the reflection and transmission coefficients for one-dimensional dielectric layers. This method is used for finite structures, where one can not speak of a “band gap”, as the concept of a band gap is meaningful only for perfectly periodic structures of infinite extent. Of course for finite structures, we should be able to see the “band gaps” as regions where the transmission coefficient is extremely small.

4.1 One-dimensional Dielectric Layer

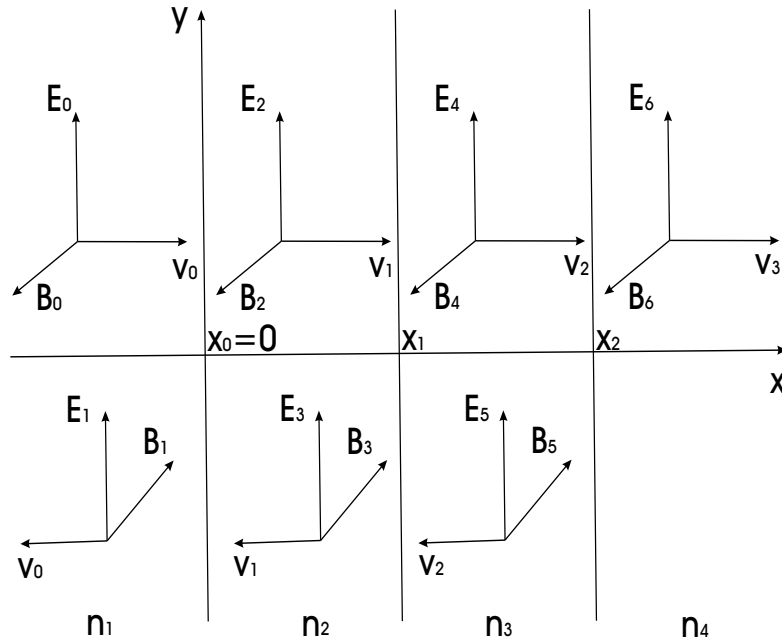


Figure 4.1: Illustration of 1D Dielectric Layer.

A plane-wave of frequency ω , travelling in the x direction and polarized in the y direction is represented

$$\mathbf{E}(x, t) = E_0 e^{i(kx - \omega t)} \hat{y} \quad (4.1)$$

$$\mathbf{B}(x, t) = \frac{1}{v} E_0 e^{i(kx - \omega t)} \hat{z}. \quad (4.2)$$

In our problem we have reflected and transmitted waves and we take $t = 0$.

Writing \mathbf{E} and \mathbf{B} for each region,

$$\mathbf{E}_0(x, t) = E_0 e^{ik_0 x} \quad (4.3)$$

$$\mathbf{B}_0(x, t) = \frac{E_0}{v_0} e^{ik_0 x} \quad (4.4)$$

$$\mathbf{E}_1(x, t) = E_1 e^{-ik_0 x} \quad (4.5)$$

$$\mathbf{B}_1(x, t) = -\frac{E_1}{v_0} e^{-ik_0 x}, \quad (4.6)$$

$$\mathbf{E}_2(x, t) = E_2 e^{ik_1 x} \quad (4.7)$$

$$\mathbf{B}_2(x, t) = \frac{E_2}{v_1} e^{ik_1 x} \quad (4.8)$$

$$\mathbf{E}_3(x, t) = E_3 e^{-ik_1 x} \quad (4.9)$$

$$\mathbf{B}_3(x, t) = -\frac{E_3}{v_1} e^{-ik_1 x}, \quad (4.10)$$

$$\mathbf{E}_4(x, t) = E_4 e^{ik_2 x} \quad (4.11)$$

$$\mathbf{B}_4(x, t) = \frac{E_4}{v_2} e^{ik_2 x}. \quad (4.12)$$

Boundary conditions for our system are ;

$$\epsilon_1 E_1^\perp = \epsilon_2 E_2^\perp$$

$$B_1^\perp = B_2^\perp$$

$$E_1^\parallel = E_2^\parallel$$

$$\frac{1}{\mu_1} B_1^\parallel = \frac{1}{\mu_2} B_2^\parallel.$$

Applying boundary conditions at $x = 0$ and $x = d$ then At $x = 0$;

$$1 + E_1 = E_2 + E_3 \quad (4.13)$$

$$1 - E_1 = n_1 E_2 - n_1 E_3. \quad (4.14)$$

At $x = d$;

$$E_2 e^{ik_1 d} + E_3 e^{-ik_1 d} = E_4 e^{ik_2 d} \quad (4.15)$$

$$n_1 E_2 e^{ik_1 d} - n_1 E_3 e^{-ik_1 d} = n_2 E_4 e^{ik_2 d}. \quad (4.16)$$

Multiplying Eq. (4.15) by n_2 and subtracting Eq. (4.16) we obtain

$$(n_2 - n_1)E_2 e^{ik_1 d} + (n_2 + n_1)E_3 e^{-ik_1 d} = 0 \quad (4.17)$$

Multiplying Eq. (4.13) by n_1 and adding Eq. (4.14) then

$$(n_1 + 1) + (n_1 - 1)E_1 = 2n_1 E_1 \quad (4.18)$$

$$E_2 = \frac{(n_1 + 1) + (n_1 - 1)E_1}{2n_1}. \quad (4.19)$$

Multiplying Eq. (4.13) by n_1 and subtracting Eq. (4.14)

$$(n_1 - 1) + (n_1 + 1)E_1 = 2n_1 E_3 \quad (4.20)$$

$$E_3 = \frac{(n_1 - 1) + (n_1 + 1)E_1}{2n_1}. \quad (4.21)$$

From Eq. (4.17) we can write

$$(n_2 - n_1)E_2 X + (n_2 + n_1)E_3 \frac{1}{X} = 0, \quad (4.22)$$

where $X \equiv e^{ik_1 d}$. Substituting E_2 and E_3 into Eq. (4.22)

$$(n_2 - n_1) \frac{[(n_1 + 1) + (n_1 - 1)E_1]X}{2n_1} \quad (4.23)$$

$$+ (n_2 + n_1) \frac{[(n_1 - 1) + (n_1 + 1)E_1] \frac{1}{X}}{2n_1} = 0$$

$$\frac{(n_2 - n_1)[(n_1 + 1) + (n_1 - 1)E_1]X^2}{2n_1 X} \quad (4.24)$$

$$+ \frac{(n_2 + n_1)[(n_1 - 1) + (n_1 + 1)E_1]}{2n_1 X} = 0$$

$$\frac{(n_2 - n_1)(n_1 + 1)X^2 + (n_2 - n_1)(n_1 - 1)E_1 X^2}{2n_1 X} + \quad (4.25)$$

$$\frac{(n_2 + n_1)(n_1 - 1) + (n_2 + n_1)(n_1 + 1)E_1}{2n_1 X} = 0$$

$$\frac{E_1[(n_2 - n_1)(n_1 - 1)X^2 + (n_2 + n_1)(n_1 + 1)]}{2n_1X} \quad (4.26)$$

$$+ \frac{(n_2 - n_1)(n_1 + 1)X^2 + (n_2 + n_1)(n_1 - 1)}{2n_1X} = 0$$

$$E_1 = - \frac{(n_2 - n_1)(n_1 + 1)X^2 + (n_2 + n_1)(n_1 - 1)}{(n_2 + n_1)(n_1 - 1)X^2 + (n_2 + n_1)(n_1 + 1)}, \quad (4.27)$$

where $X^2 \equiv e^{2ik_1d}$ and taking $2ik_1d \equiv y$ we can write that $X^2 = \cos y + i \sin y$ then substituting this into E_1

$$E_1 = - \frac{(n_2 - n_1)(n_1 + 1)(\cos y + i \sin y) + (n_2 + n_1)(n_1 - 1)}{(n_2 + n_1)(n_1 - 1)(\cos y + i \sin y) + (n_2 + n_1)(n_1 + 1)}. \quad (4.28)$$

We assume that there is no reflection, according to this assumption we can take $E_1 = 0$ then right part of equation (4.28) is

$$- \frac{(n_2 - n_1)(n_1 + 1)(\cos y + i \sin y) + (n_2 + n_1)(n_1 - 1)}{(n_2 + n_1)(n_1 - 1)(\cos y + i \sin y) + (n_2 + n_1)(n_1 + 1)} = 0 \quad (4.29)$$

$$(n_2 - n_1)(n_1 + 1)(\cos y + i \sin y) + (n_2 + n_1)(n_1 - 1) = 0 \quad (4.30)$$

For the imaginary part ;

$$\sin y = \sin 2k_1d = 0$$

$$2k_1d = m\pi, m = 1, 3, 5, \dots$$

For the real part, $\cos y = \cos 2k_1d = -1$ using this in Eq. (4.30) we can find

$$n_1 = \sqrt{n_2} \quad (4.31)$$

For $2k_1d = \pi$;

$$d = \frac{\lambda}{4n_1} = \frac{\lambda'}{4} \quad (4.32)$$

Eq. (4.31) and Eq. (4.32) are known as antireflection coating conditions. If the refractive index of second region is square root of third region and width of slab is a quarter wavelength, we do not have any reflected wave. These two conditions are not related with incident region and also refractive index and dielectric constant. We can write this problem in matrix form. Rewriting Eq. (4.13), Eq. (4.14), Eq. (4.15) and Eq. (4.16).

$$E_1 - E_2 - E_3 = -1 \quad (4.33)$$

$$E_1 + n_1E_2 - n_1E_3 = 1 \quad (4.34)$$

$$E_2 e^{ik_1d} + E_3 e^{-ik_1d} - E_4 e^{ik_2d} = 0 \quad (4.35)$$

$$n_1E_2 e^{ik_1d} - n_1E_3 e^{-ik_1d} - n_2E_4 e^{ik_2d} = 0 \quad (4.36)$$

This linear system can be written as $AX = B$. Here A,B and X matrixes are defined as

$$A = \begin{bmatrix} 1 & -1 & -1 & 0 \\ 1 & n_1 & -n_1 & 0 \\ 0 & e^{ik_1d} & e^{-ik_1d} & -e^{ik_2d} \\ 0 & n_1e^{ik_1d} & -n_1e^{-ik_1d} & -n_2e^{ik_2d} \end{bmatrix} \quad (4.37)$$

$$B = \begin{bmatrix} -1 \\ 1 \\ 0 \\ 0 \end{bmatrix} \quad X = \begin{bmatrix} E_1 \\ E_2 \\ E_3 \\ E_4 \end{bmatrix}. \quad (4.38)$$

The calculations above are performed for one dielectric layer. Now we are going to investigate two dielectric layers. Our purpose is to generalize this problem to N dielectric layers, solving this linear system of equations.

First media ;

$$\mathbf{E}_0(x, t) = E_0 e^{ik_0x} \quad (4.39)$$

$$\mathbf{B}_0(x, t) = \frac{E_0}{v_0} e^{ik_0x} \quad (4.40)$$

$$\mathbf{E}_1(x, t) = E_1 e^{-ik_0x} \quad (4.41)$$

$$\mathbf{B}_1(x, t) = \frac{E_1}{v_0} e^{-ik_0x} \quad (4.42)$$

Second media ;

$$\mathbf{E}_2(x, t) = E_2 e^{ik_1x} \quad (4.43)$$

$$\mathbf{B}_2(x, t) = \frac{E_2}{v_1} e^{ik_1x} \quad (4.44)$$

$$\mathbf{E}_3(x, t) = E_3 e^{-ik_1x} \quad (4.45)$$

$$\mathbf{B}_3(x, t) = \frac{E_3}{v_1} e^{-ik_1x} \quad (4.46)$$

Third media ;

$$\mathbf{E}_4(x, t) = E_4 e^{ik_2x} \quad (4.47)$$

$$\mathbf{B}_4(x, t) = \frac{E_4}{v_2} e^{ik_2x} \quad (4.48)$$

$$\mathbf{E}_5(x, t) = E_5 e^{-ik_2x} \quad (4.49)$$

$$\mathbf{B}_5(x, t) = \frac{E_5}{v_2} e^{-ik_2x} \quad (4.50)$$

Fourth media ;

$$\mathbf{E}_6(x, t) = E_6 e^{ik_3x} \quad (4.51)$$

$$\mathbf{B}_6(x, t) = \frac{E_6}{v_3} e^{ik_3x} \quad (4.52)$$

Using boundary conditions for each media At $x = 0$

$$1 + E_1 = E_2 + E_3 \quad (4.53)$$

$$1 - E_1 = n_1 E_2 - n_1 E_3 \quad (4.54)$$

At $x = x_1$

$$E_2 e^{ik_1x_1} + E_3 e^{-ik_1x_1} = E_4 e^{ik_2x_1} + E_5 e^{-ik_2x_1} \quad (4.55)$$

$$n_1 E_2 e^{ik_1x_1} - n_1 E_3 e^{-ik_1x_1} = n_2 E_4 e^{ik_2x_1} - n_2 E_5 e^{-ik_2x_1} \quad (4.56)$$

At $x = x_2$

$$E_4 e^{ik_2x_2} + E_5 e^{-ik_2x_2} = E_6 e^{ik_3x_2} \quad (4.57)$$

$$n_2 E_4 e^{ik_2x_2} - n_2 E_5 e^{-ik_2x_2} = n_3 E_6 e^{ik_3x_2} \quad (4.58)$$

Rearranging these equations we obtain

$$\begin{aligned} E_1 - E_2 - E_3 &= -1 \\ E_1 + n_1 E_2 - n_1 E_3 &= 1 \\ E_2 e^{ik_1x_1} + E_3 e^{-ik_1x_1} - E_4 e^{ik_2x_1} - E_5 e^{-ik_2x_1} &= 0 \\ n_1 E_2 e^{ik_1x_1} - n_1 E_3 e^{-ik_1x_1} - n_2 E_4 e^{ik_2x_1} + n_2 E_5 e^{-ik_2x_1} &= 0 \\ E_4 e^{ik_2x_2} + E_5 e^{-ik_2x_2} - E_6 e^{ik_3x_2} &= 0 \\ n_2 E_4 e^{ik_2x_2} - n_2 E_5 e^{-ik_2x_2} - n_3 E_6 e^{ik_3x_2} &= 0. \end{aligned}$$

In matrix form

$$A = \begin{bmatrix} 1 & -1 & -1 & 0 & 0 & 0 \\ 1 & n_1 & -n_1 & 0 & 0 & 0 \\ 0 & e^{ik_1x_1} & e^{-ik_1x_1} & -e^{ik_2x_1} & -e^{-ik_2x_1} & 0 \\ 0 & n_1 e^{ik_1x_1} & -n_1 e^{-ik_1x_1} & -n_2 e^{ik_2x_1} & n_2 e^{-ik_2x_1} & 0 \\ 0 & 0 & 0 & e^{ik_2x_2} & e^{-ik_2x_2} & -e^{ik_3x_2} \\ 0 & 0 & 0 & n_2 e^{ik_2x_2} & -n_2 e^{-ik_2x_2} & -n_3 e^{ik_3x_2} \end{bmatrix} \quad (4.59)$$

$$B = \begin{bmatrix} -1 \\ 1 \\ 0 \\ 0 \\ 0 \\ 0 \end{bmatrix} \quad X = \begin{bmatrix} E_1 \\ E_2 \\ E_3 \\ E_4 \\ E_5 \\ E_6 \end{bmatrix}. \quad (4.60)$$

4.2 Calculation of Transmission and Reflection Coefficients

In this section we are going to examine the energy density of electromagnetic waves which is important to understand the behavior of the incident wave. Before doing this, we should calculate the reflection and transmission coefficients. They measure the fraction of the incident energy that is reflected and transmitted. In order to obtain these two coefficients, we need to consider the poynting vectors of reflected, transmitted, and incident waves. The formula of the poynting vector is

$$\mathbf{S} = \frac{1}{\mu} \mathbf{E} \times \mathbf{B}. \quad (4.61)$$

For $\mu = 1$ reflection and transmission coefficients are

$$R = \frac{S_r}{S_i} \quad T = \frac{S_t}{S_i}, \quad (4.62)$$

where S_r, S_i, S_t are respectively poynting vectors of reflected, incident, and transmitted waves. These are calculated below

$$\mathbf{S}_i = \mathbf{E} \times \mathbf{B} = \frac{n_i}{c} E_i E_i = \frac{n_i}{c} E_i^2 \quad (4.63)$$

$$\mathbf{S}_r = \frac{n_r}{c} E_r E_r = \frac{n_r}{c} E_r^2 \quad (4.64)$$

$$\mathbf{S}_t = \frac{n_t}{c} E_t E_t = \frac{n_t}{c} E_t^2 \quad (4.65)$$

$$R = \frac{S_r}{S_i} = \frac{\frac{n_i}{c} E_r^2}{\frac{n_i}{c} E_i^2} = \left[\frac{E_r}{E_i} \right]^2 \quad (4.66)$$

$$T = \frac{S_t}{S_i} = \frac{\frac{n_t}{c} E_t^2}{\frac{n_i}{c} E_i^2} \frac{n_t}{n_i} \left[\frac{E_t}{E_i} \right]^2. \quad (4.67)$$

In this problem we take the coefficient of electric field of incident wave $E_i = 1$. Substituting this into R and T we obtain reflection and transmission coefficients as

$$R = E_r^2 \quad (4.68)$$

$$T = \frac{n_t}{n_i} E_t^2. \quad (4.69)$$

According to equations above, we can say that the reflection coefficient only depends on the electric field coefficient of reflected wave but the transmission coefficient also depends on the electric field coefficient of transmitted wave and refractive index of transmitted and incident regions.

At the beginning of our calculations we have illustrated our medium and problem. Using the parameters of each medium we have calculated transmission coefficients of dielectric layers using Eq. (4.69). In order to see first three band gap clearly, we have taken natural logarithm of the transmission coefficient.

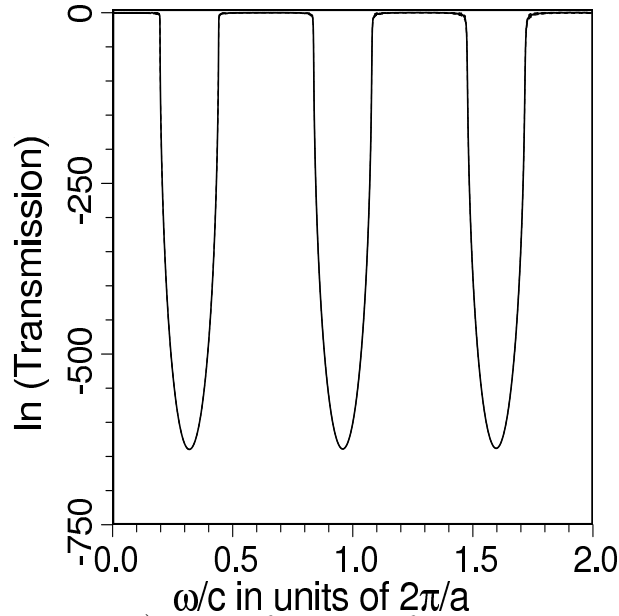


Figure 4.2: $\ln(\text{Transmission})$ versus frequency for $\epsilon_1 = 1$, $\epsilon_2 = 13$, $d_1 = 3.6055$, $d_2 = 1$.

In this graph we have taken number of slab as 500 that means 250 unit cells.

Chapter 5

RANDOMNESS IN PERIODIC LAYERED MEDIA AND ONE-DIMENSIONAL PHOTONIC CRYSTAL

Bandgaps in photonic crystals depend on two crucial properties: an infinite and perfect translational symmetry. In real life no crystal is infinite in size or perfect. When one introduces randomness, one has to give up the idea of a complete bandgap, i.e. a region where the density of states is exactly zero. Instead one needs to look for bands of frequencies for which the density of states is very small. Similarly when the crystal is finite, a quantity of interest would be the transmission coefficient vs frequency. In this chapter, we will consider both approaches, and demonstrate that the bandgaps for the infinite perfect lattice show up as large depressions in the transmission coefficient and the density of states.

5.1 Supercell Method

To calculate the density of states, we use a supercell which contains many unit cells, but the geometrical parameters in each unit cell are randomly perturbed. This unit cell, however is repeated in space so the Bloch formalism still applies to the supercell. Clearly, the larger the supercell size, the better. The supercell is illustrated in Fig. (5.1). There are n layers in the supercell each with a dielectric constant ϵ_i . The Fourier transform of $\epsilon(x)$ can be written as

$$\begin{aligned}\epsilon(G) &= \frac{1}{V_{\text{cell}}} \sum_{m=1}^n \int_{m-1}^m \epsilon_m e^{-i G x} dx \\ &= \frac{1}{V_{\text{cell}}} \sum_{m=1}^n \epsilon_m \int_{m-1}^m e^{-i G x} dx \\ &= \frac{1}{V_{\text{cell}}} \sum_{m=1}^n \epsilon_m \int_{m-1}^m (\cos(G x) - i \sin(G x)) dx \\ &= \frac{1}{V_{\text{cell}}} \sum_{m=1}^n \epsilon_m \left[\frac{1}{G} (\sin(G x) + i \cos(G x)) \right]_{x_{m-1}}^{x_m}\end{aligned}$$

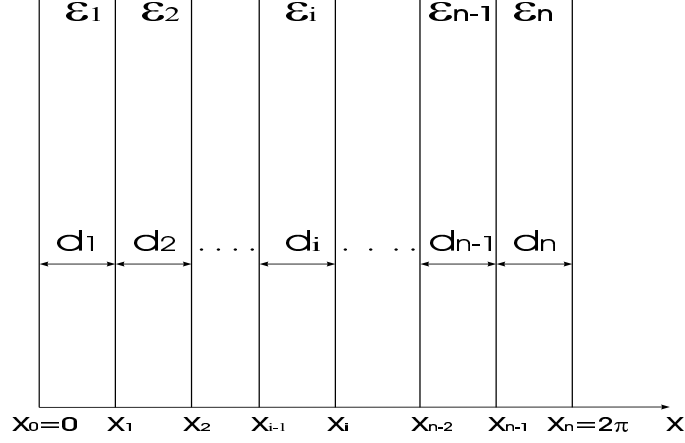


Figure 5.1: General Picture of the Supercell Method where ϵ_i is dielectric constant of each medium, d_i is the thickness of each medium, and supercell size is taken 2π .

$$\begin{aligned}
&= \frac{1}{V_{\text{cell}}} \sum_{m=1}^n \epsilon_m \left[\frac{1}{G} \{(\sin(G x_m) + i \cos(G x_m)) - (\sin(G x_{m-1}) + i \cos(G x_{m-1}))\} \right] \\
\epsilon(G) &= \frac{1}{V_{\text{cell}}} \sum_{m=1}^n \epsilon_m \left[\frac{1}{G} (\sin(G x_m) - \sin(G x_{m-1})) + \frac{i}{G} (\cos(G x_m) - \cos(G x_{m-1})) \right].
\end{aligned}$$

Up to now we have derived the general Fourier transform of $\epsilon(G)$ including both cosine and sine terms without any assumption. For a perfectly periodic medium

$$\epsilon_i = \begin{cases} \epsilon_a, & \text{for } i \text{ odd,} \\ \epsilon_b, & \text{for } i \text{ even,} \end{cases} \quad (5.1)$$

$$d_i = \begin{cases} d_a, & \text{for } i \text{ odd,} \\ d_b, & \text{for } i \text{ even.} \end{cases} \quad (5.2)$$

Now we are going to write Fourier transform of dielectric constant for a given lattice parameters. According to the Fig. (5.1),

$$\begin{aligned}
\epsilon(G) &= \frac{1}{2\pi} \int dx e^{-i G x} \epsilon(x) \\
\epsilon(G) &= \frac{1}{2\pi} \left\{ \sum_{i=1,3,5\dots}^{n-1} \epsilon_a \int_{\frac{(i-1)}{2}(d_a+d_b)}^{d_a+\frac{(i-1)}{2}(d_a+d_b)} e^{-i G x} dx + \sum_{i=2,4,6\dots}^n \epsilon_b \int_{\frac{(i-2)}{2}(d_a+d_b)+d_a}^{\frac{i}{2}(d_a+d_b)} e^{-i G x} dx \right\}
\end{aligned}$$

To consider the effect of randomness, we added a random variation to the thickness of each layer in the unit cell.

$$d = d_0 \left[1 + (r - 0.5) \left(\frac{2p}{100} \right) \right], \quad (5.3)$$

where d_0 is unperturbed thickness, r is uniformly distributed random number between 0 and 1, and p is percentage of randomness.

5.2 Randomness in 1-D Photonic Crystal

In disordered one-dimensional photonic crystal, we deal with the density of states and sketch the density of states vs normalized frequency graph. We are interested in the first three band gaps and the effect of uniform random numbers on the band gaps. The density of states graph in Fig. (5.2) is for $p = 0$, i.e. a perfect structure. The medium parameters that we have used are $\epsilon_a = 13$, $\epsilon_b = 1$, the thicknesses of a and b layers are $d_a = 1$, $d_b = 3.6055$ and the supercell contains 250 unit cells. We have taken 500 layers for our calculations because size of structure is important. If we take small number of layer for example 8 layer, the result can be a little bit different from the real one. This difference appears because of the interaction between the neighboring unit cells.

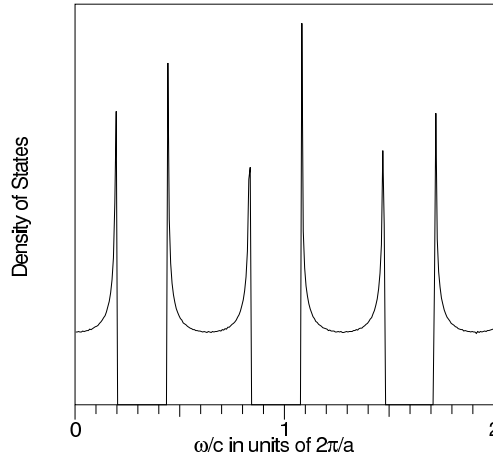


Figure 5.2: Density of States graph of periodic structure for $\epsilon_a = 13$, $\epsilon_b = 1$, $d_a = 1$, $d_b = 3.6055$, number of plane-waves = 10000, and number of layers = 500.

All figures are sketched for $\epsilon_a = 13$, $\epsilon_b = 1$, the thicknesses of a and b layers are $d_a = 1$, $d_b = 3.6055$ and the number of layer is 500. In Fig. (5.3), there is no change in the band gap size but we can see the fluctuations according to random thickness. When we increase the percentage of uniform random numbers we see the third band gap is starting to get smaller but there is no damage in the first band gap even the randomness percentage is 10. In Fig. (5.5), second and third band gaps disappeared according to 50% percentage. For 100% randomness, there is no band gap and periodicity and the structure is completely random. In order to observe and find where these three band gaps will disappear, we have

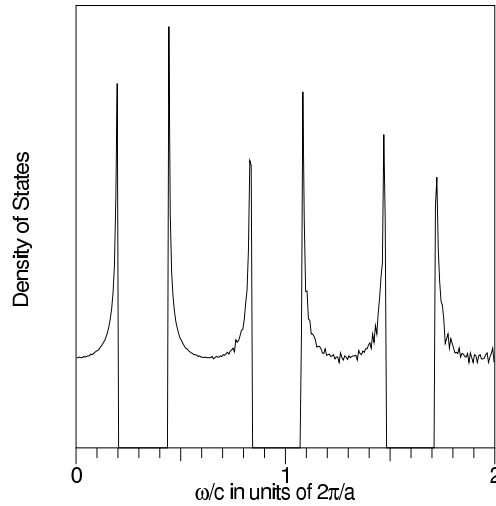


Figure 5.3: Density of States graph for 1% randomness where $\epsilon_a = 13$, $\epsilon_b = 1$, $d_a = 1$, $d_b = 3.6055$, number of plane-waves = 10000, and number of layers = 500.

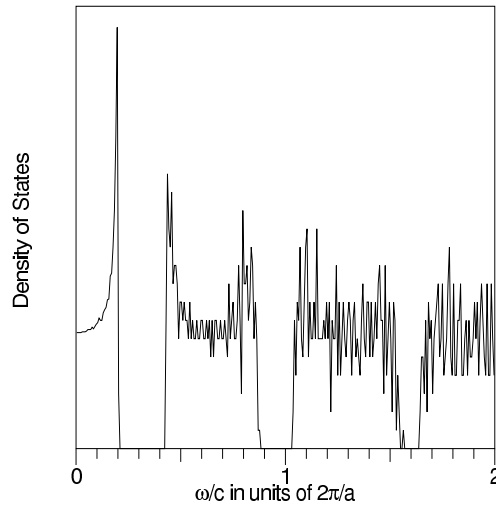


Figure 5.4: Density of States graph for 10% randomness where $\epsilon_a = 13$, $\epsilon_b = 1$, $d_a = 1$, $d_b = 3.6055$, number of plane-waves = 10000, and number of layers = 500.

made an animation and sketched the change of first three band gaps with the increasing percentage.

From Fig. (5.7) we have found the disappearing percentages of each band gaps. According to this figure, it is clear that the damages are beginning from the high frequencies and finally first band gap disappeared. Third, second, and first band gaps disappeared when the randomness is %11, %21, and 68% respectively.

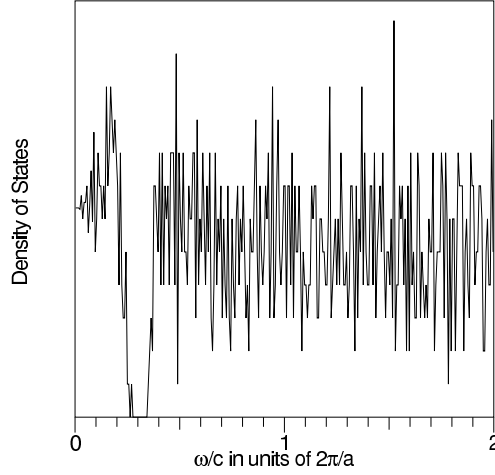


Figure 5.5: Density of States graph for 50% randomness where $\epsilon_a = 13$, $\epsilon_b = 1$, $d_a = 1$, $d_b = 3.6055$, number of plane-waves = 10000, and number of layers = 500.

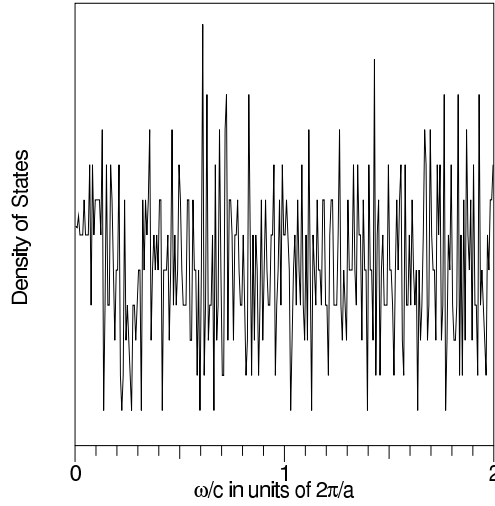


Figure 5.6: Density of States graph for 100% randomness where $\epsilon_a = 13$, $\epsilon_b = 1$, $d_a = 1$, $d_b = 3.6055$, number of plane-waves = 10000, and number of layers = 500.

In Fig. (5.8), Fig. (5.9), and Fig. (5.10) we have shown first three band gaps of one-dimensional photonic crystal with 10% randomness and band structure of one-dimensional perfectly periodic photonic crystal. Band structure of photonic crystal is calculated for $\epsilon_a = 13$, $\epsilon_b = 1$, filling ratio = 0.22, and 3000 plane-waves. Using the same parameters we have calculated band gap widths with 10% randomness in the thickness of each medium and sketched the graph normalized frequency vs number of layers. These three figures are also calculated for different sample size. We have taken different number of samples and looked at the fact that how much sample we need to take for accurate result. In figures we have seen that 100 samples is sufficient but taking only 1 sample is not good enough. When we have taken less number of samples we come across

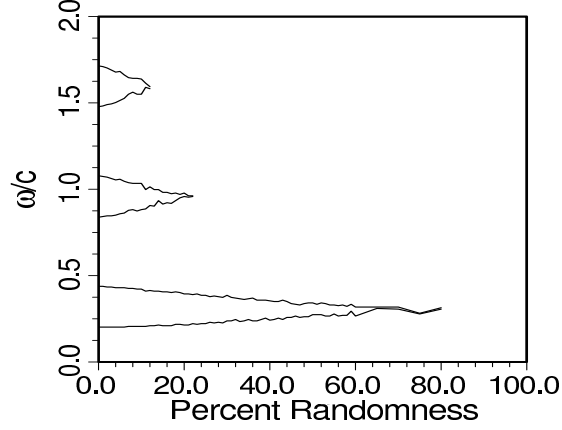


Figure 5.7: Frequency vs % Randomness where $\epsilon_a = 13$, $\epsilon_b = 1$, $d_a = 1$, $d_b = 3.6055$, number of plane-waves = 10000, and number of layers = 500.

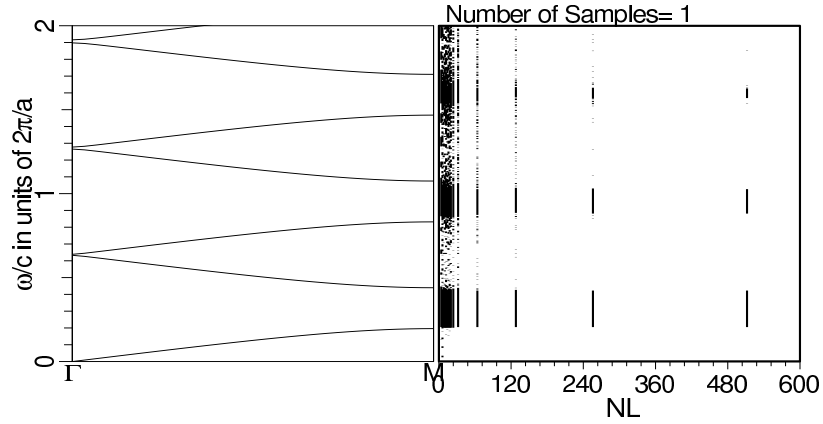


Figure 5.8: Band structure of 1D photonic crystal and 1st three band gaps of the same structure with 10% randomness for (1 sample) where $\epsilon_a = 13$, $\epsilon_b = 1$, $d_a = 1$, $d_b = 3.6055$, number of plane-waves = 10000.

with virtual band gaps. Taking enough number of sample we can get rid of these kind of virtual band gaps. There is also another fact about the number of layer parameter because if we have increase the number of layers we have approached the real band gap width and obstructed the interaction between the unit cells.

5.3 Randomness in Periodic Layered Media

In this section we have investigated how transmission is influenced from the randomness. Uniform random numbers are added or subtracted to thicknesses of each slabs after that transmission coefficients are calculated and $\ln(\text{transmission})$ versus frequency graphs are sketched. While we are studying this problem we have searched the importance of sample and structure sizes as in the case of randomness in one-dimensional photonic crystal section. We have also calculated the standard deviation of transmission coefficients for each frequencies. We have

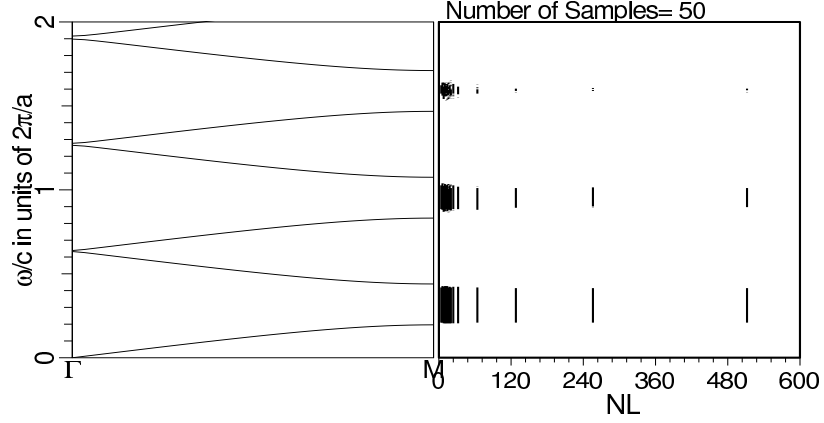


Figure 5.9: Band structure of 1D photonic crystal and 1st three band gaps of the same structure with 10% randomness (for 50 sample) where $\epsilon_a = 13$, $\epsilon_b = 1$, $d_a = 1$, $d_b = 3.6055$, number of plane-waves = 10000.

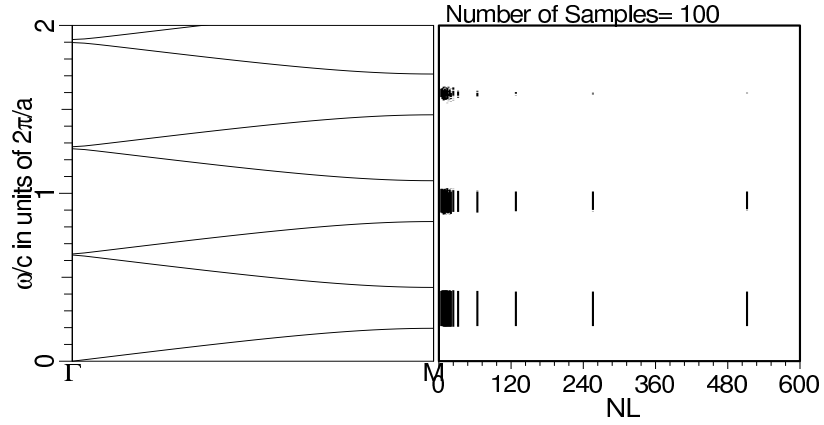


Figure 5.10: Band structure of 1D photonic crystal and 1st three band gaps of the same structure with 10% randomness (for 100 sample) where $\epsilon_a = 13$, $\epsilon_b = 1$, $d_a = 1$, $d_b = 3.6055$, number of plane-waves = 10000.

looked at the standard deviations because we would like to see and understand how the change in size of the structure influences the fluctuations in the transmission. Now we are giving graphs for different number of slabs and percent randomness.

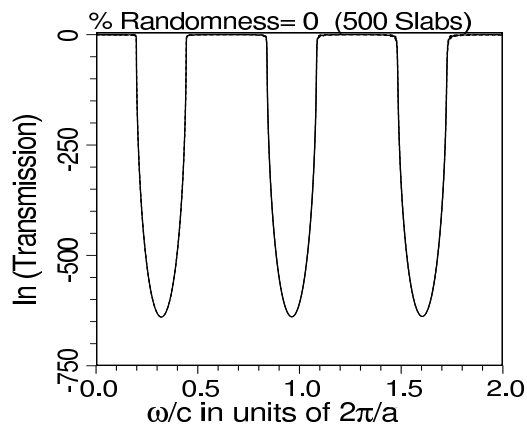


Figure 5.11: $\ln(\text{Transmission})$ of periodic layered structure where $\epsilon_a = 13$, $\epsilon_b = 1$, $d_a = 1$, $d_b = 3.6055$.

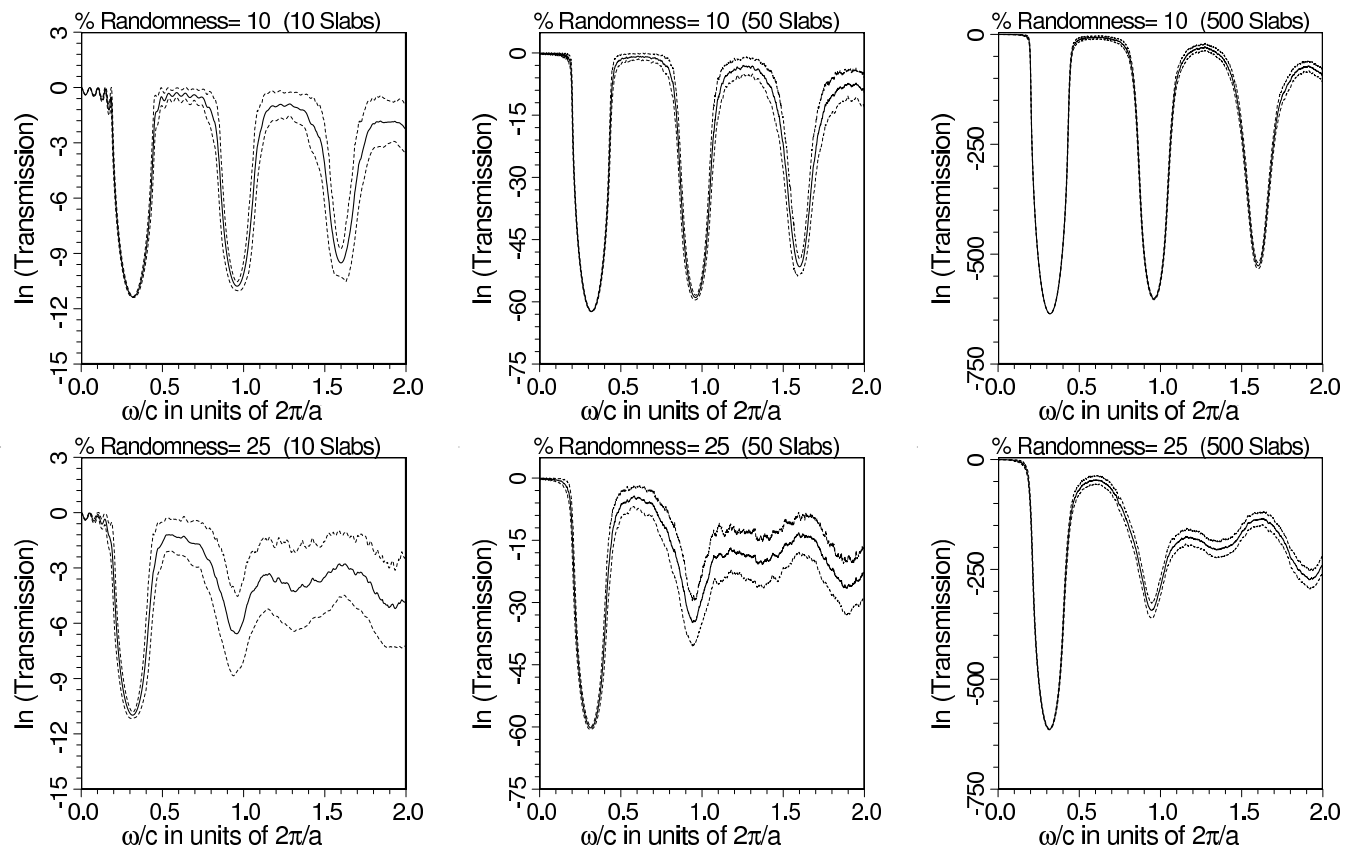


Figure 5.12: $\ln(\text{Transmission})$ vs Normalized frequency for 10% and 25% randomness where $\epsilon_a = 13$, $\epsilon_b = 1$, $d_a = 1$, $d_b = 3.6055$.

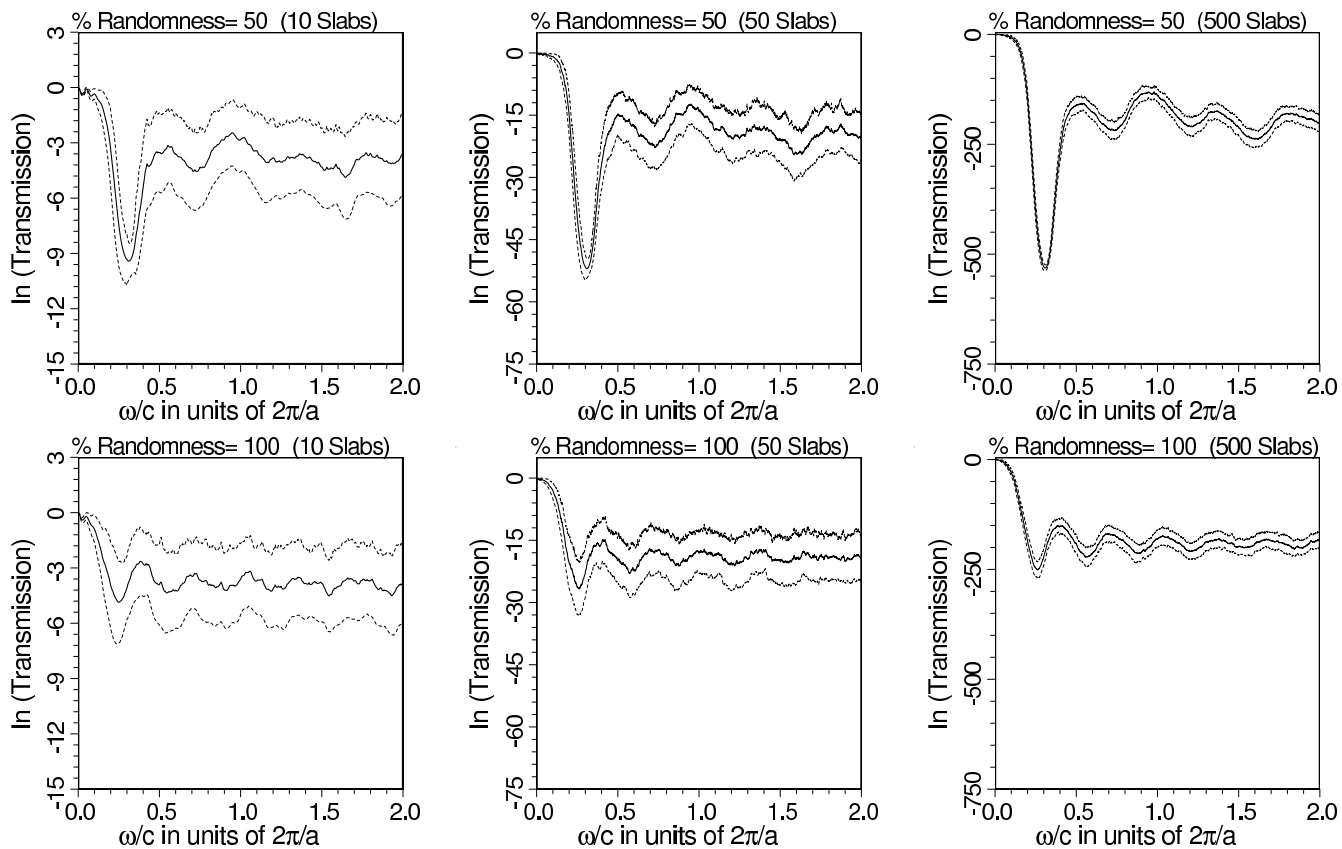


Figure 5.13: $\ln(\text{Transmission})$ vs Normalized frequency for 50% and 100% randomness where $\epsilon_a = 13$, $\epsilon_b = 1$, $d_a = 1$, $d_b = 3.6055$. Making the comparison between graphs for different number of slabs and same percent randomness for instance this figure and previous figure we can easily see that if we increase the number of slabs we can minimize the fluctuations in transmission.

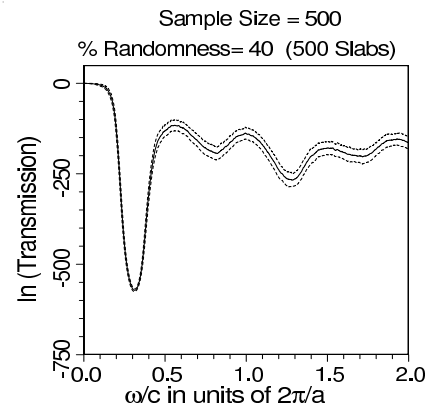
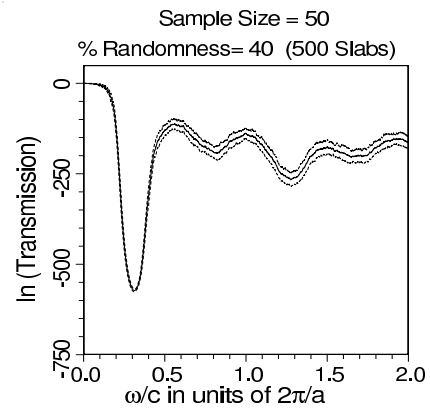
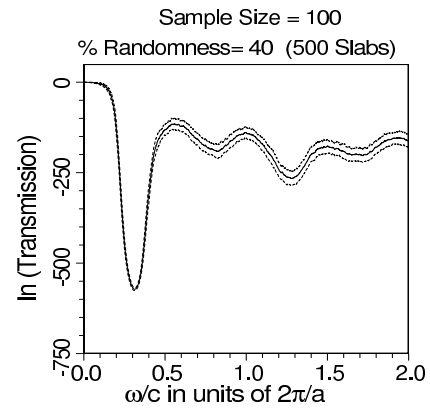
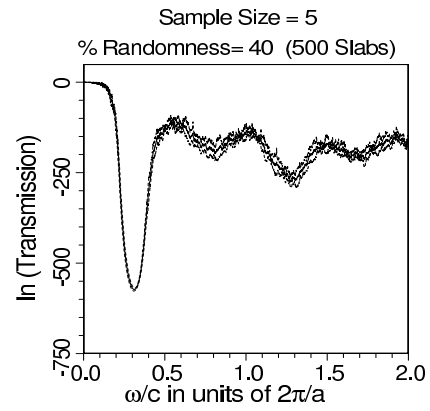


Figure 5.14: $\ln(\text{Transmission})$ vs Normalized frequency with different sample size for 40% randomness where $\epsilon_a = 13$, $\epsilon_b = 1$, $d_a = 1$, $d_b = 3.6055$.

Chapter 6

ONE-DIMENSIONAL PHOTONIC CRYSTAL WAVEGUIDE

6.1 Supercell Method: Derivation and Illustration

This method is the second method which we used for band structure calculations. The plane-wave method is always valid for band gap calculation of periodic dielectric structures such as perfect photonic crystals. If we would like to produce a defect into the periodic dielectric structure we have to change our method. The plane-wave method based supercell approach allows us to model the combined photonic crystals defects by a periodic system with a large unit cell centered around the defect. If the unit cell is made sufficiently large, the probability of reciprocal influence between the unit cells is going to be low and you can not observe the virtual defect modes associated with the overlap between neighboring unit cells in the photonic band gap. The figure below represent our supercell which has a small unit cell size.

Now we are going to show our derivations of supercell approach and obtain the Fourier transform of dielectric constant $\epsilon(r)$ using similar procedure for the supercell as in the case of plane-wave method. Before writing the general formula of $\epsilon(G)$, we are going to take the Fourier transform of it.

$$\begin{aligned}
 \epsilon(G) &= \frac{1}{V_{\text{cell}}} \sum_{m=1}^n \left[\int_{m-1}^m \epsilon_m e^{i G x} dx \right] \\
 &= \frac{1}{V_{\text{cell}}} \sum_{m=1}^n \epsilon_m \int_{m-1}^m e^{i G x} dx \\
 &= \frac{1}{V_{\text{cell}}} \sum_{m=1}^n \epsilon_m \int_{m-1}^m (\cos(G x) + i \sin(G x)) dx \\
 &= \frac{1}{V_{\text{cell}}} \sum_{m=1}^n \epsilon_m \left[\frac{1}{G} (\sin(G x) - i \cos(G x)) \right]_{x_{m-1}}^{x_m} \\
 &= \frac{1}{V_{\text{cell}}} \sum_{m=1}^n \epsilon_m \left[\frac{1}{G} \{ (\sin(G x_m) - i \cos(G x_m)) - (\sin(G x_{m-1}) - i \cos(G x_{m-1})) \} \right] \\
 \epsilon(G) &= \frac{1}{V_{\text{cell}}} \sum_{m=1}^n \epsilon_m \left[\frac{1}{G} (\sin(G x_m) - \sin(G x_{m-1})) - \frac{i}{G} (\cos(G x_m) - \cos(G x_{m-1})) \right].
 \end{aligned}$$

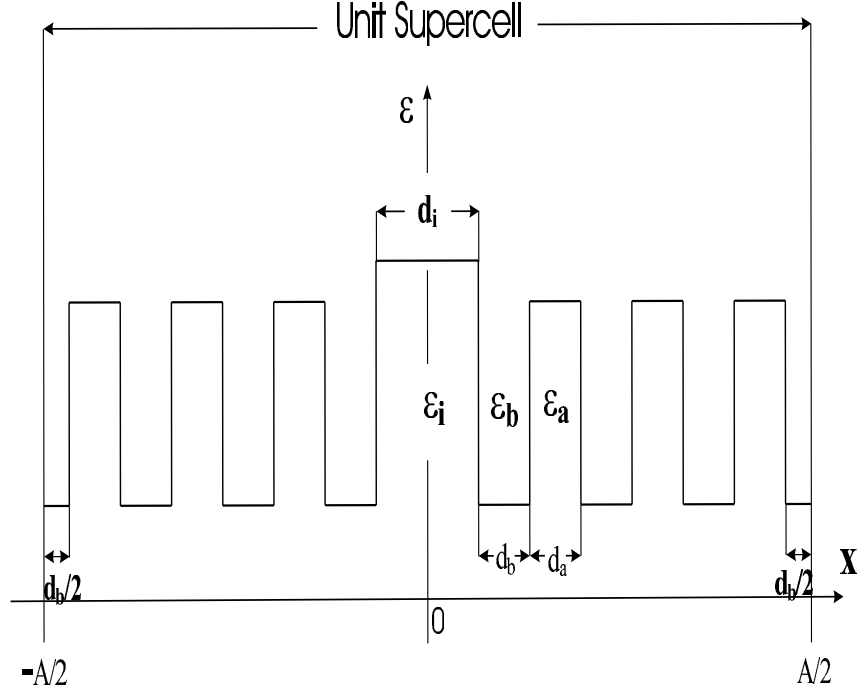


Figure 6.1: Illustration of Supercell, where ϵ_i dielectric constant of impurity layer, d_i thickness of impurity layer, ϵ_b dielectric constant of b type material, d_b thickness of b type material, ϵ_a dielectric constant of a type material, d_a thickness of a type material, n_{ϵ_a} number of epsilon of a type material, $a \equiv d_a + d_b$ lattice constant, A superlattice constant (Taken 2π).

Up to now now we have derived the general Fourier transform of $\epsilon(G)$ including both cosine and sine terms without any assumption. Now we are going to assume that ϵ_m has an even symmetry. That means, the complex part of the integral is zero and we have only cosine part as an integrant. As a result $\epsilon(G)$ depends only on sine function. According to figure 6.1 substituting the parameters and keeping it in mind, we are going to take Fourier transform of $\epsilon(G)$.

Starting point of derivation of $\epsilon(G)$ for a supercell structure is rewriting the general Fourier transform of $\epsilon(r)$.

$$\begin{aligned}
\epsilon(G) &= \frac{1}{V_{\text{cell}}} \int_{W_{\text{Scell}}} dr e^{-i \mathbf{G} \cdot \mathbf{r}} \epsilon(\mathbf{r}) \\
\epsilon(G) &= \frac{2}{V_{\text{cell}}} \left[\int_0^{d_i/2} \epsilon_i \cos(G x) dx + \sum_{m=1}^{n_{\epsilon_a}} \left\{ \epsilon_b \int_{d_i/2 + (m-1)(d_a+d_b)}^{d_i/2 + (m-1)(d_a+d_b) + d_b} \cos(G x) dx \right. \right. \\
&\quad \left. \left. + \epsilon_a \int_{d_i/2 + (m-1)(d_a+d_b) + d_b}^{d_i/2 + m(d_a+d_b)} \cos(G x) dx \right\} + \epsilon_b \int_{d_i/2 + n_{\epsilon_a}(d_a+d_b)}^{d_i/2 + n_{\epsilon_a}(d_a+d_b) + d_b/2} \cos(G x) dx \right] \\
&= \frac{2}{A} \left\{ \epsilon_i \left[\frac{\sin(G x)}{G} \right]_0^{d_i/2} + \sum_{m=1}^{n_{\epsilon_a}} \left(\epsilon_b \left[\frac{\sin(G x)}{G} \right]_{d_i/2 + (m-1)(d_a+d_b)}^{d_i/2 + (m-1)(d_a+d_b) + d_b} \right. \right. \\
&\quad \left. \left. + \epsilon_a \left[\frac{\sin(G x)}{G} \right]_{d_i/2 + (m-1)(d_a+d_b) + d_b}^{d_i/2 + m(d_a+d_b)} \right) + \epsilon_b \left[\frac{\sin(G x)}{G} \right]_{d_i/2 + n_{\epsilon_a}(d_a+d_b)}^{d_i/2 + n_{\epsilon_a}(d_a+d_b) + d_b/2} \right\}
\end{aligned}$$

$$\begin{aligned}
& + \epsilon_a \left[\frac{\sin(G x)}{G} \right]_{\frac{d_i}{2} + m(d_a + d_b)}^{\frac{d_i}{2} + m(d_a + d_b)} + \epsilon_b \left[\frac{\sin(G x)}{G} \right]_{\frac{d_i}{2} + n_{\epsilon_a}(d_a + d_b) + \frac{d_b}{2}}^{\frac{d_i}{2} + n_{\epsilon_a}(d_a + d_b) + \frac{d_b}{2}} \} \\
\epsilon(G) & = \frac{2}{A} \left\{ \epsilon_i \frac{\sin(G \frac{d_i}{2})}{G} + \sum_{m=1}^{n_{\epsilon_a}} \left\{ \epsilon_b \left[\frac{\sin(G(\frac{d_i}{2} + (m-1)(d_a + d_b) + d_b))}{G} \right. \right. \right. \\
& - \left. \left. \frac{\sin(G(\frac{d_i}{2} + (m-1)(d_a + d_b)))}{G} \right] + \epsilon_a \left[\frac{\sin(G(\frac{d_i}{2} + m(d_a + d_b)))}{G} \right. \right. \\
& - \left. \left. \frac{\sin(G(\frac{d_i}{2} + (m-1)(d_a + d_b) + d_b))}{G} \right] \right\} + \epsilon_b \left[\frac{\sin(G(\frac{d_i}{2} + n_{\epsilon_a}(d_a + d_b)) + \frac{d_b}{2})}{G} \right. \\
& \left. \left. - \frac{\sin(G(\frac{d_i}{2} + n_{\epsilon_a}(d_a + d_b)))}{G} \right] \right\}. \tag{6.1}
\end{aligned}$$

For simplification we define $x_1 = \frac{d_i}{2} + (m-1)(d_a + d_b) + d_b$ and $x_2 = \frac{d_i}{2} + n_{\epsilon_a}(d_a + d_b)$. Substituting these two new variables into the above equation and multiplying each side by the argument of sine functions yields:

$$\begin{aligned}
\epsilon(G) & = \frac{2}{A} \left\{ \epsilon_i \frac{d_i}{2} \frac{\sin(G \frac{d_i}{2})}{G \frac{d_i}{2}} + \sum_{m=1}^{n_{\epsilon_a}} \left\{ \epsilon_b \left[x_1 \frac{\sin(G x_1)}{G x_1} - (x_1 - d_b) \frac{\sin(G (x_1 - d_b))}{G (x_1 - d_b)} \right] \right. \right. \\
& + \left. \epsilon_a \left[(x_1 + d_a) \frac{\sin(G (x_1 + d_a))}{G (x_1 + d_a)} - x_1 \frac{\sin(G x_1)}{G} \right] \right\} + \epsilon_b \left[(x_2 + \frac{d_b}{2}) \frac{\sin(G (x_2 + \frac{d_b}{2}))}{G (x_2 + \frac{d_b}{2})} \right. \\
& \left. \left. - x_2 \frac{\sin(G x_2)}{G x_2} \right] \right\}. \tag{6.2}
\end{aligned}$$

The thickness values of each layer are given in units of $\frac{2\pi}{A}$. As mentioned before, the unit cell size A has a value of 2π .

$$\begin{aligned}
A & = 2 \left(\frac{d_i}{2} + n_{\epsilon_a} (d_a + d_b) + \frac{d_b}{2} \right) \\
\frac{d_i}{2} & = \frac{2\pi}{A} \frac{d_i}{2} \\
d_a & = \frac{2\pi}{A} d_a \\
d_b & = \frac{2\pi}{A} d_b
\end{aligned}$$

To obtain comparable results with the outputs of the 1-D photonic crystal, we normalize the frequency as $\omega = \frac{\omega}{2 n_{\epsilon_a} + 1}$

6.2 H Method in One-Dimensional Photonic Crystal Waveguide

If we have decided to solve one-dimensional photonic crystal by using H method we can follow different way for this method. We start on the left hand side of Eq. (2.61) for a given \mathbf{G}

$$(\mathbf{k} + \mathbf{G}') \times \eta(\mathbf{G}' - \mathbf{G})(\mathbf{k} + \mathbf{G}) \times \mathbf{H}(\mathbf{k} + \mathbf{G}) \tag{6.3}$$

At the beginning of our derivation , we have chosen $(\mathbf{k} + \mathbf{G}')$ as \mathbf{q} . Again using \mathbf{q} into matrix element ,we are going to obtain the matrix A. This is not the only way to calculate matrix elements but it is an easy way to do it.

$$\begin{aligned}\mathbf{q} &= (\mathbf{k} + \mathbf{G}) \\ \mathbf{q}' &= (\mathbf{k} + \mathbf{G}')\end{aligned}$$

From Eq. (6.3)

$$\mathbf{q}' \times \eta \mathbf{q} \times \mathbf{H} = \eta \mathbf{q}' \times \mathbf{q} \times \mathbf{H}. \quad (6.4)$$

Here \mathbf{q} , \mathbf{q}' , and \mathbf{H} have been chosen for one-dimensional photonic crystal waveguide as $\mathbf{q}' = G\mathbf{i} + k\mathbf{j}$, $\mathbf{q} = G'\mathbf{i} + k\mathbf{j}$, and $\mathbf{H} = H_x\mathbf{i} + H_y\mathbf{j} + H_z\mathbf{k}$. Using the appropriate vector identity

$$\mathbf{q}' \times \mathbf{q} \times \mathbf{H} = (\mathbf{q} \cdot \mathbf{q}')\mathbf{H} - (\mathbf{H} \cdot \mathbf{q}')\mathbf{q},$$

$$(\mathbf{q} \cdot \mathbf{q}')\mathbf{H} = (k^2 + GG')H_x\mathbf{i} + (k^2 + GG')H_y\mathbf{j} + (k^2 + GG')H_z\mathbf{k} \quad (6.5)$$

$$\begin{aligned}(\mathbf{H} \cdot \mathbf{q}')\mathbf{q} &= (G'H_x + kH_y)(k\mathbf{j} + G\mathbf{i}) \\ &= (G'H_x + kH_y)k\mathbf{j} + (G'H_x + kH_y)G\mathbf{i}.\end{aligned} \quad (6.6)$$

From Eq. (6.5) and Eq. (6.6)

$$\begin{aligned}\mathbf{q}' \times \mathbf{q} \times \mathbf{H} &= k^2H_x\mathbf{i} + GG'H_x\mathbf{i} + k^2H_y\mathbf{j} + GG'H_y\mathbf{j} + k^2H_z\mathbf{k} \\ &+ GG'H_z\mathbf{k} - kG'H_x\mathbf{j} - k^2H_y\mathbf{j} - GG'H_x\mathbf{i} - kGH_y\mathbf{i} \\ &= \mathbf{i}(k^2H_x - kGH_y) + \mathbf{j}(-kG'H_x + GG'H_y) \\ &+ \mathbf{k}(k^2 + GG')H_z.\end{aligned} \quad (6.7)$$

If we write this equation in matrix form

$$\mathbf{q}' \times \mathbf{q} \times \mathbf{H} = \begin{bmatrix} k^2 & -kG & 0 \\ -kG & GG' & 0 \\ 0 & 0 & (k^2 + GG') \end{bmatrix}. \quad (6.8)$$

Our eigenvalue problem is going to be

$$\eta \begin{bmatrix} k^2 & -kG & 0 \\ -kG & GG' & 0 \\ 0 & 0 & (k^2 + GG') \end{bmatrix} \begin{bmatrix} H_x \\ H_y \\ H_z \end{bmatrix} = \frac{\omega^2}{c^2} \begin{bmatrix} H_x \\ H_y \\ H_z \end{bmatrix}. \quad (6.9)$$

From Eq. (6.9), matrix A can be written for two reciprocal lattice vectors G_1 and G_2

$$A = \begin{bmatrix} k^2\eta_{11} & -kG_1\eta_{11} & 0 & k^2\eta_{12} & -kG_1\eta_{12} & 0 \\ -kG_1\eta_{11} & G_1^2 & 0 & -kG_2\eta_{12} & G_1G_2\eta_{12} & 0 \\ 0 & 0 & (k^2 + G_1^2)\eta_{11} & 0 & 0 & (k^2 + G_1G_2)\eta_{12} \\ k^2\eta_{21} & -kG_2\eta_{21} & 0 & k^2\eta_{22} & -kG_2\eta_{22} & 0 \\ -kG_2\eta_{21} & G_2G_1\eta_{21} & 0 & -kG_2\eta_{22} & G_2^2\eta_{22} & 0 \\ 0 & 0 & (k^2 + G_2G_1)\eta_{21} & 0 & 0 & (k^2 + G_2^2)\eta_{22} \end{bmatrix},$$

$$H = \begin{bmatrix} H_x(G_1) \\ H_y(G_1) \\ H_z(G_1) \\ H_x(G_2) \\ H_y(G_2) \\ H_z(G_2) \end{bmatrix}.$$

We can reduce this $3N \times 3N$ system into $2N \times 2N$ and $N \times N$ systems by doing some column and row operations. After solving $N \times N$ eigenvalue problem, we obtain information about dispersion relation of H_z and guided modes for a given system. Now we are going to apply column and row operations to our system step by step. Exchanging column $3 \leftrightarrow 4$ and row $3 \leftrightarrow 4$ in matrix A

$$\begin{bmatrix} k^2\eta_{11} & kG_1\eta_{11} & k^2\eta_{12} & 0 & -kG_1\eta_{12} & 0 \\ -kG_1\eta_{11} & G_1^2\eta_{11} & -kG_2\eta_{12} & 0 & G_1G_2\eta_{12} & 0 \\ k^2\eta_{21} & -kG_2\eta_{21} & k^2\eta_{22} & 0 & -kG_2\eta_{22} & 0 \\ 0 & 0 & 0 & (k^2 + G_1)\eta_{11} & 0 & (k^2 + G_1G_2)\eta_{12} \\ -kG_1\eta_{21} & G_2G_1\eta_{21} & -kG_2\eta_{22} & 0 & G_2^2\eta_{22} & 0 \\ 0 & 0 & 0 & (k^2 + G_2G_1)\eta_{21} & 0 & (k^2 + G_2^2)\eta_{22} \end{bmatrix}.$$

Exchanging column 4 \leftrightarrow 5 and row 4 \leftrightarrow 5

$$\begin{bmatrix} k^2\eta_{11} & -kG_1\eta_{11} & k^2\eta_{12} & -kG_1\eta_{12} & 0 & 0 \\ -kG_1\eta_{11} & G_1^2\eta_{11} & -kG_2\eta_{12} & G_1G_2\eta_{12} & 0 & 0 \\ k^2\eta_{21} & -kG_2\eta_{21} & k^2\eta_{22} & -kG_2\eta_{22} & 0 & 0 \\ -kG_1\eta_{21} & G_2G_1\eta_{21} & -kG_2\eta_{22} & G_2^2\eta_{22} & 0 & 0 \\ 0 & 0 & 0 & 0 & (k^2 + G_1^2)\eta_{11} & (k^2 + G_1G_2)\eta_{12} \\ 0 & 0 & 0 & 0 & (k^2 + G_2G_1)\eta_{21} & (k^2 + G_2^2)\eta_{22} \end{bmatrix}.$$

These operations show us that we have two different ordinary eigenvalue problems. As in the form

$$\begin{aligned} A_1 H_{xy} &= \lambda_1 H_{xy} \\ A_2 H_z &= \lambda_2 H_z. \end{aligned}$$

If we write the separated eigenvalue equations in matrix form

$$\begin{bmatrix} k^2\eta_{11} & -kG_1\eta_{11} & \eta_{12}k^2 & -kG_1\eta_{12} \\ -kG_1\eta_{11} & G_1^2\eta_{11} & -kG_2\eta_{12} & G_1G_2\eta_{12} \\ k^2\eta_{21} & -kG_2\eta_{21} & k^2\eta_{22} & -kG_2\eta_{12} \\ -kG_2\eta_{21} & G_2G_1\eta_{21} & -kG_2\eta_{22} & G_2^2\eta_{22} \end{bmatrix} \begin{bmatrix} H_x(G_1) \\ H_y(G_1) \\ H_x(G_2) \\ H_y(G_2) \end{bmatrix} = \lambda_1 \begin{bmatrix} H_x(G_1) \\ H_y(G_1) \\ H_x(G_2) \\ H_y(G_2) \end{bmatrix},$$

and

$$\begin{bmatrix} (k^2 + G_1^2)\eta_{11} & (k^2 + G_1G_2)\eta_{12} \\ (k^2 + G_2G_1)\eta_{21} & (k^2 + G_2^2)\eta_{22} \end{bmatrix} \begin{bmatrix} H_z(G_1) \\ H_z(G_2) \end{bmatrix} = \lambda_2 \begin{bmatrix} H_z(G_1) \\ H_z(G_2) \end{bmatrix}.$$

We are going to solve $N \times N$ eigenvalue problem as in the case of E-polarization. As an analogy we are going to use another notation in our calculations and results is B-polarization. Transverse electric (TE) and transverse magnetic (TM) polarization are equivalent to E-polarization and B-polarization. We will sometimes use TE and TM polarizations instead of E and B-polarizations.

6.3 1-D Photonic Crystal Waveguide

We are beginning this section by considering a photonic crystal waveguide as illustrated in Fig.(6.2). Guiding direction will be taken as the y axis, the time variation of the modes is of the form $e^{i\omega t}$, and β represents the propagation vector in the y direction. In this medium $\mu \equiv 1$ and ϵ is the dielectric constant of the dielectric structure and is a function of x .

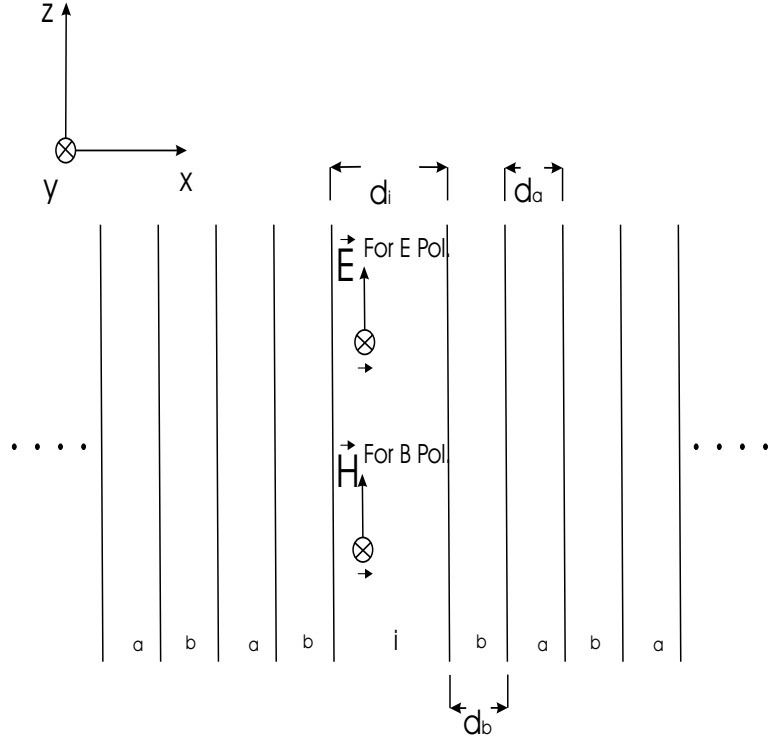


Figure 6.2: 1D Waveguide, where d_i thickness of impurity layer, $d_a \equiv$ thickness of a type material, $d_b \equiv$ thickness of b type material, $\epsilon_i \equiv$ dielectric constant of impurity layer, $\epsilon_a \equiv$ dielectric constant of a type material, $\epsilon_b \equiv$ dielectric constant of b type material and em waves moving in y direction.

$$\beta = \beta \mathbf{j}$$

Since the whole dielectric structure is homogeneous along the y axis, solutions to the wave equation can be taken as

$$\mathbf{E}(x, y, t) = \mathbf{E}(x) e^{i(\beta y - \omega t)} \quad (6.10)$$

$$\mathbf{B}(x, y, t) = \mathbf{B}(x) e^{i(\beta y - \omega t)}, \quad (6.11)$$

where $\mathbf{E}(x)$ and $\mathbf{B}(x)$ are

$$\mathbf{E}(x) = E_{x0}(x) \mathbf{i} + E_{y0}(x) \mathbf{j} + E_{z0}(x) \mathbf{k}$$

$$\mathbf{B}(x) = B_{x0}(x) \mathbf{i} + B_{y0}(x) \mathbf{j} + B_{z0}(x) \mathbf{k}$$

$$\mathbf{E}(x, y, t) = [E_{x0}(x) \mathbf{i} + E_{y0}(x) \mathbf{j} + E_{z0}(x) \mathbf{k}] e^{i(\beta y - \omega t)} \quad (6.12)$$

$$\mathbf{B}(x, y, t) = [B_{x0}(x) \mathbf{i} + B_{y0}(x) \mathbf{j} + B_{z0}(x) \mathbf{k}] e^{i(\beta y - \omega t)}. \quad (6.13)$$

Maxwell's equations ;

$$\nabla \cdot \mathbf{D} = 0 \quad (6.14)$$

$$\nabla \cdot \mathbf{B} = 0 \quad (6.15)$$

$$\nabla \times \mathbf{E} = -\frac{1}{c} \frac{\partial \mathbf{B}}{\partial t} \quad (6.16)$$

$$\nabla \times \mathbf{H} = \frac{1}{c} \frac{\partial \mathbf{D}}{\partial t} \quad (6.17)$$

From Eq. (6.14) we obtain

$$\nabla \cdot (\epsilon(x) \mathbf{E}(\mathbf{x})) = 0$$

or similarly

$$\frac{\partial(\epsilon(x) E_{x0})}{\partial x} + \frac{\partial(\epsilon(x) E_{y0})}{\partial y} + \frac{\partial(\epsilon(x) E_{z0})}{\partial z} = 0.$$

Since ϵ is not a function of y and z , we can take ϵ outside of derivatives with respect to the y and z .

$$\frac{\partial(\epsilon(x) E_{x0})}{\partial x} + \epsilon(x) \frac{\partial E_{y0}}{\partial y} + \epsilon(x) \frac{\partial E_{z0}}{\partial z} = 0$$

From Eq. (6.15) we obtain

$$\frac{\partial B_{x0}}{\partial x} + \frac{\partial B_{y0}}{\partial y} + \frac{\partial B_{z0}}{\partial z} = 0 \quad (6.18)$$

From Eq. (6.16) ;

$$\begin{aligned} \nabla \times \mathbf{E} &= \begin{vmatrix} \mathbf{i} & \mathbf{j} & \mathbf{k} \\ \partial_x & \partial_y & \partial_z \\ E_x(x, y) & E_y(x, y) & E_z(x, y) \end{vmatrix} \\ &= \mathbf{i} [\partial_y(E_{z0}(x) e^{i(\beta y - \omega t)}) - \partial_z(E_{y0}(x) e^{i(\beta y - \omega t)})] \\ &\quad - \mathbf{j} [\partial_x(E_{z0}(x) e^{i(\beta y - \omega t)}) - \partial_z(E_{x0}(x) e^{i(\beta y - \omega t)})] \\ &\quad + \mathbf{k} [\partial_x(E_{y0}(x) e^{i(\beta y - \omega t)}) - \partial_y(E_{x0}(x) e^{i(\beta y - \omega t)})] \\ &= \mathbf{i} (i\beta E_{z0}(x) e^{i(\beta y - \omega t)} - 0) \\ &\quad - \mathbf{j} (E'_{z0}(x) e^{i(\beta y - \omega t)} - 0) \\ &\quad + \mathbf{k} (E'_{y0}(x) e^{i(\beta y - \omega t)} - i\beta E_{x0}(x) e^{i(\beta y - \omega t)}) \end{aligned} \quad (6.19)$$

$$\begin{aligned} &- \frac{\partial \mathbf{B}(x, y)}{\partial t} = i\omega \mathbf{B}(x, y) \\ &= i\omega (B_{x0}(x) \mathbf{i} + B_{y0}(x) \mathbf{j} + B_{z0}(x) \mathbf{k}) e^{i(\beta y - \omega t)} \end{aligned} \quad (6.20)$$

From Eq. (6.17) ;

$$\nabla \times \mathbf{B} = \epsilon \frac{\partial \mathbf{E}}{\partial t} \quad (6.21)$$

$$\begin{aligned} \nabla \times \mathbf{B} &= \begin{vmatrix} \mathbf{i} & \mathbf{j} & \mathbf{k} \\ \partial_x & \partial_y & \partial_z \\ B_x(x, y) & B_y(x, y) & B_z(x, y) \end{vmatrix} \\ &= \mathbf{i} [\partial_y(B_{z0}(x) e^{i(\beta y - \omega t)}) - \partial_z(B_{y0}(x) e^{i(\beta y - \omega t)})] \\ &\quad - \mathbf{j} [\partial_x(B_{z0}(x) e^{i(\beta y - \omega t)}) - \partial_z(B_{x0}(x) e^{i(\beta y - \omega t)})] \\ &\quad + \mathbf{k} [\partial_x(B_{y0}(x) e^{i(\beta y - \omega t)}) - \partial_y(B_{x0}(x) e^{i(\beta y - \omega t)})] \\ &= \mathbf{i} (i\beta B_{z0}(x) e^{i(\beta y - \omega t)} - 0) \\ &\quad - \mathbf{j} (B'_{z0}(x) e^{i(\beta y - \omega t)} - 0) \\ &\quad + \mathbf{k} (B'_{y0}(x) e^{i(\beta y - \omega t)} - i\beta B_{x0}(x) e^{i(\beta y - \omega t)}) \end{aligned} \quad (6.22)$$

$$\begin{aligned} \frac{\partial(\epsilon(x)\mathbf{E}(x, y))}{\partial t} &= \epsilon(x)(-i\omega)\mathbf{E}(x, y) \\ &= -i\omega(E_{x0}\mathbf{i} + E_{y0}\mathbf{j} + E_{z0}\mathbf{k}) \end{aligned} \quad (6.23)$$

where $E_m(x, y)$ and $B_m(x, y)$ denote $E_{m0}(x) e^{i(\beta y - \omega t)}$ and $B_{m0}(x) e^{i(\beta y - \omega t)}$ respectively and $m \equiv x, y, z$.

In Eq. (6.16) and Eq. (6.17) comparing both left and right sides we obtain;

$$\beta E_{z0} = \omega B_{x0} \quad (6.24)$$

$$E'_{z0} = -i\omega B_{y0} \quad (6.25)$$

$$E'_{y0} = i\beta E_{x0} + i\omega B_{z0} \quad (6.26)$$

$$\beta B_{z0} = -\omega\epsilon E_{x0} \quad (6.27)$$

$$B'_{z0} = i\omega\epsilon E_{y0} \quad (6.28)$$

$$B'_{y0} = i\beta B_{x0} - i\omega\epsilon E_{z0} \quad (6.29)$$

If we rewrite the above equations in terms of E_{z0} and B_{z0} after obtaining E_{z0} and B_{z0} we can find other components of electric and magnetic fields,

$$B_{x0} = \frac{\beta}{\omega} E_{z0} \quad (6.30)$$

$$B_{y0} = \frac{1}{-i\omega} E'_{z0} \quad (6.31)$$

$$E_{x0} = \frac{-\beta}{\omega\epsilon} B_{z0} \quad (6.32)$$

$$E_{y0} = \frac{1}{i\omega\epsilon} B'_{z0} \quad (6.33)$$

Now we are going to rewrite the electric and magnetic field components in terms of E_{z0} and B_{z0} using the equations above.

6.3.1 Solution of One-dimensional Photonic Crystal Waveguide for E-polarization

If we set $B_{z0} \equiv 0$ we have only E_{z0} component of electric field and the solution of the wave equation gives only E_{z0} . If we know E_{z0} we can find B_{x0} and B_{y0} components of the magnetic field. In this case we have E polarized waves or transverse electric modes (TE). We are going to first derive the wave equation of electric field in real space, next take the Fourier transform of it and then obtain ordinary eigenvalue equation of electric field in reciprocal lattice space. From Eq. (6.25) and Eq. (6.28)

$$B_{y0} = -\frac{E'_{z0}}{i\omega} \quad (6.34)$$

$$E_{y0} = -\frac{B'_{z0}}{i\omega\epsilon}. \quad (6.35)$$

Taking derivative of Eq. (6.34) with respect to x ;

$$B'_{y0} = \frac{iE''_{z0}}{\omega}. \quad (6.36)$$

From Eq. (6.29)

$$\begin{aligned} i\beta B_{x0} - i\omega\epsilon E_{z0} &= \frac{iE''_{z0}}{\omega} \\ \beta\omega B_{x0} - \omega^2\epsilon E_{z0} &= E''_{z0} \end{aligned} \quad (6.37)$$

Substituting B_{x0} into equation Eq. (6.37)

$$\begin{aligned} \beta\omega\frac{\beta}{\omega}E_{z0} - \omega^2\epsilon E_{z0} &= E''_{z0} \\ E''_{z0} + (\omega^2\epsilon - \beta^2)E_{z0} &= 0 \\ E''_{z0} - \beta^2 E_{z0} &= -\omega^2\epsilon E_{z0}. \end{aligned} \quad (6.38)$$

We know that $\epsilon(x)$ is periodic and we can represent $\epsilon(x)$ as a summation over reciprocal lattice vectors G and $E_{z0}(x)$ as follows :

$$\begin{aligned} \epsilon(x) &= \sum_G \epsilon(G) e^{iGx} \\ E_{z0}(x) &= \sum_G E_{z0}(G) e^{iGx} \end{aligned}$$

Taking second derivative of $E_{z0}(x)$ with respect to x then,

$$E''_{z0}(x) = - \sum_G G E_{z0}(G) e^{iGx}, \quad (6.39)$$

and plugging $\epsilon(x)$ and $E''_{z0}(x)$ into Eq. (6.38) then

$$\begin{aligned} - \sum_G G^2 E_{z0}(G) e^{iGx} - \beta^2 \sum_G E_{z0}(G) e^{iGx} &= -\omega^2 \sum_G \epsilon(G) e^{iGx} \sum_{G'} E_{z0}(G') e^{iG'x} \\ \sum_G (\beta^2 + G^2) E_{z0}(G) e^{iGx} &= \omega^2 \sum_G \sum_{G'} \epsilon(G) e^{iGx} E_{z0}(G') e^{iG'x} \\ \sum_G (\beta^2 + G^2) E_{z0}(G) e^{iGx} &= \omega^2 \sum_G \sum_{G'} \epsilon(G) E_{z0}(G') e^{i(G'+G)x}. \end{aligned}$$

Changing indices as $G' + G \equiv G''$ and $G \equiv G'' - G'$ on the right hand side then

$$\sum_G (\beta^2 + G^2) E_{z0}(G) e^{iGx} = \omega^2 \sum_{G''} \sum_G \epsilon(G'' - G') E_{z0}(G') e^{iG''x} \quad (6.40)$$

Then defining $G'' \equiv G'$ and $G' \equiv G$

$$\sum_G (\beta^2 + G^2) E_{z0}(G) e^{iGx} = \omega^2 \sum_{G'} \sum_G \epsilon(G' - G) E_{z0}(G) e^{iG'x} \quad (6.41)$$

Following this equation we can obtain matrix equation for a given G as

$$(\beta^2 + G^2) E_{z0}(G) = \omega^2 \epsilon(G' - G) E_{z0}(G'). \quad (6.42)$$

This equation is generalized eigenvalue problem for E-polarization as in the form of $AX = \lambda BX$. We can reduce this generalized equation in ordinary eigenvalue equation because we do not want to store two different matrices. In the ordinary eigenvalue problem we should only have one matrix and therefore we can reach results in shorter time than the generalized case. Now we are going to reduce generalized problem multiplying both sides of Eq. (6.3.1) by $\epsilon^{-1}(G' - G)$, from the left then

$$\epsilon^{-1}(G' - G) (\beta^2 + G^2) E_{z0}(G) = \omega^2 E_{z0}(G) \quad (6.43)$$

In this case we have $A'X = \lambda X$ where $A_{G',G} \equiv \epsilon^{-1}(G' - G) (\beta^2 + G^2)$ and $X_G \equiv E_{z0}(G)$.

Solving this ordinary eigenvalue equation we are going to obtain solution of one-dimensional photonic crystal waveguide for E-polarization.

6.3.2 Solution of One-dimensional Photonic Crystal Waveguide for B-polarization

If we set $E_{z0} \equiv 0$ we have only B_{z0} component of magnetic field and wave equation of the magnetic field. This case is known as B-polarization or transverse magnetic (TM). The solution of the wave equation gives us B_{z0} and using it we can find E_{x0} and E_{y0} . In order to find B polarized solutions of the wave equation we write the wave equation of magnetic field and following the same procedure as in the case of E-polarization we can obtain eigenvalue equation. First of all we are going to derive wave equation in real space. Now we are going to rewrite Eq. (6.35) by setting $\eta(x) \equiv \epsilon^{-1}(x)$ in order to simplify our calculations.

$$E_{y0} = -\frac{\eta(x)B'_{z0}}{i\omega} \quad (6.44)$$

We want to find and solve second order differential equation with respect to B_{z0} . In order to derive the equation, we are going to take the derivative of equation Eq. (6.44).

$$E'_{y0} = \frac{1}{i\omega} (\eta' B'_{z0} + \eta B''_{z0}) \quad (6.45)$$

Substituting Eq. (6.26)

$$\begin{aligned} i\beta E_{x0}(x) + i\omega B_{z0}(x) &= \frac{1}{i\omega} (\eta'(x) B'_{z0}(x) + \eta(x) B''_{z0}(x)) \\ -\beta\omega E_{x0}(x) + -\omega^2 B_{z0}(x) &= \eta'(x) B'_{z0}(x) + \eta(x) B''_{z0}(x) \\ -\beta\omega \frac{\beta\eta(x)}{(-\omega)} B_{z0}(x) + -\omega^2 B_{z0}(x) &= \eta'(x) B'_{z0}(x) + \eta(x) B''_{z0}(x) \\ \beta^2 \eta(x) B_{z0}(x) + -\omega^2 B_{z0}(x) &= \eta'(x) B'_{z0}(x) + \eta(x) B''_{z0}(x). \end{aligned} \quad (6.46)$$

$$\eta(x) B''_{z0}(x) + \eta'(x) B'_{z0}(x) + (\omega^2 - \beta^2\eta(x)) B_{z0}(x) = 0 \quad (6.47)$$

Equation Eq. (6.47) can be written in the form

$$(\eta(x) B'_{z0}(x))' + \left(\frac{\omega^2}{c^2} - \beta^2 \eta(x)\right) B_{z0}(x) = 0. \quad (6.48)$$

Since $\eta(x)$ is periodic it can be represented as a summation over reciprocal lattice vectors G .

$$\eta(x) = \sum_G \eta(G) e^{iGx} \quad (6.49)$$

$$\begin{aligned}
B_{z0}(x) &= \int_{-\infty}^{\infty} dq B_{z0}(q) e^{iqx} \\
&= \int_{\text{BZ}} dk B_{z0}(k+G) e^{ikx} e^{iGx} \\
&= \int_{\text{BZ}} dk e^{ikx} \left[\sum_G B_{z0}(G) e^{iGx} \right] \tag{6.50}
\end{aligned}$$

In our calculations we can use two different ways for obtaining $B_{z0}(x)$ in supercell method. First one is taking different k values and for each value taking G values, second one is taking $k = 0$ and different G values for this k value. In the second method, for instance if we define our superlattice size as $A100a$ in terms of lattice constant we have reciprocal lattice vector as $G = \frac{2\pi}{A}n = \frac{2\pi}{a} \frac{n}{100}$. That means we have divided our reciprocal lattice vector in 100 pieces and we have 100 different lattice vectors. The second method brings us scanning reciprocal lattice space with small lattice vectors for $k = 0$. That is why we can write $B_{z0}(x)$ as

$$B_{z0}(x) = \sum_G B_{z0}(G) e^{iGx}.$$

Taking derivative of $B_{z0}(x)$ with respect to x and then multiplying by $\eta(x)$ we obtain

$$\begin{aligned}
B'_{z0}(x) &= \sum_G iG B_{z0}(G) e^{iGx} \\
\eta(x) B'_{z0}(x) &= \sum_G \eta(G) e^{iGx} \sum_{G'} iG' B_{z0}(G') e^{iG'x} \\
&= \sum_G \sum_{G'} iG' \eta(G) B_{z0}(G') e^{i(G'+G)x}.
\end{aligned}$$

Changing the summation indices as $G + G' = G''$ and $G = G'' - G'$ then

$$\begin{aligned}
\eta(x) B'_{z0}(x) &= \sum_{G''} \sum_{G'} \eta(G'' - G') e^{iG''x} \sum_{G'} iG' B_{z0}(G') \\
&= \sum_{G''} \sum_{G'} \eta(G'' - G') iG' B_{z0}(G') e^{iG''x}
\end{aligned}$$

$$(\eta(x) B'_{z0}(x))' = \sum_{G''} \sum_{G'} \eta(G'' - G') iG'' iG' B_{z0}(G') e^{iG''x}$$

Substituting the above equation into equation Eq. (6.48)

$$-\sum_{G''} \sum_{G'} \eta(G'' - G') G' G'' B_{z0}(G') e^{iG''x} + \left(\frac{\omega^2}{c^2} - \beta^2 \sum_G \eta(G) e^{iGx} \right) \sum_{G'} B_{z0}(G') e^{iG'x} = 0$$

Using the same procedure for ηB_{z0} term as in the case of $\eta B'_{z0}$,

$$\begin{aligned}
& - \sum_{G''} \sum_{G'} \eta(G'' - G') G' G'' B_{z0}(G') e^{iG''x} + \frac{\omega^2}{c^2} \sum_{G'} B_{z0}(G') e^{iG'x} \\
& \quad - \beta^2 \sum_{G'',G'} \eta(G'' - G') B_{z0}(G') e^{iG''x} = 0 \\
& \sum_{G''} \sum_{G'} \eta(G'' - G') (\beta^2 + G' G'') B_{z0}(G') e^{iG''x} = \frac{\omega^2}{c^2} \sum_{G'} B_{z0}(G') e^{iG'x}. \quad (6.51)
\end{aligned}$$

Again changing indices as $G'' \equiv G'$ and $G' \equiv G$

$$\begin{aligned}
& \sum_{G'} \sum_G \eta(G' - G) (\beta^2 + GG') B_{z0}(G) e^{iG'x} = \frac{\omega^2}{c^2} \sum_{G'} B_{z0}(G') e^{iG'x} \\
& \sum_{G'} e^{iG'x} \left\{ \sum_G \eta(G' - G) (\beta^2 + GG') B_{z0}(G) - \frac{\omega^2}{c^2} B_{z0}(G') \right\} = 0 \quad (6.52)
\end{aligned}$$

If this equation is equal to zero, the part which is in the parenthesis must be equal to zero. From this equality,

$$\sum_G \eta(G' - G) (\beta^2 + GG') B_{z0}(G) = \frac{\omega^2}{c^2} B_{z0}(G') \quad (6.53)$$

We have reduced our second order differential equation into eigenvalue problem as;

$AX = \lambda X$ (Ordinary Eigenvalue problem)

Where matrix element A , B_{z0} , and λ are

$A_{G',G} \equiv \eta(G' - G) (\beta^2 + GG')$, $B_{z0} \equiv X$ and $\lambda = \frac{\omega^2}{c^2}$.

6.4 Results and Discussion on 1-D Photonic Crystal Waveguide

6.4.1 Analytical Solution of Single Slab Symmetric Waveguide

In this section the analytical solution of the single slab symmetric waveguide will be compared with the numerical solutions. We have done this comparison because we would like to be sure about our method and calculations. The analytical solutions are obtained from [22] and [23]. Some of the procedures, mathematical operations, and figure of single slab symmetric waveguide are given below .

Maxwell's equations can be written in the form

$$\nabla \times \mathbf{E} = -i \omega \mu \mathbf{H} \quad (6.54)$$

$$\nabla \times \mathbf{H} = i \omega \epsilon_0 n^2 \mathbf{E} \quad (6.55)$$

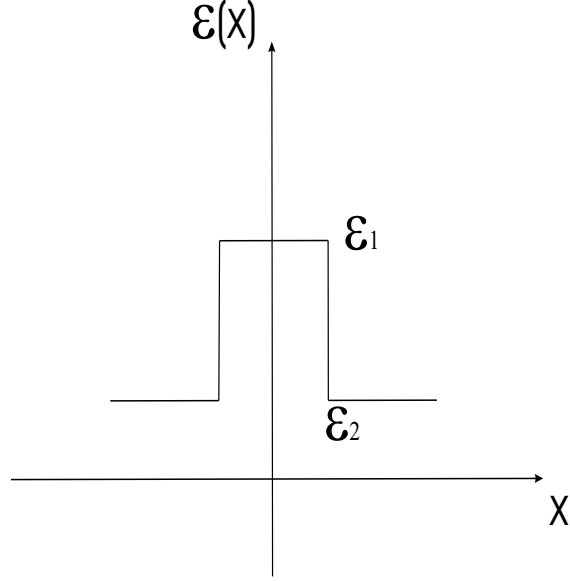


Figure 6.3: Figure of Single Slab Symmetric Waveguide, where $\epsilon_1 \equiv$ dielectric constant of guiding layer, $\epsilon_2 \equiv$ dielectric constant of outside.

Since the whole structure is homogeneous along the z axis, solutions to the wave equations Eq. (6.54) and Eq. (6.55) can be taken as;

$$\mathbf{E}(x, t) = \mathbf{E}_m(x) e^{i(\omega t - \beta z)} \quad (6.56)$$

$$\mathbf{H}(x, t) = \mathbf{H}_m(x) e^{i(\omega t - \beta z)} \quad (6.57)$$

The wave equation can be obtained by eliminating \mathbf{H} from Eq. (6.55):

$$\left[\frac{d^2}{dx^2} + \left(\frac{\omega}{c} n \right)^2 - \beta^2 \right] \mathbf{E}_m(x) = 0. \quad (6.58)$$

The electric field amplitude of the guided \mathbf{E} polarized modes can be written in the form

$$E_y(x, z, t) = E_m(x) e^{i(\omega t - \beta z)}. \quad (6.59)$$

The mode function $E_m(x)$ is taken as

$$E_m(x) = \begin{cases} A \sin hx + B \cos hx, & |x| < \frac{1}{2}d, \\ C e^{-qx}, & \frac{1}{2}d < x, \\ D e^{qx}, & x < -\frac{1}{2}d, \end{cases} \quad (6.60)$$

where A , B , C , and D are constants, and parameters h and q are related to the propagation constant by

$$h = \left[\left(\frac{n_2 \omega}{c} \right)^2 - \beta^2 \right]^{1/2}, \quad (6.61)$$

$$q = \left[\beta^2 - \left(\frac{n_1 \omega}{c} \right)^2 \right]^{1/2}. \quad (6.62)$$

The parameter h may be considered as the transverse component of the wave vector in the guiding layer. To have acceptable solutions, the tangential component of the electric and magnetic fields E_y , H_z must be continuous at the interfaces. After some mathematical operations, the solutions of E polarized modes may be divided into two classes: for the first class (for even solutions)

$$A = 0, \quad C = D, \quad h \tan \left(\frac{1}{2} h d \right) = q, \quad (6.63)$$

and for the second class (for odd solutions)

$$B = 0, \quad C = -D, \quad h \cot \left(\frac{1}{2} h d \right) = -q. \quad (6.64)$$

The continuity of H_y and E_z at the two interfaces $x = \pm \frac{1}{2}$ leads to the solutions of B polarized modes that may be divided into two groups as even and odd solutions respectively

$$h \tan \left(\frac{1}{2} h d \right) = \frac{n_2^2}{n_1^2} q, \quad (6.65)$$

$$h \cot \left(\frac{1}{2} h d \right) = -\frac{n_2^2}{n_1^2} q. \quad (6.66)$$

We have taken both E and B polarized solutions of single slab symmetric waveguide and written a small program for analytical solutions. After giving the parameters of the medium which we want to solve, we have sketched the frequency versus propagation constant graph. At the same time for the same physical medium we have obtained the same graph as a result of our photonic crystal waveguide program.

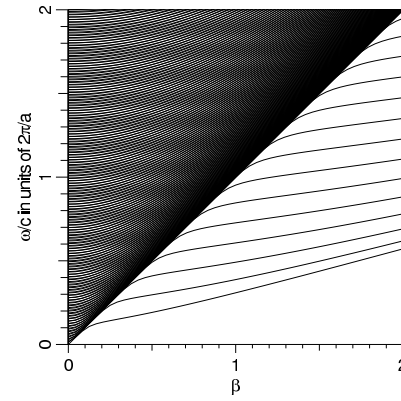
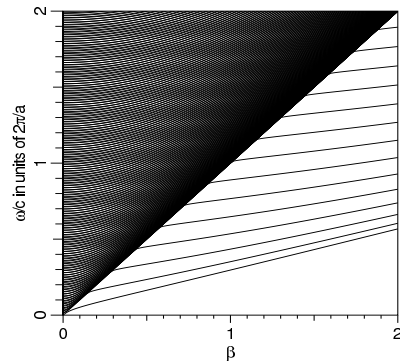
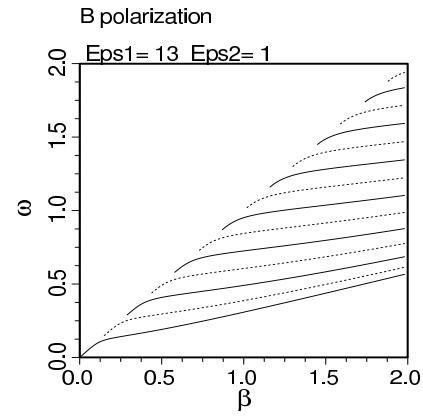
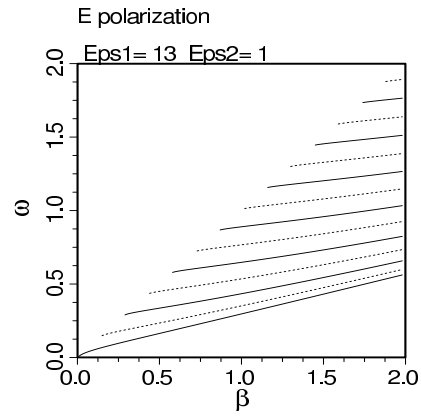


Figure 6.4: Exact and Numerical Solution of Single Slab Symmetric Waveguide for $\epsilon_1 = 13$, $\epsilon_2 = 1$, $d_1 = 0.1$, $d_2 = 0.05$ for E Polarization and B Polarization. Straight and dashed lines denote even and odd modes respectively.

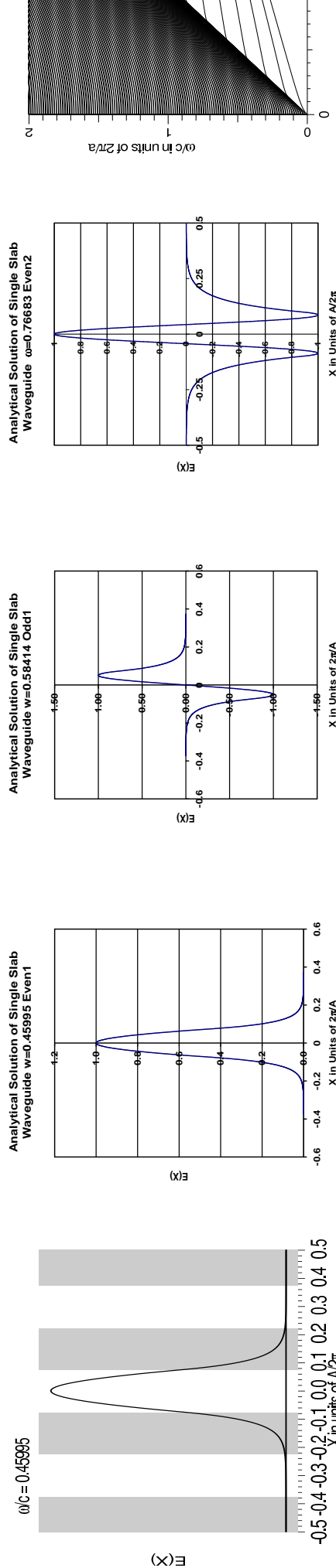
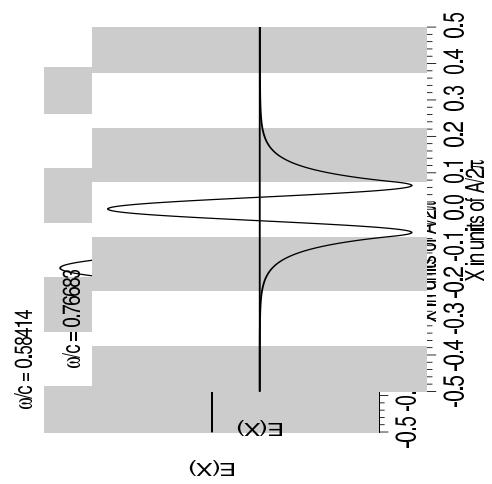


Figure 6.5: Exact and Numerical Solution and Band Structure of Single Slab Symmetric Waveguide for $\epsilon_1 = 13$, $\epsilon_2 = 1$, $d_1 = 0.1$, $d_2 = 0.05$ for E Polarization. First even, first odd, and second even modes are given.



For exact solution of single slab symmetric waveguide, modes are calculated for dielectric constant of guiding layer $\epsilon_1 = 13$ and dielectric constant of outside region $\epsilon_2 = 1$. Numerical solutions of single slab symmetric waveguide is obtained for dielectric constant of guiding (impurity) layer $\epsilon_i = 13$, dielectric constants of outside region $\epsilon_a = 1$ and $\epsilon_b = 1$ by using supercell method and 10000 plane-waves are taken. In Fig. (6.4), straight and dashed lines are denoted respectively even and odd solutions of single slab symmetric waveguide. When we compare these two solutions for E-polarization we can easily see that the guided modes exactly match with each other. In Fig. (6.5), the region where there is no guidance is keeping radiation modes inside. In this region the modes can have a phase velocity that is greater than the speed of light and the boundary of this region is known as a light cone. If the phase velocity of modes is less than the slope of this line the modes can be guided modes and the phase velocity of these modes is less than the speed of light. For B-polarization, the solutions of single slab symmetric waveguide is

For exact solution of single slab symmetric waveguide, modes are calculated for dielectric constant of guiding layer $\epsilon_1 = 13$ and dielectric constant of outside region $\epsilon_2 = 1$. Numerical solutions of single slab symmetric waveguide is obtained for dielectric constant of guiding (impurity) layer $\epsilon_i = 13$, dielectric constants of outside region $\epsilon_a = 1$ and $\epsilon_b = 1$ by using supercell method and 10000 plane-waves are taken. In Fig. (6.4), straight and dashed lines are denoted respectively even and odd solutions of single slab symmetric waveguide. When we compare these two solutions for B-polarization we can easily see that the guided modes exactly match with each other. The concept about phase velocity which we have mentioned that in the E polarized solutions is valid for B polarized solutions.

When we look at the electric fields of analytical and numerical solutions of single slab symmetric waveguide for making comparison between them we have seen that the modes are matched. This calculations are performed for $\beta = 1.57$. In Fig. (6.5), we have seen that frequencies of the first even, first odd, and second even modes are 0.45995, 0.58414, and 0.76683 respectively.

6.4.2 1-D Photonic Crystal Waveguide

Light propagation in photonic crystal waveguide is a topic under intense investigation. It is expected that the control of photons in photonic crystal structure can be realized by introducing artificial defects that have the way for

propagating modes confined within the defect. Because of that reason we have constituted impurity into our structures by using supercell method. This impurity can be constituted by using two ways. One of them depends on changing the dielectric constant and the other depends on changing the thickness of impurity layer. In our calculations we use both of them. Now we will show two dispersion diagrams for periodic structure and the structure with defect.

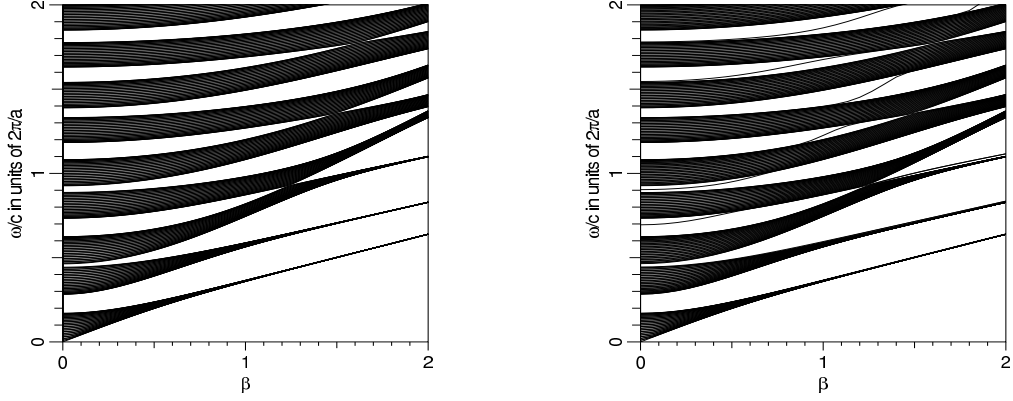
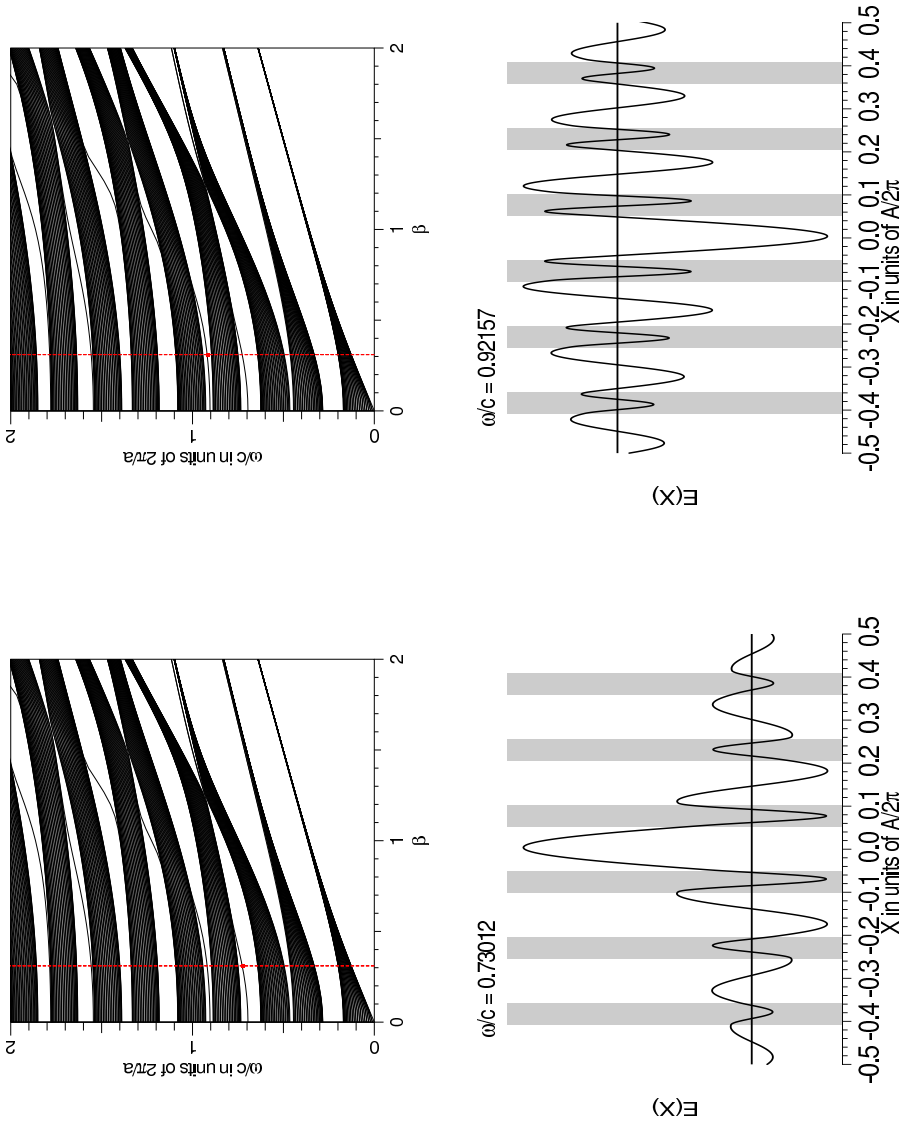


Figure 6.6: Perfect Periodic Structure for $\epsilon_a = 2.43$, $\epsilon_b = 12.25$, $\epsilon_i = 2.43$, $d_a : d_b = 1 : 2$, $d_i = d_a$, $\beta = 0.32786$ and Structure with defect for $\epsilon_a = 2.43$, $\epsilon_b = 12.25$, $\epsilon_i = 1$, $d_a : d_b = 1 : 2$, $d_i \equiv \frac{2}{3}(d_a + d_b)$, $\beta = 0.32786$ for E-Polarization.

Here is the first even and odd modes of Fig. (6.6). Both even and odd modes have fluctuations outside the impurity layer and these modes are not perfectly localized modes. The phase velocity of these modes is greater than the speed of light.

Figure 6.7: Comparison of guided modes for $\epsilon_a = 2.43$, $\epsilon_b = 12.25$, $\epsilon_i = 1$, $d_a : d_b = 1 : 2$, $d_i \equiv \frac{2}{3}(d_a + d_b)$, $\beta = 0.32786$.



In the dispersion relation of perfect periodic structure that we have given in Fig. (6.6) the medium parameters are $\epsilon_i = 2.43$, $\epsilon_a = 2.43$, $\epsilon_b = 12.25$ for periodic structure and for structure with defect parameters are $\epsilon_i = 1$, $\epsilon_a = 2.43$, $\epsilon_b = 12.25$. From the parameters we can easily see that the impurity is constituted by changing the ϵ_i . Because of this defect we obtained the modes that is different from the modes from Fig. (6.6). When we investigate these modes we find out that these are guided modes and that means we have photonic crystal waveguide.

In order to check our results with the literature we have obtained band diagram of one-dimensional photonic crystal waveguide structure with different parameters and compared our guided modes with [25]. In Fig. (6.8) we have seen that five guided modes are matched for E-polarization but the other modes do not match. We think the way what we have used is different from this paper or they could not catch these guided modes.

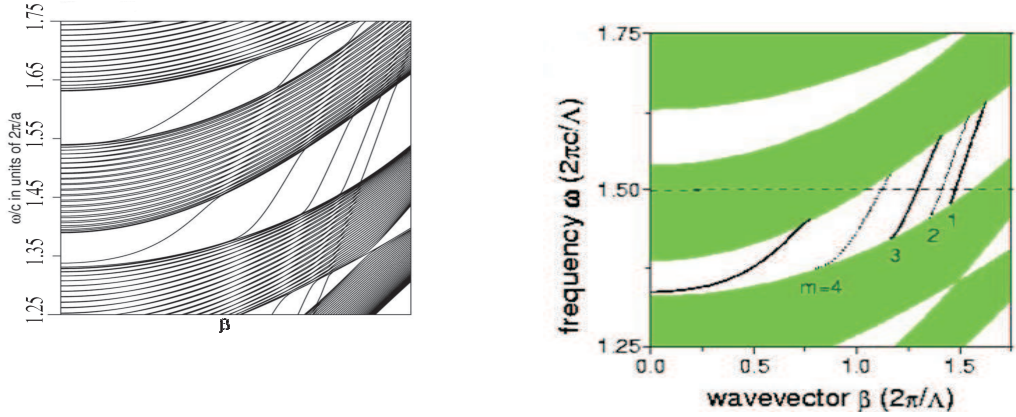


Figure 6.8: Comparison of guided modes [25] for $\epsilon_a = 2.43$, $\epsilon_b = 12.25$, $\epsilon_i = 1$, $d_a : d_b = 1 : 2$, $d_i = \frac{2}{3}(d_a + d_b)$.

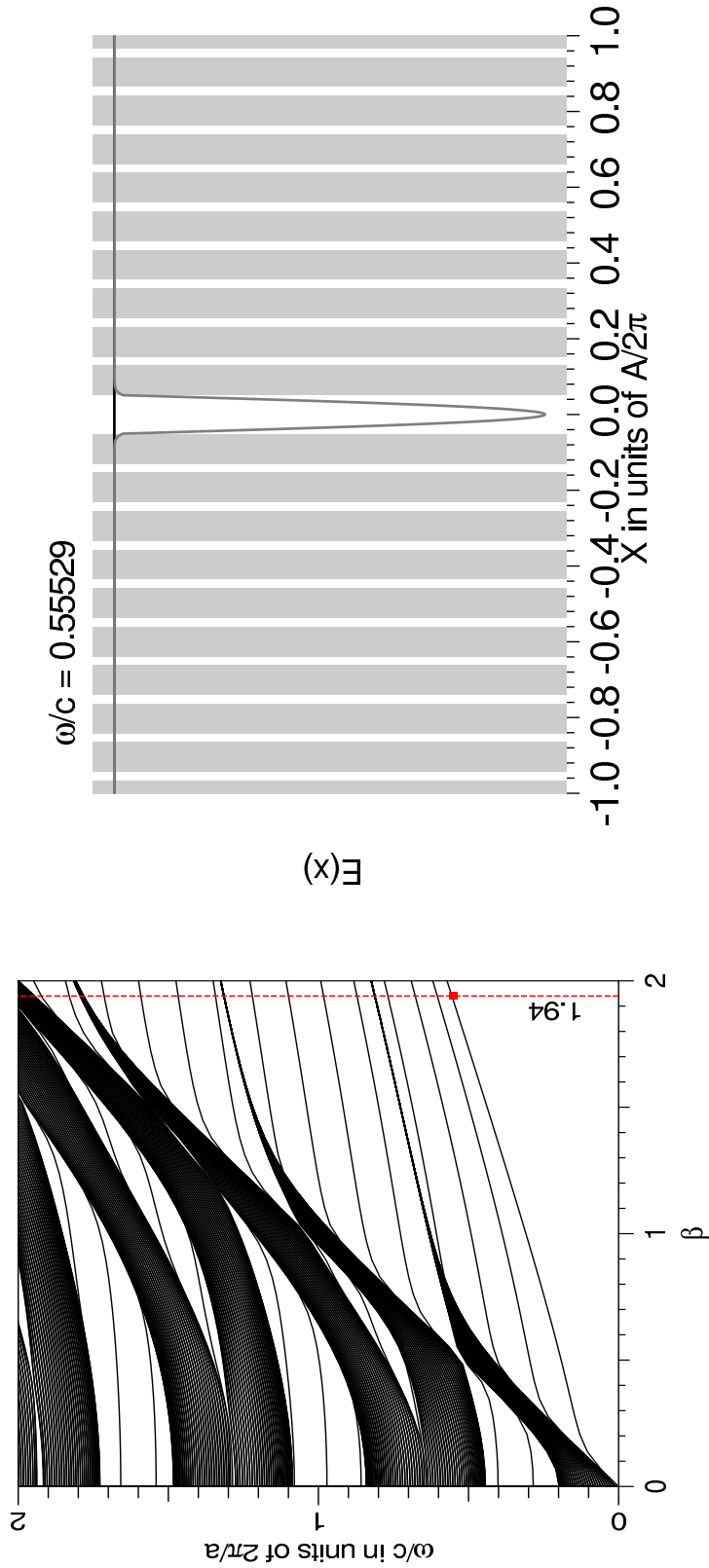


Figure 6.9: Dispersion relation and $E(x)$ vs x graph of 1st even mode for $\epsilon_a = 13$, $\epsilon_b = 1$, $\epsilon_i = 13$, $d_a = 0.02$, $d_b = 0.08$, $d_i = 0.1$ (B-polarization).

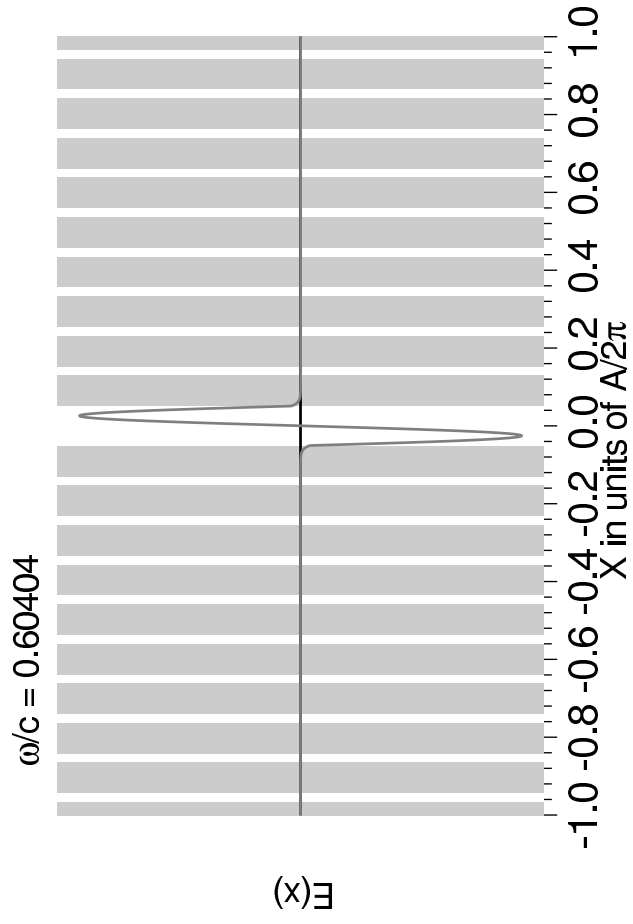
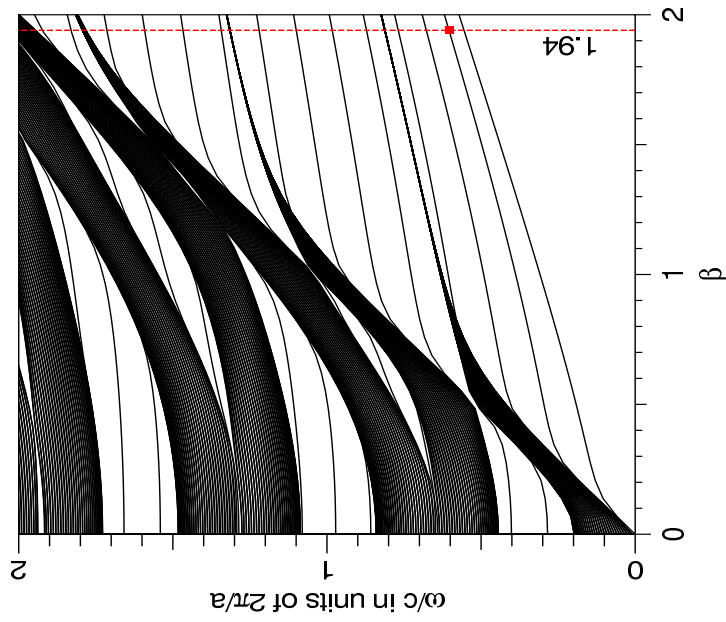


Figure 6.10: Dispersion relation and $E(x)$ vs x graph of 1st odd mode for $\epsilon_a = 13$, $\epsilon_b = 1$, $\epsilon_i = 13$, $d_a = 0.02$, $d_b = 0.08$, $d_i = 0.1$ (B-polarization).

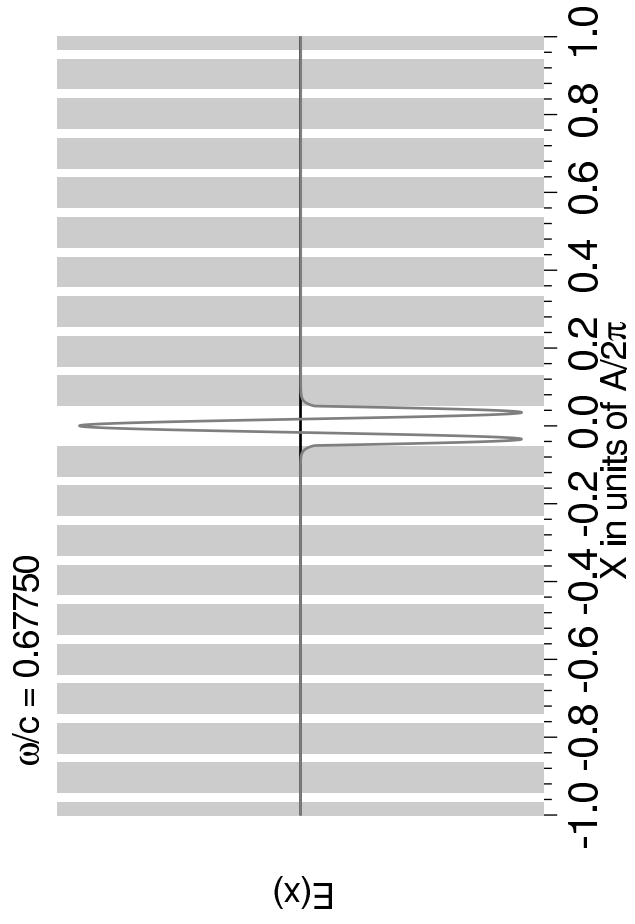
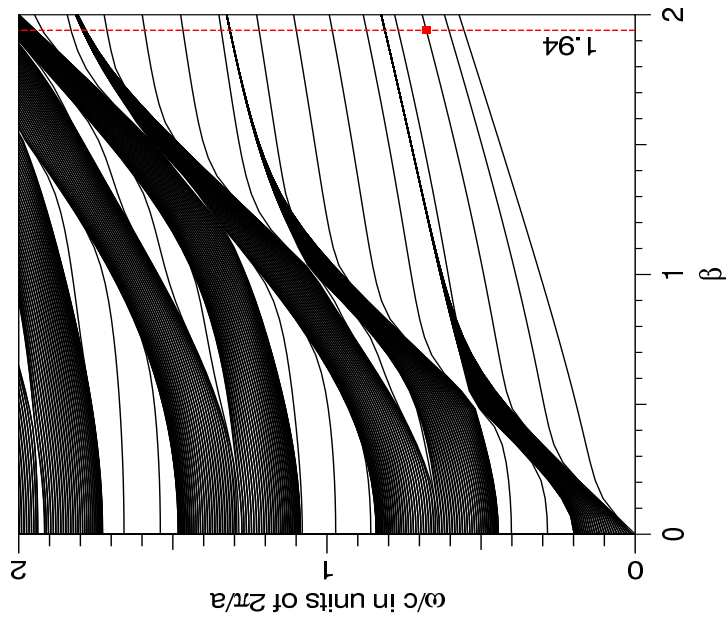


Figure 6.11: Dispersion relation and $E(x)$ vs x graph of 2nd even mode for $\epsilon_a = 13$, $\epsilon_b = 1$, $\epsilon_i = 13$, $d_a = 0.02$, $d_b = 0.08$, $d_i = 0.1$ (B-polarization).

In Fig. (6.9), we have shown the band diagram of first even guided mode and electric fields in real spaces for B-polarization. All the calculations are done for propagation constant value 1.94 and 10000 plane-waves. We use this propagation constant β value because we need to look all the guided modes clearly that we have seen in the figures. we can easily see that electric field of first even modes is localized and confined into guided layer. The thing that we have considered both localization and confinement in it. The frequency value of this mode for this β value is 0.55529. Therefore we have single mode one-dimensional photonic crystal waveguide up to this frequency. After this frequency we are going to have multi mode waveguide. In Fig. (6.10) and Fig. (6.11), we have first odd guided mode and second even guided mode. The localization is also valid for these two modes. Frequency values are 0.60404 and 0.6775 of these modes respectively. From these values we can say that this waveguide is still a single mode up to the frequency value 0.60404 because there is no other mode between first even and odd modes.

There is an interesting thing that we have to mention here. When we compare the band diagrams of single slab symmetric waveguide and one-dimensional photonic crystal waveguide we see that there is a perfect matching between guided modes. That means our photonic crystal waveguide behaves like single slab symmetric waveguide.

When we come to guided modes of E-polarization we should look at Fig. (6.12), Fig. (6.13), and Fig. (6.14). As in the case of B-polarization on the left hand side there are band diagrams of one-dimensional photonic crystal and on the right side electric fields in real spaces. The frequency values of first even, first odd and second even guided modes are 0.551, 0.58869, and 0.64815 respectively. Until 0.58869 frequency value we have single mode waveguide. There is also a correspondence between guided modes of single slab symmetric waveguide and one-dimensional photonic crystal waveguide for E-polarization.

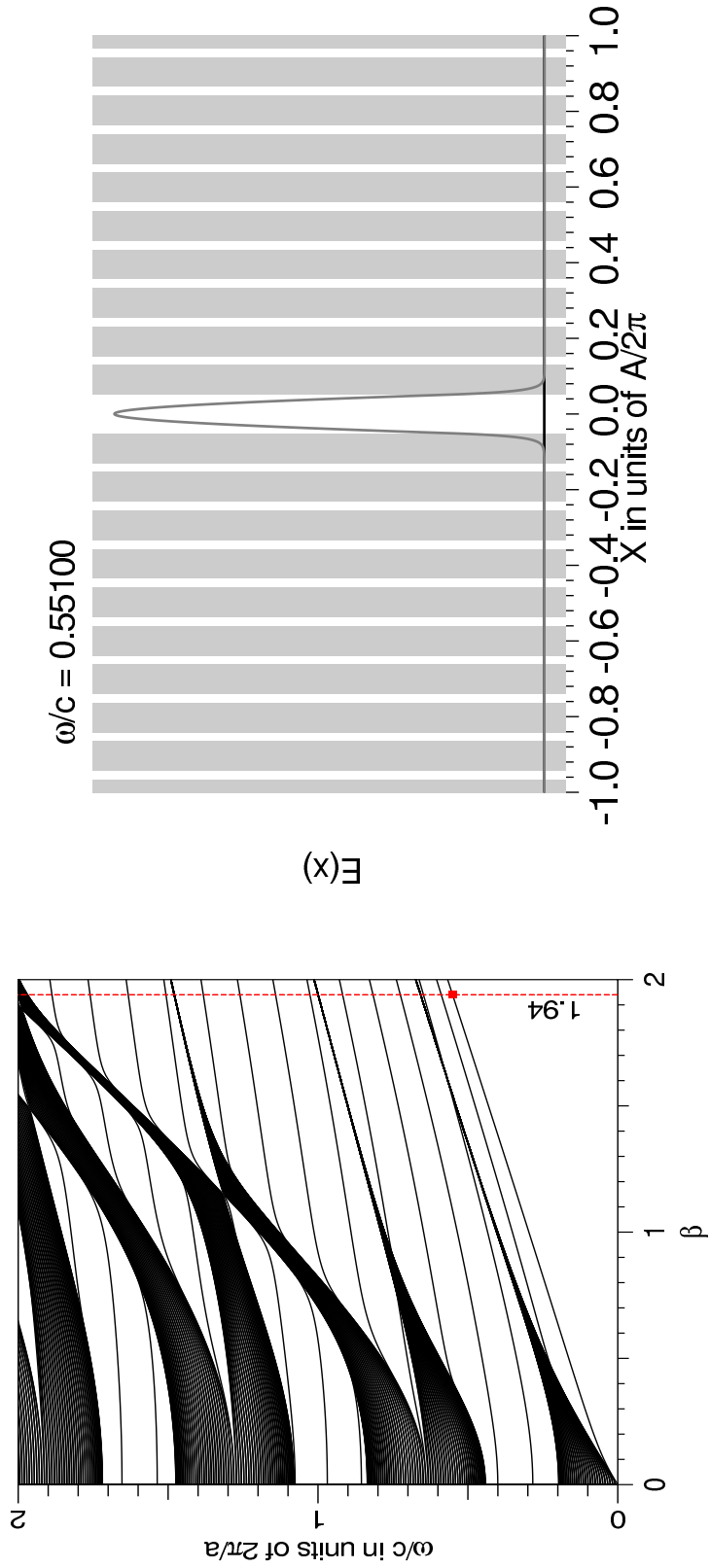


Figure 6.12: Dispersion relation and $E(x)$ vs x graph of 1st even mode for $\epsilon_a = 13$, $\epsilon_b = 1$, $\epsilon_i = 13$, $d_a = 0.02$, $d_b = 0.08$, $d_i = 0.1$ (E-polarization).

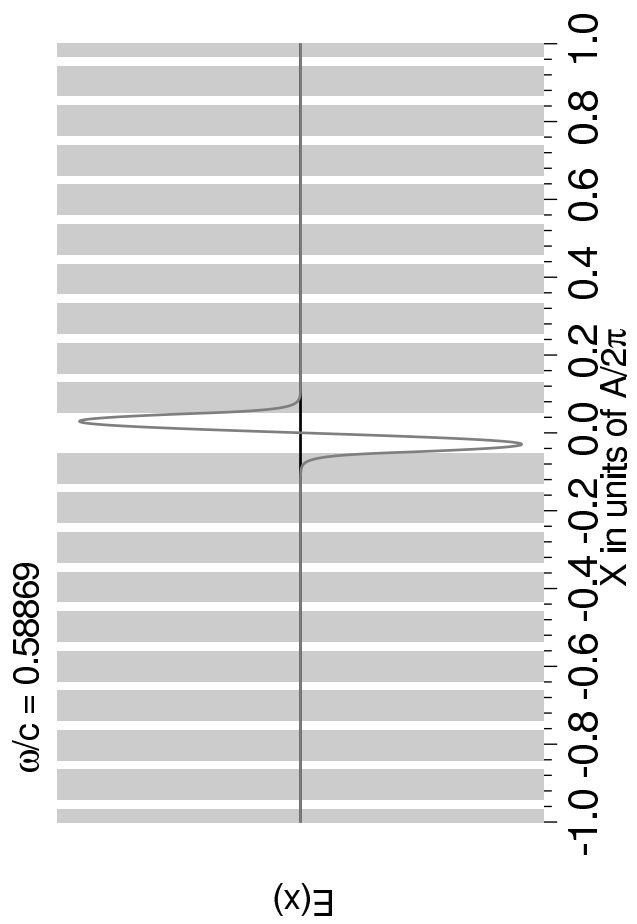
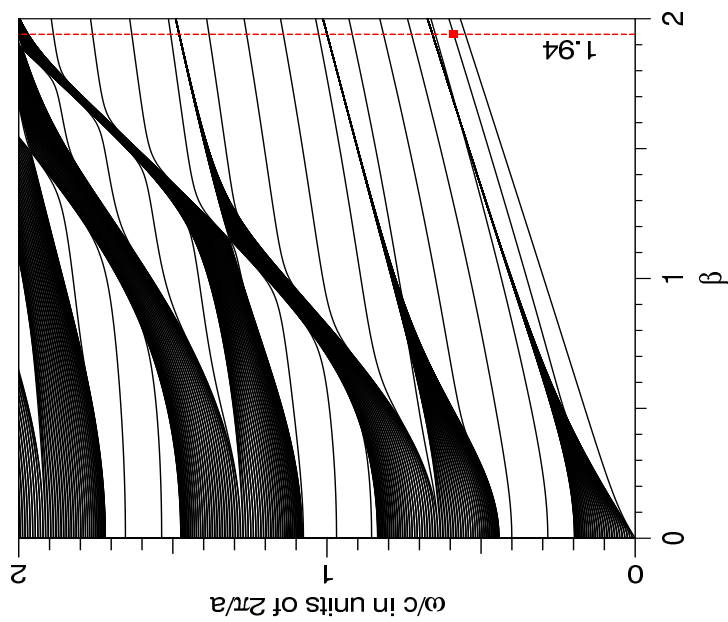


Figure 6.13: Dispersion relation and $E(x)$ vs x graph of 1st odd mode for $\epsilon_a = 13$, $\epsilon_b = 1$, $\epsilon_i = 13$, $d_a = 0.02$, $d_b = 0.08$, $d_i = 0.1$ (E-polarization).

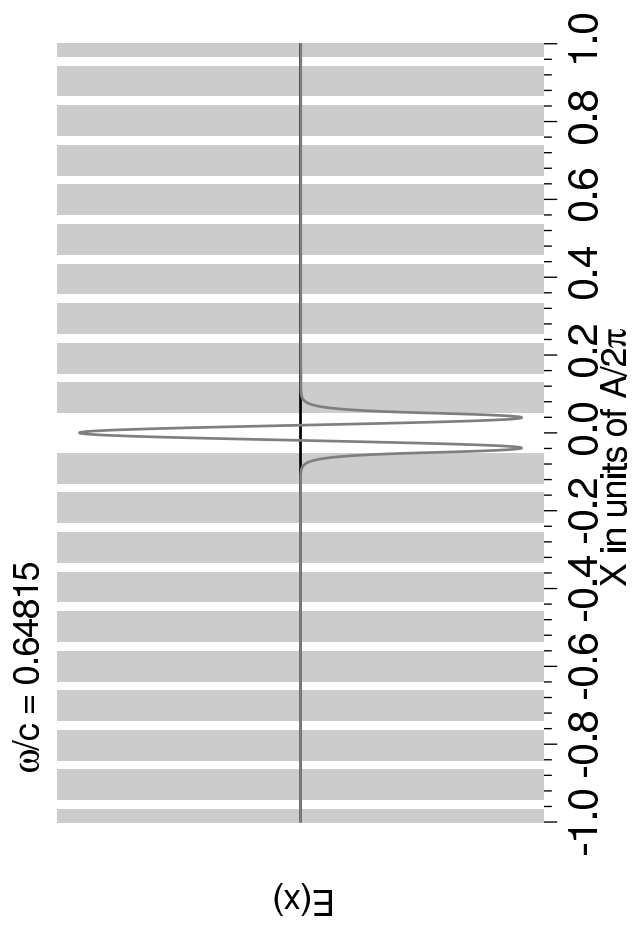
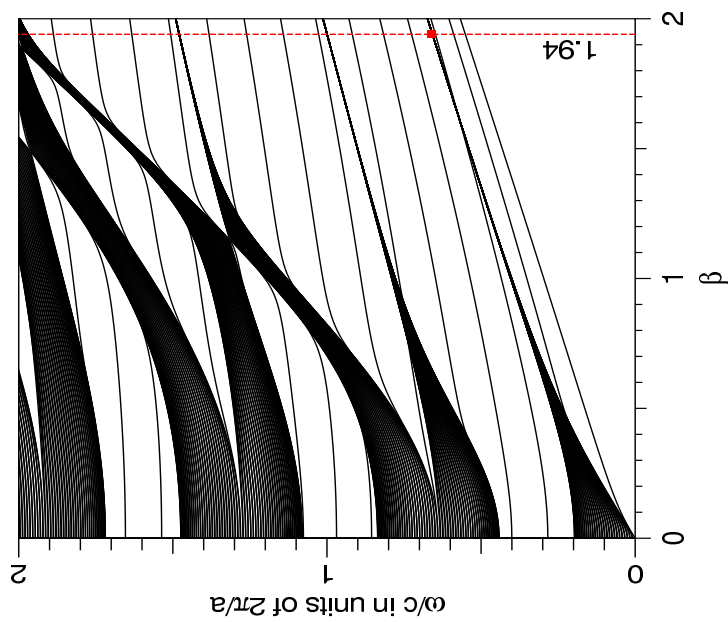


Figure 6.14: Dispersion relation and $E(x)$ vs x graph of 2nd even mode for $\epsilon_a = 13$, $\epsilon_b = 1$, $\epsilon_i = 13$, $d_a = 0.02$, $d_b = 0.08$, $d_i = 0.1$ (E-polarization).

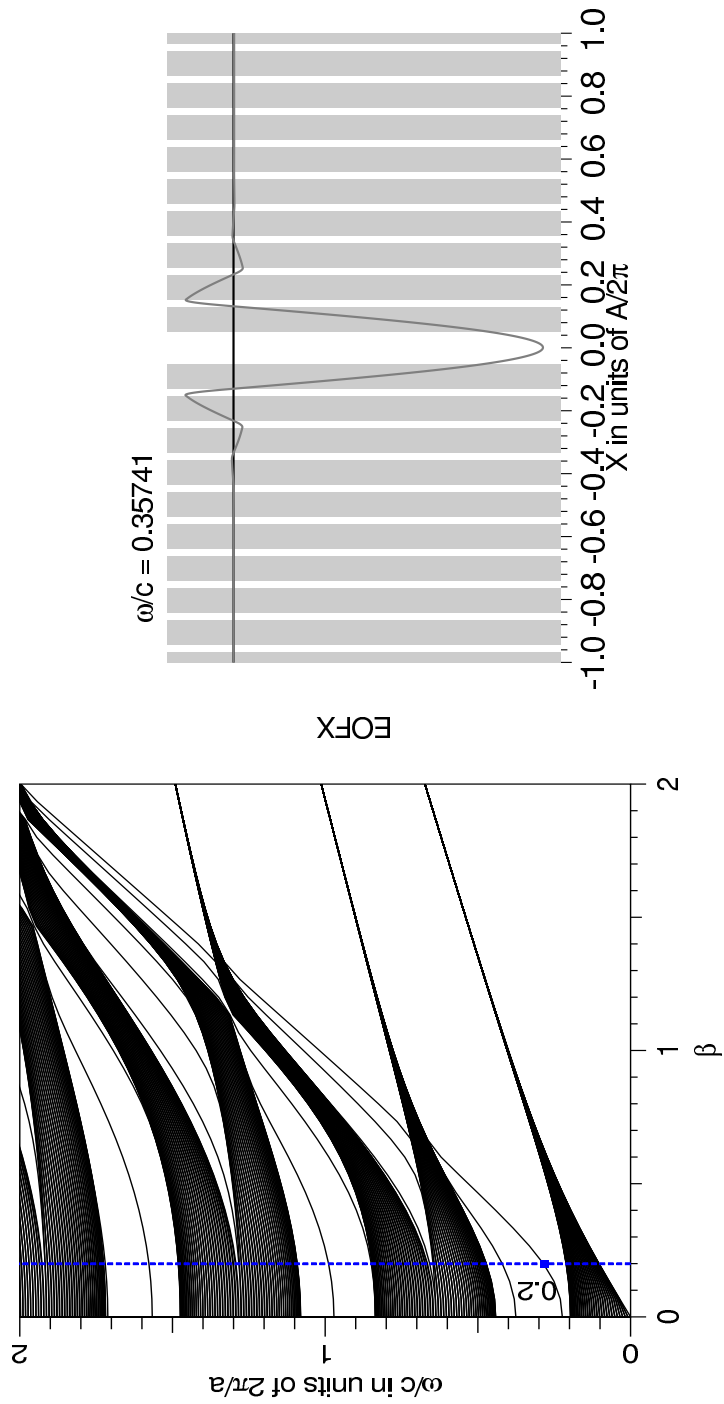


Figure 6.15: Dispersion relation and $E(x)$ vs x graph of 1st even mode for $\epsilon_a = 13$, $\epsilon_b = 1$, $\epsilon_i = 1$, $d_a = 0.02$, $d_b = 0.08$, $d_i = 0.1$ (E-polarization).

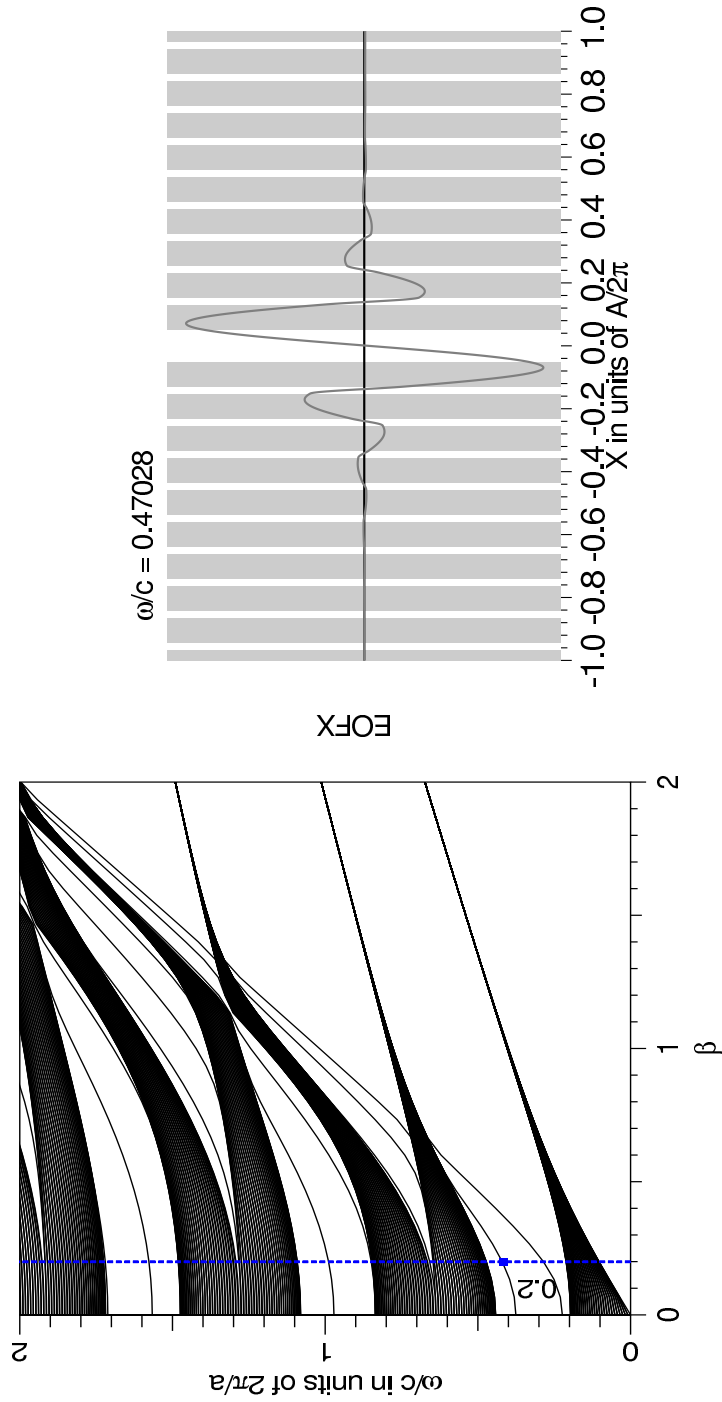


Figure 6.16: Dispersion relation and $E(x)$ vs x graph of 1st odd mode for $\epsilon_a = 13$, $\epsilon_b = 1$, ϵ_{i1} , $d_a = 0.02$, $d_b = 0.08$, $d_i = 0.1$ (E-polarization).

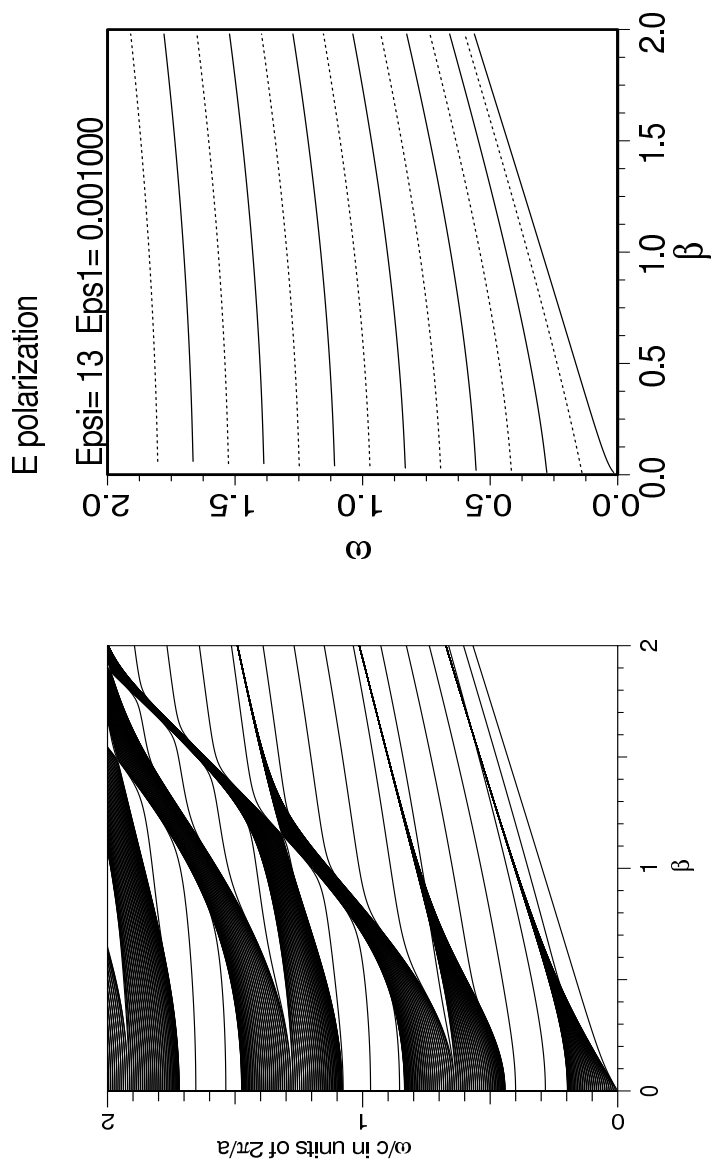
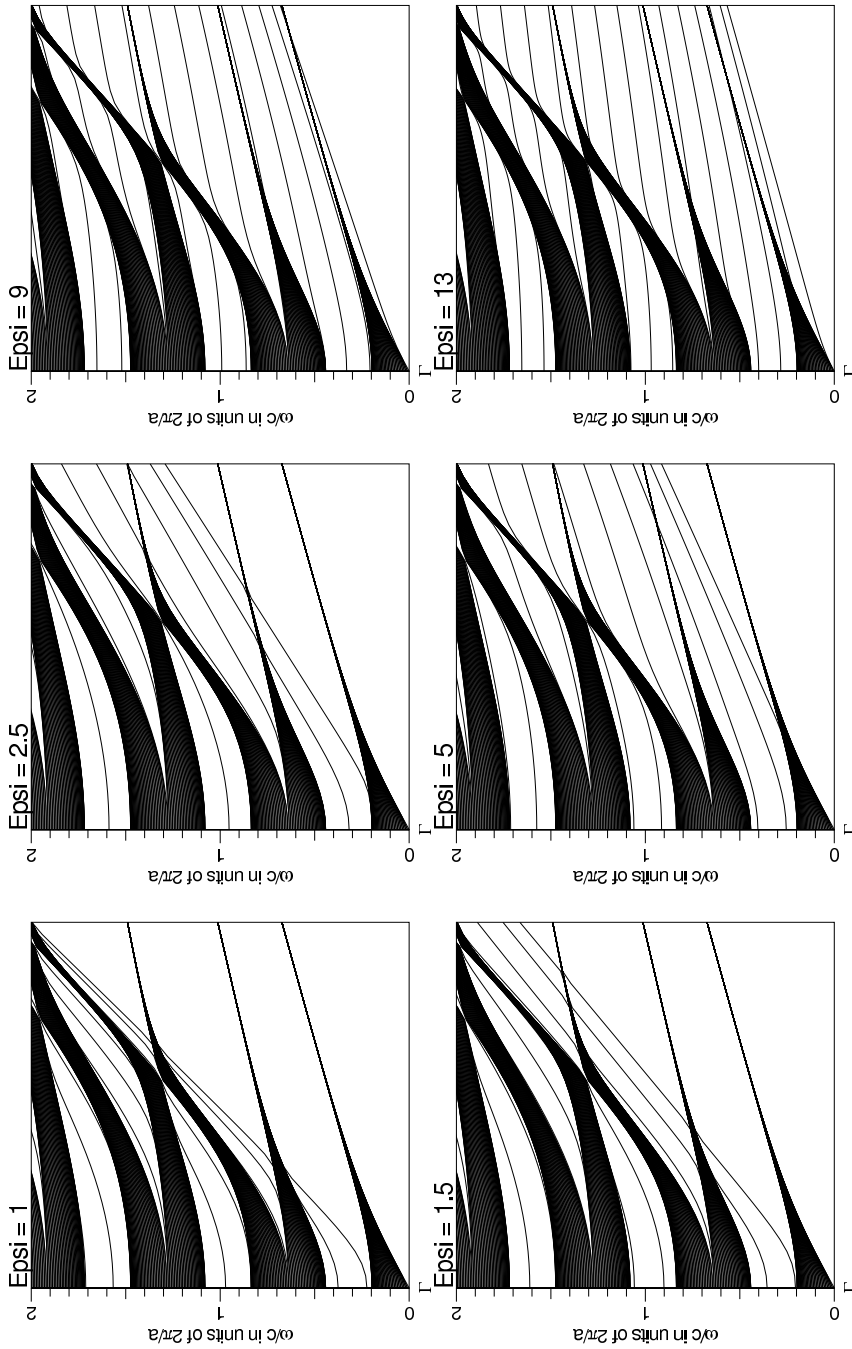


Figure 6.17: Dispersion relation and $E(x)$ vs x graph for $\epsilon_a = 13$, $\epsilon_b = 1$, $\epsilon_i = 13$, $d_a = 0.02$, $d_b = 0.08$, $d_i = 0.1$ and analytical solution of single slab waveguide for $\epsilon_i = 13$, $\epsilon_1 0.001$ (E-polarization). In this graph, if we choose the dielectric constant of outside region close to zero we have obtained the same guided modes in the case of one dimensional photonic crystal waveguide. This kind of materials which have zero dielectric constant known as perfect dielectric materials.

Figure 6.18: Band diagrams of one-dimensional photonic crystal waveguide for increasing ϵ_i , where $\epsilon_a=13$, $\epsilon_b = 1$ (E-Polarization).



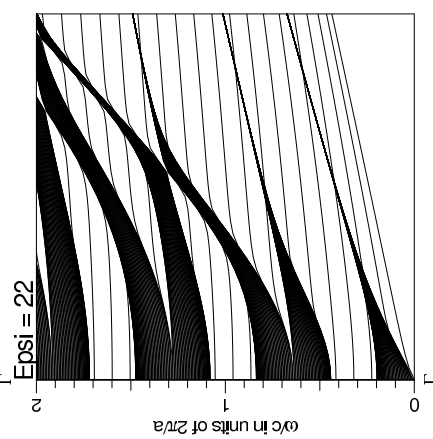
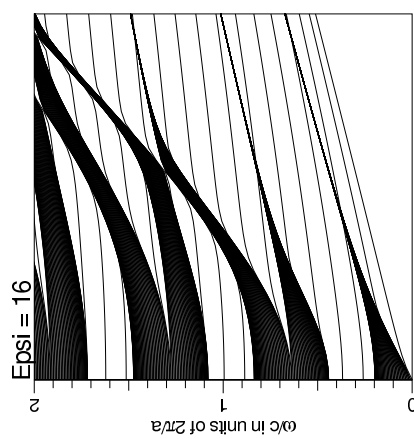
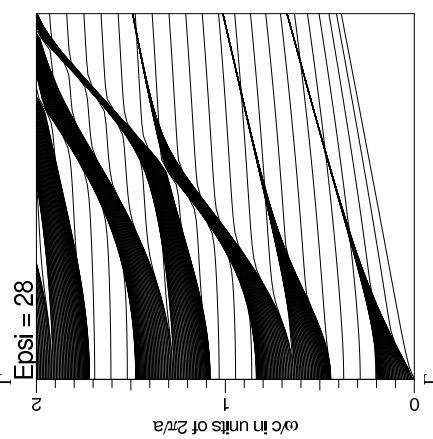
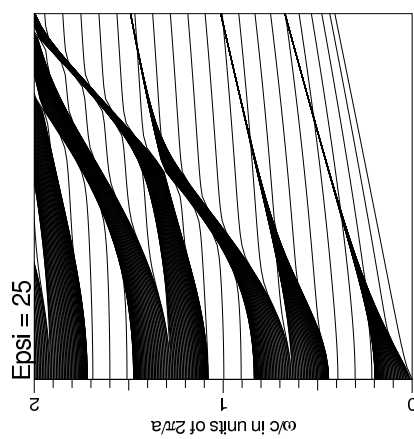
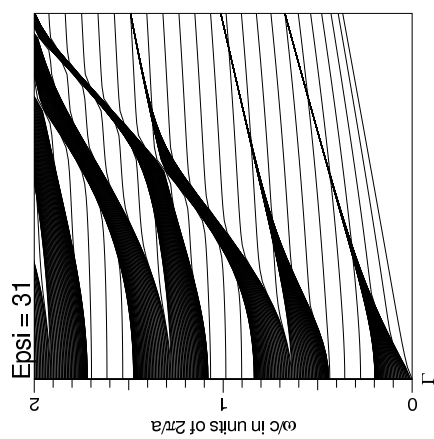


Figure 6.19: Band diagrams of one-dimensional photonic crystal waveguide for increasing ϵ_i , where $\epsilon_a = 13$, $\epsilon_b = 1$ (E-Polarization).

Figure 6.20: Band diagrams of one-dimensional photonic crystal waveguide for increasing ϵ_i , where $\epsilon_a = 13$, $\epsilon_b = 1$ (B-Polarization).

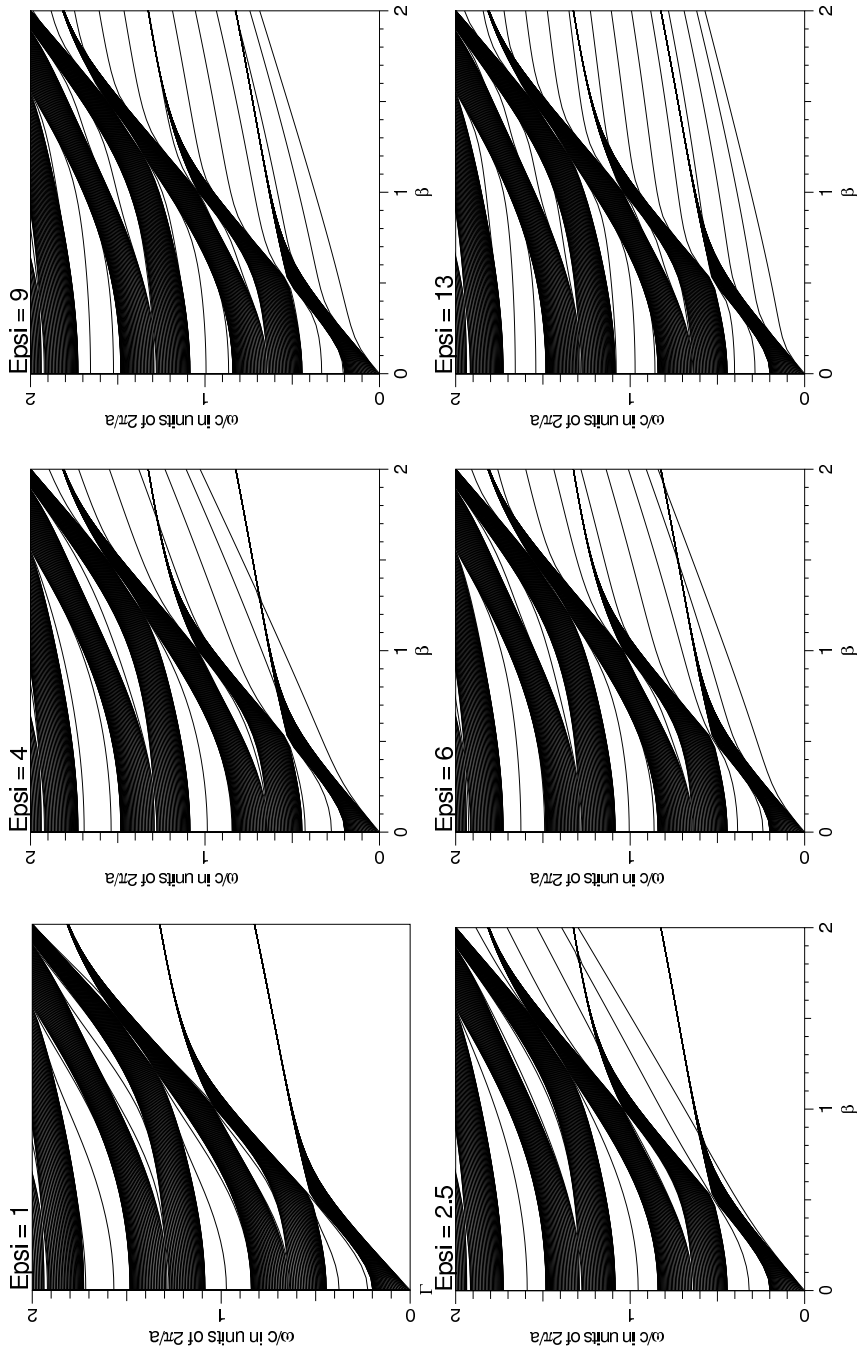
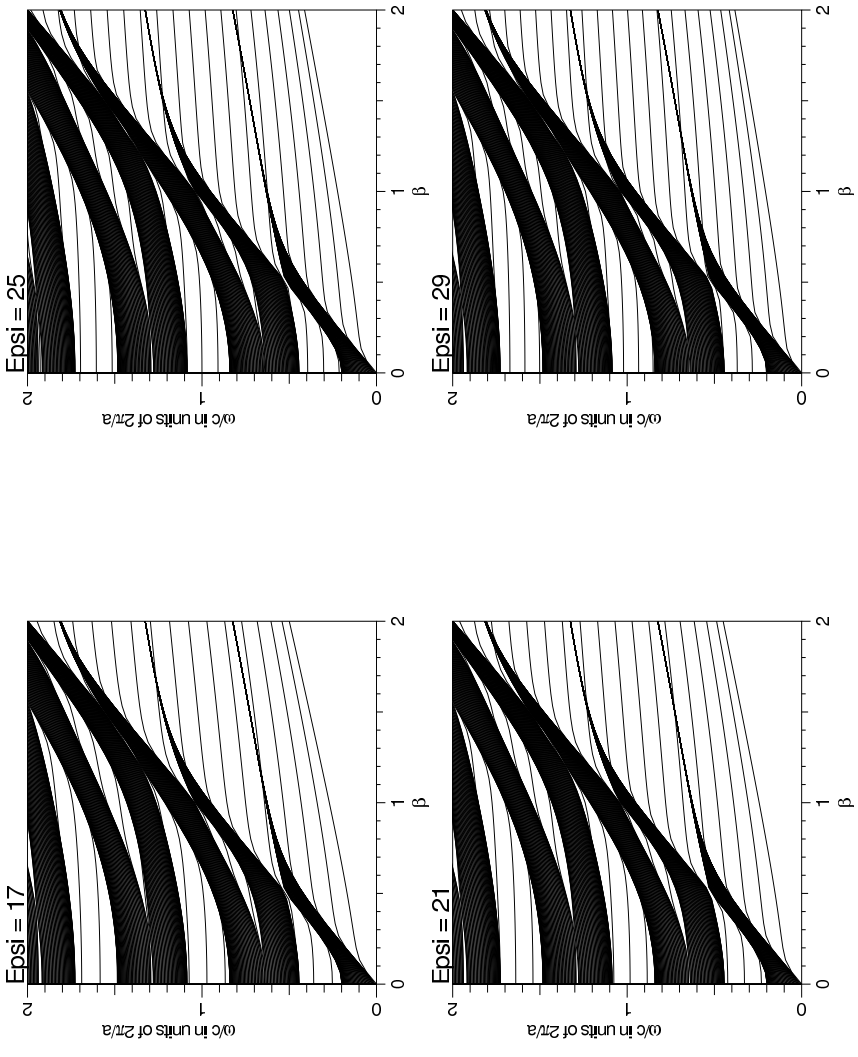


Figure 6.21: Band diagrams of one-dimensional photonic crystal waveguide for increasing ϵ_i , where $\epsilon_a = 13$, $\epsilon_b = 1$ (B-Polarization).



Chapter 7

DISCUSSION AND CONCLUSIONS

In this thesis, one-dimensional photonic crystals and photonic crystal waveguides are investigated by using different methods. We have begun to study our research with the plane-wave method and then calculated reflection and transmission coefficients of layered structure. Since we have obtained the band diagram of one-dimensional photonic crystal for a certain medium and the structure parameters, we have found transmission coefficients of layered structure for the same parameters and compared the photonic band gaps with the frequency region where the transmission was zero. After compared the results, we would like to observe the impurities in the band structure of one-dimensional photonic crystal. Using the transmission and reflection coefficients method, we could observe the impurities by changing the thickness of layers, but the impurities can not be obtained by using the plane-wave method. This method is valid only for the periodic photonic band gap structures. Because of this reason we have decided to use another method to create impurity into the structure. This method is known as the supercell method. By using this method, we have observed impurity in the middle of the supercell and chosen the convenient parameters, geometry, and the direction of electromagnetic waves, we have obtained the one-dimensional photonic crystal waveguide.

In the photonic crystal waveguide part of this thesis, we have calculated our modes for two polarizations E (TE) and B (TM). In order to check our results whether they are true or not, we have found the modes of single slab symmetric waveguide and compared it with the analytical solutions for E and B polarizations. We have seen that there is a good harmony between analytical and numerical results. After this check, we have constituted one-dimensional photonic crystal waveguide that has a different guiding mechanism than the conventional waveguide. This guiding mechanism is called photonic crystal guidance. The occurrence of this guidance is the reason of periodic photonic crystal which is placed outside of the guiding layer. In the calculation process of the modes of one-dimensional photonic crystal waveguide, the importance of structure size and

the number of plane-waves investigated for obtaining a good results. If we have taken small supercell size, the supercells are influenced with each other. Because of the fact that we have to take big supercell size to have reliable results. The second important parameter is the number of plane-waves which we have to take enough number of plane-waves for convergence [8].

As the second part of this research, we have tried to observe randomness in one-dimensional photonic crystal. In this study, we have used uniform random numbers which were added or subtracted to the thickness of each layer as a percentage. We have also calculated the same structure for a different percentages and looked at the variation of the first three band gaps of it. We have seen that how the randomness is important in the fabrication process of photonic crystals and how it affects the band gaps and the characteristics of the structure.

7.1 FUTURE WORKS

There are many possibilities for future work to extend and build upon the ideas put forward here. Specifically there a several key directions we would like to follow up.

- Design different photonic crystal waveguides which have different modes, confinements etc.
- Doing this research in 2-D structures for investigating the photonic crystal optical fibers.
- Randomness in 2-D or 3-D structures.
- Randomness in Supercell Method.
- Randomness in 1-D Photonic Crystal Waveguide.

We hope that these ideas will be attempted in the near future.

APPENDIX A

DERIVATION OF EIGENVALUE EQUATION OF H METHOD

First of all we are going to write general form of our equation,

$$-\sum_G (\mathbf{k} + \mathbf{G}') \times \eta(\mathbf{G}' - \mathbf{G})(\mathbf{k} + \mathbf{G}) \times H(\mathbf{k} + \mathbf{G}) = \frac{\omega^2}{c^2} H(\mathbf{k} + \mathbf{G}') \quad (\text{A.1})$$

The equation above is an ordinary eigenvalue problem in the form

$$AH = \frac{\omega^2}{c^2} H. \quad (\text{A.2})$$

In Eq. (A.1) we have $3N \times 3N$ matrix equation and we can reduce in $2N \times 2N$ eigenvalue problem. From the left hand side

$$\mathbf{q}' \times \mathbf{q} \times \mathbf{H}_G = \begin{bmatrix} q'_1 q_1 - \mathbf{q}' \cdot \mathbf{q} & q'_2 q_2 & q'_3 q_1 \\ q'_1 q_2 & q'_2 q_2 - \mathbf{q}' \cdot \mathbf{q} & q'_3 q_2 \\ q'_1 q_3 & q'_2 q_3 & q'_3 q_3 - \mathbf{q}' \cdot \mathbf{q} \end{bmatrix} \begin{bmatrix} H_x \\ H_y \\ H_z \end{bmatrix} \quad (\text{A.3})$$

We can write our equation in the form

$$\sum_G A_{GG'} H_G = \frac{\omega^2}{c^2} H_{G'} \quad (\text{A.4})$$

Multiplying both sides from left by S_G then

$$\sum_{G,G'} S_G A_{GG'} H_G = \frac{\omega^2}{c^2} S_{G'} H_{G'} \quad (\text{A.5})$$

Using identity matrix as $I \equiv S_{G'}^\dagger S_G$ then

$$\sum_{G,G'} S_G A_{GG'} S_{G'}^\dagger S_G H_G = \frac{\omega^2}{c^2} S_{G'} H_{G'} \quad (\text{A.6})$$

Now we have another eigenvalue problem

$$\sum_{G,G'} S_G A_{GG'} S_{G'}^\dagger H_G^* = \frac{\omega^2}{c^2} H_{G'}^* \quad (\text{A.7})$$

where

$$S_G = \begin{pmatrix} e_{1x} & e_{1y} & e_{1z} \\ e_{2x} & e_{2y} & e_{2z} \\ e_{3x} & e_{3y} & e_{3z} \end{pmatrix} \quad (\text{A.8})$$

$$S_{G'}^\dagger = \begin{pmatrix} e'_{1x} & e'_{2x} & e'_{3x} \\ e'_{1y} & e'_{2y} & e'_{3y} \\ e'_{1z} & e'_{2z} & e'_{3z} \end{pmatrix} \quad (\text{A.9})$$

$$\tilde{A} = \begin{bmatrix} e_{1x} & e_{1y} & e_{1z} \\ e_{2x} & e_{2y} & e_{2z} \\ e_{3x} & e_{3y} & e_{3z} \end{bmatrix} \begin{bmatrix} q'_1 q_1 - \mathbf{q}' \cdot \mathbf{q} & q'_2 q_2 & q'_3 q_1 \\ q'_1 q_2 & q'_2 q_2 - \mathbf{q}' \cdot \mathbf{q} & q'_3 q_2 \\ q'_1 q_3 & q'_2 q_3 & q'_3 q_3 - \mathbf{q}' \cdot \mathbf{q} \end{bmatrix} \begin{bmatrix} e'_{1x} & e'_{2x} & e'_{3x} \\ e'_{1y} & e'_{2y} & e'_{3y} \\ e'_{1z} & e'_{2z} & e'_{3z} \end{bmatrix}$$

Where $\tilde{A} \equiv S_G A_{GG'} S_{G'}^\dagger$. Using $\mathbf{q} \equiv q \hat{e}_3$ and $\mathbf{q}' \equiv q' \hat{e}'_3$ into equation above,

$$= qq' \begin{bmatrix} e_{1x} & e_{1y} & e_{1z} \\ e_{2x} & e_{2y} & e_{2z} \\ e_{3x} & e_{3y} & e_{3z} \end{bmatrix} \left\{ \begin{bmatrix} e'_{3x} e_{3x} & e'_{3y} e_{3y} & e'_{3z} e_{3z} \\ e'_{3x} e_{3y} & e'_{3y} e_{3y} & e'_{3z} e_{3y} \\ e'_{3x} e_{3z} & e'_{3y} e_{3z} & e'_{3z} e_{3z} \end{bmatrix} - \hat{e}'_3 \cdot \hat{e}_3 I \right\} \begin{bmatrix} e'_{1x} & e'_{2x} & e'_{3x} \\ e'_{1y} & e'_{2y} & e'_{3y} \\ e'_{1z} & e'_{2z} & e'_{3z} \end{bmatrix}$$

In order to simplify our calculations we denote that

$$E_{ij} = \begin{bmatrix} e_{1x} & e_{1y} & e_{1z} \\ e_{2x} & e_{2y} & e_{2z} \\ e_{3x} & e_{3y} & e_{3z} \end{bmatrix}$$

$$Q_{ij} = \begin{bmatrix} e'_{3x} e_{3x} & e'_{3y} e_{3y} & e'_{3z} e_{3z} \\ e'_{3x} e_{3y} & e'_{3y} e_{3y} & e'_{3z} e_{3y} \\ e'_{3x} e_{3z} & e'_{3y} e_{3z} & e'_{3z} e_{3z} \end{bmatrix}$$

$$E'_{ij} = \begin{bmatrix} e'_{1x} & e'_{2x} & e'_{3x} \\ e'_{1y} & e'_{2y} & e'_{3y} \\ e'_{1z} & e'_{2z} & e'_{3z} \end{bmatrix}$$

We can write $E_{ij} \equiv \hat{\mathbf{e}}_i \cdot \mathbf{u}_j$, $Q_{ij} \equiv (\hat{\mathbf{e}}'_3 \cdot \mathbf{u}_i)(\hat{\mathbf{e}}_3 \cdot \mathbf{u}_j)$, and $E'_{ij} \equiv \mathbf{u}_i \cdot \hat{\mathbf{e}}'_j$ into above equation. As we can see from the equation we have two part. For the first part we can write,

$$\begin{aligned}
\tilde{A}_{ij} &= qq' \sum_{k,l} E_{ik} Q_{kl} E'_{lj} \\
&= qq' \sum_{k,l} (\hat{\mathbf{e}}_i \cdot \mathbf{u}_k) (\hat{\mathbf{e}}'_3 \cdot \mathbf{u}_k) (\hat{\mathbf{e}}_3 \cdot \mathbf{u}_l) (\mathbf{u}_l \cdot \hat{\mathbf{e}}'_j) \\
&= qq' (\hat{\mathbf{e}}_i \cdot \hat{\mathbf{e}}'_3) (\hat{\mathbf{e}}_3 \hat{\mathbf{e}}'_j) \\
&= qq' \begin{bmatrix} (\mathbf{e}_1 \cdot \mathbf{e}'_3)(\mathbf{e}_3 \cdot \mathbf{e}'_1) & (\mathbf{e}_1 \cdot \mathbf{e}'_3)(\mathbf{e}_3 \cdot \mathbf{e}'_2) & (\mathbf{e}_1 \cdot \mathbf{e}'_3)(\mathbf{e}_3 \cdot \mathbf{e}'_3) \\ (\mathbf{e}_2 \cdot \mathbf{e}'_3)(\mathbf{e}_3 \cdot \mathbf{e}'_1) & (\mathbf{e}_2 \cdot \mathbf{e}'_3)(\mathbf{e}_3 \cdot \mathbf{e}'_2) & (\mathbf{e}_2 \cdot \mathbf{e}'_3)(\mathbf{e}_3 \cdot \mathbf{e}'_3) \\ (\mathbf{e}_3 \cdot \mathbf{e}'_3)(\mathbf{e}_3 \cdot \mathbf{e}'_1) & (\mathbf{e}_3 \cdot \mathbf{e}'_3)(\mathbf{e}_3 \cdot \mathbf{e}'_2) & (\mathbf{e}_3 \cdot \mathbf{e}'_3)(\mathbf{e}_3 \cdot \mathbf{e}'_3) \end{bmatrix} \quad (\text{A.10})
\end{aligned}$$

For the second part of our equation,

$$\begin{aligned}
&= -qq' \hat{\mathbf{e}}'_3 \cdot \hat{\mathbf{e}}_3 \begin{bmatrix} \mathbf{e}_1 \cdot \mathbf{e}'_1 & \mathbf{e}_1 \cdot \mathbf{e}'_2 & \mathbf{e}_1 \cdot \mathbf{e}'_3 \\ \mathbf{e}_2 \cdot \mathbf{e}'_1 & \mathbf{e}_2 \cdot \mathbf{e}'_2 & \mathbf{e}_2 \cdot \mathbf{e}'_3 \\ \mathbf{e}_3 \cdot \mathbf{e}'_1 & \mathbf{e}_3 \cdot \mathbf{e}'_2 & \mathbf{e}_3 \cdot \mathbf{e}'_3 \end{bmatrix} \\
&= -qq' \begin{bmatrix} (\mathbf{e}'_3 \cdot \mathbf{e}_3)(\mathbf{e}_1 \cdot \mathbf{e}'_1) & (\mathbf{e}'_3 \cdot \mathbf{e}_3)(\mathbf{e}_1 \cdot \mathbf{e}'_2) & (\mathbf{e}'_3 \cdot \mathbf{e}_3)(\mathbf{e}_1 \cdot \mathbf{e}'_3) \\ (\mathbf{e}'_3 \cdot \mathbf{e}_3)(\mathbf{e}_2 \cdot \mathbf{e}'_1) & (\mathbf{e}'_3 \cdot \mathbf{e}_3)(\mathbf{e}_2 \cdot \mathbf{e}'_2) & (\mathbf{e}'_3 \cdot \mathbf{e}_3)(\mathbf{e}_2 \cdot \mathbf{e}'_3) \\ (\mathbf{e}'_3 \cdot \mathbf{e}_3)(\mathbf{e}_3 \cdot \mathbf{e}'_1) & (\mathbf{e}'_3 \cdot \mathbf{e}_3)(\mathbf{e}_3 \cdot \mathbf{e}'_2) & (\mathbf{e}'_3 \cdot \mathbf{e}_3)(\mathbf{e}_3 \cdot \mathbf{e}'_3) \end{bmatrix} \quad (\text{A.11})
\end{aligned}$$

Combining Eq. (A.10) and Eq. (A.11) and arranging some terms then

$$\tilde{A} = qq' \begin{bmatrix} \mathbf{e}_1 \cdot [(\mathbf{e}_3 \cdot \mathbf{e}'_1)\mathbf{e}'_3 - (\mathbf{e}'_3 \cdot \mathbf{e}_3)\mathbf{e}'_1] & \mathbf{e}_1 \cdot [(\mathbf{e}_3 \cdot \mathbf{e}'_2)\mathbf{e}'_3 - (\mathbf{e}'_3 \cdot \mathbf{e}_3)\mathbf{e}'_2] & 0 \\ \mathbf{e}_2 \cdot [(\mathbf{e}_3 \cdot \mathbf{e}'_1)\mathbf{e}'_3 - (\mathbf{e}'_3 \cdot \mathbf{e}_3)\mathbf{e}'_1] & \mathbf{e}_2 \cdot [(\mathbf{e}_3 \cdot \mathbf{e}'_2)\mathbf{e}'_3 - (\mathbf{e}'_3 \cdot \mathbf{e}_3)\mathbf{e}'_2] & 0 \\ 0 & 0 & 0 \end{bmatrix}$$

Using $(B.A)C - (C.A)B$ rule for each matrix element, we have obtain $S_{G'}^\dagger A S_G$ as

$$S_G A_{GG'} S_{G'}^\dagger = q'q \begin{pmatrix} -\mathbf{e}'_2 \cdot \mathbf{e}_2 & \mathbf{e}'_1 \cdot \mathbf{e}_2 & 0 \\ \mathbf{e}'_2 \cdot \mathbf{e}_1 & -\mathbf{e}'_1 \cdot \mathbf{e}_1 & 0 \\ 0 & 0 & 0 \end{pmatrix} \quad (\text{A.12})$$

Using this matrix into Eq. (A.1) and substituting $q' \equiv |k + G'|$ and $q \equiv |k + G|$

we have

$$\sum_{\mathbf{G}} |\mathbf{k} + \mathbf{G}'| |\mathbf{k} + \mathbf{G}| \eta(\mathbf{G}' - \mathbf{G}) \begin{bmatrix} \mathbf{e}'_2 \cdot \mathbf{e}_2 & -\mathbf{e}'_1 \cdot \mathbf{e}_2 \\ -\mathbf{e}'_2 \cdot \mathbf{e}_1 & \mathbf{e}'_1 \cdot \mathbf{e}_1 \end{bmatrix} \begin{bmatrix} \mathbf{H}_1(\mathbf{G}) \\ \mathbf{H}_2(\mathbf{G}) \end{bmatrix} = \frac{\omega^2}{c^2} \begin{bmatrix} \mathbf{H}_x(\mathbf{G}) \\ \mathbf{H}_y(\mathbf{G}) \end{bmatrix}.$$

Here we have reduced $3N \times 3N$ problem in $2N \times 2N$ problem.

REFERENCES

- [1] E. Yablonovitch, Phys. Rev. Lett. 58, 2059 (1987).
- [2] A. Mekis, J. C. Chen, I. Kurland, S. Fan, P. R. Villeneuve, and J. D. Joannopoulos, Phys. Rev. Lett. 77, 3787 (1996).
- [3] J. D. Joannopoulos, P. R. Villeneuve, and S. Fan, Nature 386, 143 (1997).
- [4] S. John, Phys. Rev. Lett. 58, 2486 (1987).
- [5] S.-Y. Lin, E. Chow, V. Hietala, P. R. Villeneuve, and J. D. Joannopoulos, Science 282, 274 (1998).
- [6] Satpathy, S., Zhang, Z. and Salehpour, Phys. Rev. Lett. 64, 1239 (1990).
- [7] K. M. Leung, Y. F. Liu, Phys. Rev. B 41, 10188 (1990).
- [8] H. Sami Sözüer, J.W. Haus, R. Inguva, Phys. Rev. B 45 13962 (1992).
- [9] H. Sami Sözüer, J.W. Haus, J. Opt. Soc. Am. B V 10 No: 2 (1993).
- [10] H. S. Sözüer, J. P. Dowling, J. Mod. Opt. 41, 231 (1994).
- [11] K. M. Ho, C. T. Chan, C. M. Soukoulis, R. Biswas, M. Sigalas, Solid State Commun. 89, 413 (1994).
- [12] V. N. Astratov *et al.*, Nuovo Cimento 17, 1349 (1995).
- [13] S. Y. Lin, V. M. Hietala, L. Wang, E. D. Jones, Opt. Lett. 21, 1771 (1996).
- [14] J.C. Knight, T.A. Birks, P.St.J. Russell, and D.M. Atkin, Opt. Lett., 21:1547, 1996.
- [15] T. A. Birks *et al.*, Opt. Let. 22 961 (1997).
- [16] J. C. Knight *et al.*, Science 282 1476 (1998).
- [17] J. G. Fleming, S. Y. Lin, Opt. Lett. 24, 49 (1999).
- [18] A. Blanco *et al.*, Nature 405, 437 (2000).

- [19] K. Sakoda, *Optical Properties of Photonic Crystals*, Springer Press, (2001).
- [20] S. G. Johnson, J. D. Joannopolous, *Photonic Crystals The Road from Theory to practice*, Kluwer Academic Pub. (2001).
- [21] J. D. Joannopolous, R. D. Meade, J. N. Winn, *Photonic Crystals Molding the Flow of Light*, Princeton University Press, (1995).
- [22] Pochi Yeh, *Optical Waves in Layered Media*, Wiley Interscience, (1988).
- [23] Amnon Yariv, Pochi Yeh, *Optical Waves in Crystals*, Wiley Interscience, (1983).
- [24] J. Cozens, R. Syms, *Optical Guided Waves and Devices*, Mc Graw Hill, (1992).
- [25] J. Soong, Y. Park, H. Jeon , *Journal of Korean Phys. Soc.* 39, 56 (2001).